CYPRUS UNIVERSITY OF TECHNOLOGY

FACULTY OF ENGINEERING & TECHNOLOGY

THESIS

INVESTIGATION OF SPECTROSCOPY REMOTE SENSING FOR MAPPING PAVEMENT SYSTEMS CONDITION

ELIAS TSIRIPILLOS

Limassol 2015

CYPRUS UNIVERSITY OF TECHNOLOGY

FACULTY OF ENGINEERING & TECHNOLOGY

DEPARTMENT OF CIVIL ENGINEERING AND GEOMATICS

INVESTIGATION OF SPECTROSCOPY REMOTE SENSING FOR MAPPING PAVEMENT SYSTEMS CONDITION

ELIAS TSIRIPILLOS

Limassol 2015

APPROVAL FORM

Thesis

Investigation of Spectroscopy Remote Sensing for mapping pavement systems conditions

Presented by

Elias Tsiripillos

Supervisor ____

[Title and name]

Member of Committee ____

[Title and name]

Member of Committee ____

[Title and name]

Cyprus University of Technology

[December, 2015]

Copyrights

ACKNOWLEDGEMENTS

I would like to express sincere gratitude to my supervisor Athos Agapiou for his kind encouragement and strong support in this investigation throughout the whole period, and for his enlightenment, which deepens my understanding of this area. Without his consistent and illuminating instruction this thesis could not reach its present form. Besides my supervisor, I would like to acknowledge and to personally thank Christodoulos Mettas for the help he provided me. Last but not least, I would like to thank my family for the support they provided me during my research.

ABSTRACT

An investigation of spectroscopy remote sensing for mapping pavement systems conditions is undertaken in this research. Spectral data were acquired by the HR1024 spectroradiometer and were analysed, processed and interpreted. A spectral library was developed in order to define the attributes of the different pavement systems. This research has plot the spectral profiles of each pavement system that are investigated and found that the older roads have high reflectance and the areas with the deformations or cracks can be identified as they have lower reflectance than the un-cracked – healthy areas. Several t – test were applied followed the spectral profiles in order to indicate whether there is a difference in the means between the pavement systems. After the t – test, Pearson correlation coefficient and Euclidean distance were used in order to observe wavelengths that are going to be used in the spectral experiment. Through the spectral experiment these wavelengths were used in a try to identify cracked areas or deformations. The results of the spectral experiment have shown that the cracked areas or deformations are not visible in the wavelengths.

TABLE OF CONTENTS

LIST OF TABLES

LIST OF FIGURES

1 Introduction

The knowledge of rigid and flexible pavement systems spectral characteristics plays an important role in several applications such as imagery calibration and validation, land cover analysis and civil engineering (Mei 2014). In order to manage and maintain the transportation infrastructures detailed and accurate information is vital. Information regarding the use of infrastructures, the damages of infrastructures, the age of the infrastructures, how the infrastructures act under the weather conditions and the oxidation of the infrastructures. All of the above information have high importance for urban planning and transportation engineering. Ground spectroscopy can provide this vital information. It can monitor built up areas as it can detect the growth and spatial distribution of urban infrastructures such as roads (Shahi 2014). Remote sensing has been evolved a lot, as the measurements from ground spectroscopy and hyperspectral remote sensing can provide precise investigations and understanding the properties of the material and on surface geometry. According to Herold (2002) 'remote sensing can solve the road condition mapping by applying cheap methods to evaluate the surface defects/deformations of rigid and flexible pavement systems'.

In this research, measurements from ground spectrometry will be collected and analyzed in order to map the conditions of road networks and to distinguish differences between flexible pavement system and rigid pavement system. To add this research will try to generate wavelengths from several test and to investigate whether in those wavelengths the deformations/cracks of the pavement systems are visible or not. The topic of the research was chosen with ease, as remote sensing is a relatively new topic especially in Cyprus having appeared the last decade. Remote sensing has many capabilities which make it a helpful tool to use on infrastructures projects. It was consider as a good choice as the outcomes of this research hopefully will provide the government authorities an efficient, rapid and accurate road mapping which will provide the location of the pavement systems that need maintenance.

An important aspect of this research is the creation of a comprehensive field spectral index between 350 nm to 2500 nm to interpret and analyze the characteristics. The index is consisted of two surface types asphalt and concrete which differ in their geometry, conditions, use and age.

The research is consisted by eight sections alongside with their sub sections. The first chapter is the introduction, in which chapter the purpose and the context of this research is explained. Furthermore, the introduction highlights the aims and objectives and sets an outline of the structure. Moving on, the second chapter will explain the remote sensing platforms that are used to collect data and to monitor the pavement systems. The third chapter provides information about the road types and gives explanation on the deformation and damages that occur on the pavement systems. Following on, the fourth chapter provides background on remote sensing, it explains what remote sensing is and it will review recent literature on the same topic stating out the procedure of each research and the outcomes. The fifth chapter is the methodology and it sets out the research methodology for this research, the data collection method, the methods used to analyse the data and the procedure that will be undertaken. Next, the sixth chapter which is the data analysis and discussion will present the results from the methods and the test that will be used in this research. The seventh chapter which is the conclusion it establishes the outcomes and the findings of this research. Lastly the eighth chapter will give some recommendations for future research on the topic.

2 Remote Sensing Platforms

In this chapter the most common platforms that are used to gather data are going to be explained and analyzed.

2.1 Satellite

Satellite is a platform that provides the largest spatial coverage of any remotely sensed data and is used in several aspects from earth sciences to military operations (Herold et al. 2003). The available literature seams to show that even though these data from satellite platform can cover extremely big areas in a single image, the data collection, data quality and the usability can be limited by revisit times, spatial resolution and atmospheric interferences (Schnebele 2015). The satellite's orbit and inclination will determine the data coverage and availability. Satellites with high orbit can be extremely helpful for meteorological applications for the reason that they give continuous coverage on the same area. In addition, these high orbit satellites are not suitable for road studies as they have very low spatial resolution. The satellites that are useful for earth sciences, surveillance and mapping are the polar orbiting satellites because they obtain information over every area of the Earth's surface. They can provide a variety of spatial resolutions which depends on the altitude and the velocity.

2.2 Unmanned aerial vehicles (UAV)

These low altitude systems are capable to provide high resolution, near real-time imagery with low cost when compared with manned aerial or spaceborne platforms. There are many researches that studied the UAV system; Zhang (2008) was able to identify deformations and defects on unpaved roads by using pattern recognition and image classification techniques from 2D images collected from a UAV. Furthermore, Fenger et al (2009) have shown how a UAV platform can obtain images to map roads and vehicles, and provide information with regard to traffic, accident or natural disasters within 2 hours of the event. Lastly, Zhang & Elaksher (2012) have designed a UAV system that can collect 3D high-resolution photogrammetric imagery of road surface deformations for unpaved roads. According to Tatham (2009) 'their high manoeuvrability, quick response time and high resolutions make them important tools for disaster assessment.'

2.3 Ground Penetrating Radar (GPR)

Ground penetrating radar involves electromagnetic energy in the microwave range in the Electromagnetic spectrum, using wavelengths 3m – 200mm to examine subsurface features with ground coupled antenna or air-coupled antenna (Saarenketo & Scullion 2000). The ground penetrating radar is very sensitive to water which allows the changes in materials, moisture contents and voids to be detected in the returned signal. According to the researches done by Maser (1996), Morey (1998) and Saarenketo & Scullion (2000) the most useful applications of the ground penetrating radar are the void discovery and the measurement of the thickness of the layer on a pavement system. Identifying the thickness of a layer on a pavement system can provide vital information such as load ratings and pavement life. When the GPR locates voids, either water voids or air voids, it can be really helpful. When there is moisture between the layers of the pavement system is an indicator that the pavement will deteriorate. Forest & Utsi (2004) research has shown that GPR can be useful to identify cracks in flexible pavement and to measure the cracks depths.

Moving on, Grote et al. (2005) were able to discover moisture in the subgrade of flexible pavement systems using the GPR. GPR can provide important data but for the reason that the signal is complex technicians with high level of skills are needed.

2.4 Infrared Thermography

Infrared thermograpgy is capable to identify the voids but it differs from the GPR technique. The infrared thermography can provide horizontal measurements of the voids but not depth or thickness (Weil, 1992). As Pascucci et al. (2008) have shown that infrared thermography can evaluate deformations in pavements systems. As the asphalt grows, it oily components are decreasing and the limestone increases; in their research they utilize the limestone increased absorption and they were able to identify areas of deterioration. Lastly Dumoulin et al. (2011) utilize the infrared thermography to identify non-emergent defects in pavements systems.

The reflected radiation from the surrounding environment, the atmospheric absorption of radiation, the wind, the rain and the sunlight can affect the temperatures and this will make the infrared thermography more complex (Clark et al.2003)

2.5 LiDAR (Light Detection and Ranging)

LiDAR technology obtains details by illuminating an area using light from a near infrared region and then measures the time needed between the transmission of the signal and its reflection. LiDAR technology is used for mapping and for the creation of digital elevation models. One important advantage that LiDAR technology has is that it is not depended on the sun angle, so it can be used during the day and the night. Chang et al. (2005) have indicated in their research how LiDAR can identify holes and also how to estimate the volume needed for the fill material.

2.6 Terrestrial laser scanning (TLS)

Terrestrial laser scanning is used to evaluate the conditions of pavements systems. It is usually located on a vehicle and it combines a digital camera with a laser line scanner which can produce high resolution 3D pavements surveys. There are many researches about terrestrial laser scanning; Tsai, Jiang & Wang (2012) have achieved to identify cracks 2mm and greater in asphalt pavement systems. Tsai, Wu, Ai & Pitts (2012) have achieved to detect faults in the joints of concrete pavements with an error margin of less than 1mm.

Peng & Zhou (2011) used a laser scanning system to evaluate the pavement surface texture and skid resistance.

According to Tsai and Li (2012) terrestrial laser scanning can give high resolution, continuous transverse pavement profiles and it has no sensitivity to light conditions (night or shadow). But the high cost of the use of the terrestrial laser scanning instruments and hardware makes it cost prohibitive (Schnebele, 2015).

The chapter which follows will give all the information about the types of road and will explain the difference between paved roads and unpaved. Moreover it will explain the damages that each of the road type have.

3 Road types

The majority of people think that a road is consisted by one layer of asphalt or concrete that is established over the soil in order to create a soft surface to allow traffic pass over it (Schnebele, 2015). But in fact, a road is consisted by several layers of materials, which are selected-designed-constructed under several guidelines (Schnebele, 2015). According to Huang (1993) roads can be categorized as unpaved and paved, with paved roads usually classified as flexible, rigid or composite systems. In Cyprus, the majority of the roads could be characterized as flexible paved roads. The subsurface layer differs with the road type and can play major role in the performance and life of the road. It is vital to understand the typical road profiles before assessing the road conditions.

3.1 Unpaved roads

Basically unpaved roads are being constructed using a mix of gravel, which is placed over fine grained soil (clay or silt or combination of those two) and is being compacted. The fine grained soil may be naturally deposited as part of the geological cycle or constructed as a fill as part of an artificially constructed structure such as an embankment or on top of an earth retaining structure. These finer-grained soils form the foundation of the roadway and are referred to as the subgrade (Lay 2009). Moving on, the thickness and the type of gravel that will be placed over the subgrade will depend upon the availability of the material close to the construction site. For example, if the aggregate is too coarse then a fine grained aggregate will be mixed with the coarse aggregate in order to establish a smoother surface and to fill the voids. In addition, if the subgrade is consisted by soft soil then gravel with maximum grain size will be used to minimize the deflection. But according to Giroud (2002) ‘’ the thickness of the gravel layer is usually selected based on the local experience, although there are generally accepted unpaved road design methodologies’’.

Figure 1: Cross section of unpaved road Source: Schnebele, 2015

3.2 Paved roads

As it was stated above, paved roads are categorized as a flexible pavement system or a rigid pavement system; a composite pavement, according to Huang (1993), is the combination of both flexible and rigid pavement systems; usually Portland cement concrete is used at the bottom of the pavement system in order to provide a strong foundation and asphalt is used at the top of the system to provide a smoother surface. Flexible and rigid pavement systems are very similar; as both of them appear to have subgrade, sub base and base. The only difference between them is that in a flexible pavement the surface layer is made of asphalt and a binder and in rigid pavement the surface layer is Portland cement concrete. In general, despite the type, pavement systems are constructed with the highest quality materials on the top surface where traffic stresses are at peak (Huang 1993). As it was mentioned above the paved roads have subgrade sub-base and base; the sub-base is the most important layer as it is constructed to provide foundational support to the other layers. The sub-base can be constructed with three methods: 1. Improving the subgrade with compaction machines and placing a coarse aggregate on top of it; 2. Removing a section of the soft subgrade and replacing it with more suitable soil; 3. Adding chemical additives like tack coat and prime coat into the ground followed by compaction (Lay 2009). According to the research of Edil (2002) and Kim (2006), when a road needs reinforcement, then the use of geotextiles or resembling plastic material is taking place. Subsequently, the base layer, which acts as the drainage layer for the pavement system will be discussed. Empirically speaking, the base layer is constructed over the sub-base layer but according to Huang (1993) 'it can be placed directly over the subgrade if the subgrade soils are classified as competent for road construction' Wade (1997) and Buck (1977) stated in their research that is possible to use recycled concrete aggregates for the base layer without losing strength, and these recycled concrete aggregates can give the same performance to the pavement system.

Furthermore and as already mentioned, for flexible pavement system the layer above the base is consisted of a binder course, the binder course is a mix of large aggregates and asphalt and it has small thickness between 5 -10 cm. The surface course or wearing course is the last layer of the pavement system, the one that the traffic will pass directly over it. For that reason, the surface layer needs to be smooth and in the same time it needs to provide skid resistance.

Moving on to the rigid pavement systems the layer above the base layer will be the last one and it will be consisted by 15-30 cm thick Portland cement concrete. The surface of the rigid pavement is much stiffer than the surface of the asphalt pavement and is customarily constructed directly over the base course (Schnebele 2015). Schnebele develops the claim that in rigid pavement systems a form of reinforcement is needed. The reinforcement can contain elements such as dowels, wired mesh and deformed bars.

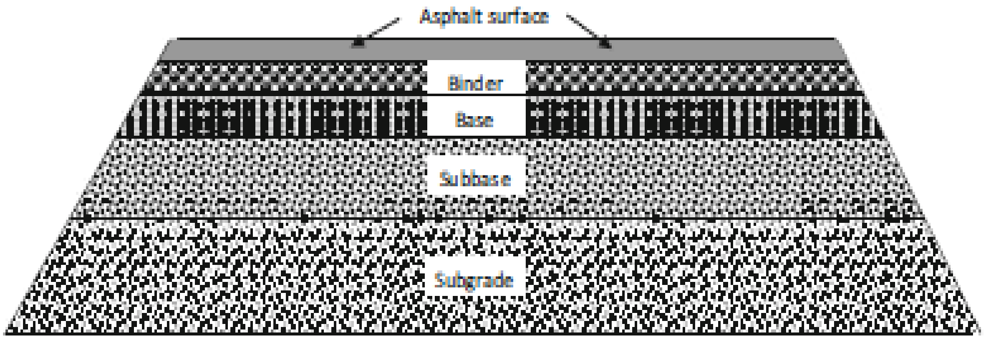

Figure 2: Cross section of flexible pavement system Source: Schnebele, 2015

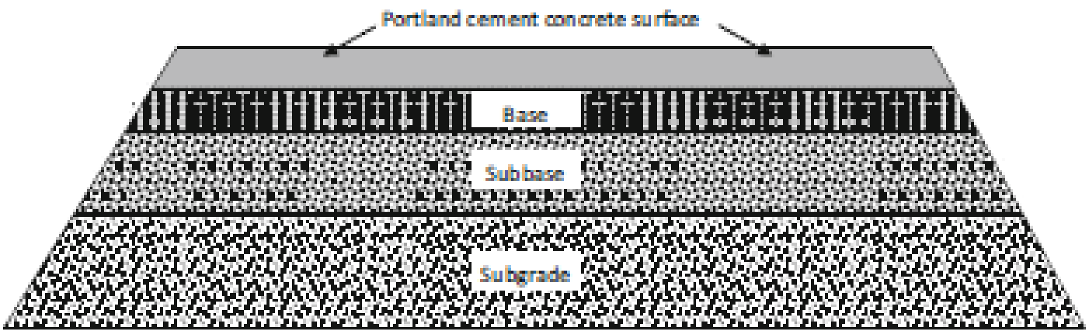

Figure 3: Cross section of rigid pavement system Source: Schnebele, 2015

3.2.1 Flexible pavement deformations and damages

Fwa (2006), Huang (1993), Sanrai (2000), Tsai & Li (2012) and Schnebele (2015) have researched about these deformations and damages which in fact affect the performance of the system; below there is a list of the most common deformations on flexible pavement system.

- Cracking: According to the researchers above there are two types of cracking common to the flexible pavement system: surface cracking and fatigue cracking.
  - Surface cracking derives from the aging and deterioration of the surface layer due to the shrinking and hardening. The applied load from the traffic has nothing to do with the surface cracking.
  - In addition the fatigue cracking is associated with the applied load from traffic and it usually appears along the vehicles wheel path. Fatigue cracking is known as alligator cracking because it resembles the alligator's skin. As Schnebele (2015) states 'Early signs can be detected from observations of fine parallel longitudinal cracks along the wheel-paths'.
- Shoving: these deformations are observed frequently in areas where the cars start and stop. It is the result of shear forces induced by traffic loads.
- Polished asphalt: This deformation is usually observed in roads with high traffic; the traffic takes away the sharp edges of the surface layer which will result in a much smoother and slippery surface and will impact the skid resistance.
- Bleeding of asphalt: This deformation appears due to the hot temperatures; the liquid asphalt migrates in hot temperatures along the pavement surface.

3.2.2 Rigid pavement deformations and damages

Moving on to the rigid pavement, and according to Chou & McCullough (1987) Faiz &Yoder (1974), Huang (1993), Wijk (1985) and Schnebele (2015) studies about the deformations that affect the pavement performance; the most common deformations on rigid pavements are:

- Cracking: researches have shown that there are four types of cracking for the rigid pavement; surface cracking, durability cracking, cluster cracking and diagonal cracking.

    - Surface cracking derives from the aging and deterioration of the surface concrete layer, it does not extend deep into the concrete slab.
    - Durability cracking forms adjacent to joints and cracks of the pavement and is initiated at the intersection of the cracks and a free edge.
    - Cluster cracking is associated with changes in conditions below the surface (settlement within the subsurface, poor drainage condition and high base friction). It is a closely spaced transverse cracking occurring in groups of three or more with space range between 150-650mm.
    - Diagonal cracking appears when an existing foundation has settlement or expansion and forms in a direction diagonal to the pavement centerline.
- Spalling: it is associated with a surface weakness within the concrete slab, if the spalling continues to progress and to deepen then it means that there is a structural weakness within the concrete slab. It forms a break or a crack of the slab edges within 0.5m of a joint.
- Faulting: It is created by a movement along a joint or crack which creates a difference in elevation. Faulting happens when the concrete slab losses its support due to erosion or settlement of the previous layers.
- Punch-outs: They appear when two closely spaced transverse cracks form an enclosed area alongside a short longitudinal crack and the edge of the pavement. It usually commence from the traffic load of the transverse cracks and by the corrosion of the steel within the concrete.
- Pumping: Water seeping in to the pavement system or ejecting the water out of the system through cracks or joints results in pumping. Inadequate concrete slab thickness is responsible for the pumping.

Following on, the next chapter provides background on remote sensing, it explains what remote sensing is and it will review recent literature on the same topic stating out the procedure of each research and the outcomes.

4 Background of Remote Sensing

4.1 Overview of remote sensing

As it is all known, the sun is the main source of energy. The energy that the sun produces is the electromagnetic radiation (Schnebele 2015). The electromagnetic radiation travels in the form of waves which are absorbed, reflected or scattered by the Earth's surface. According to Schnebele (2015) 'the amount of energy emitted or absorbed by an object is a function of temperature, and every object with a temperature above 0 degrees Kelvin emits electromagnetic radiation'. Electromagnetic radiation takes many forms, such as microwaves, X-rays, radio waves and gamma rays. Microwaves are located in the range of the electromagnetic spectrum between radio and Infrared. They are used for high bandwidth communications, radar and as a heat source in the industrial applications. X-rays are categorized into two categories: soft X-rays and hard X-rays. Soft X-rays are located in the range of the electromagnetic spectrum between the UV and the gamma rays. Hard X-rays are in the same position as the gamma rays in the electromagnetic spectrum but they differ in their source. Radio waves are at the lowest range in the electromagnetic spectrum. They are used primarily for communications which includes voice, data and entertainment media. Lastly the gamma rays as mentioned earlier are located above the soft X-rays in the electromagnetic spectrum. Their use is very important as they can kill cancer cells, when applied in measured doses. But an uncontrolled exposure is very dangerous to humans.

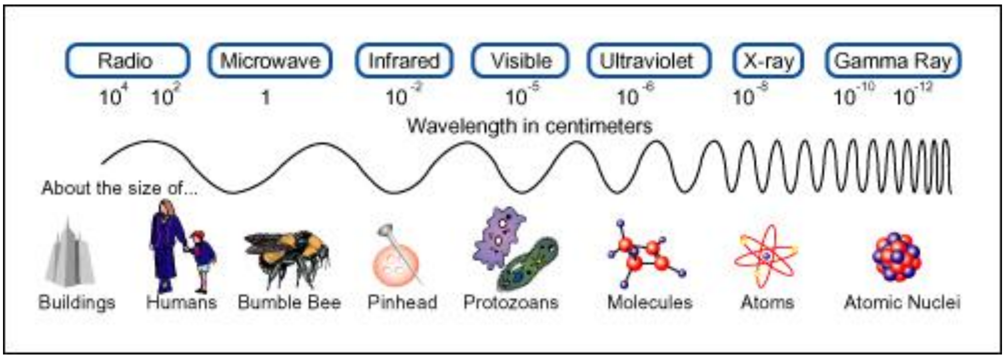

Figure 4: The Electromagnetic Spectrum Source: NASA

Moving on, scientists can gather information when they utilize the several regions of the electromagnetic spectrum. The most common method of remote sensing for pavement analysis is to collect data from the visible spectrum, such as photographs (Schnebele 2015). Moreover, remote sensing techniques such as hyperspectral imagery and laser scanner can identify and locate deformations, much quicker than other techniques. Sensors are installed on various platforms which gather the electromagnetic radiation emitted or reflected from the object.

4.2 Recent literature on remote sensing

This section will provide academic background to the research. Similar researches with this one are summarized below stating the methods that were used to obtain data and the results that were extracted from the researchers.

According to the research of Mei (2012)' recent advances in imaging spectrometry provide the possibility to detect physical and chemical properties of materials at very detailed level. There is evidence that road properties, such as aging and material composition, can affect spectral characteristics even if it is still an open question to quantify the relationship between reflectance values and specific road surface characteristics.' Mei (2012) used spectroradiometric measurements in order to characterize aggregates and asphalt mixtures that are being used for the construction of a pavement system. The use of spectroradiometric data to characterize aggregates and bituminous mixtures can lead to improve remote sensed image analyses. Measurements were taken in the wavelength range between 350-2500nm from samples that have different compositional characteristics. The researcher concludes to the following results:

1. It is possible to apply spectoradiometric analysis to aggregates and asphalt mixtures in order to evaluate physical characteristics. (lithology, porosity and water content)
2. The radiometric surveys can check the composition of bituminous mixtures and aggregates with success.

3. The field radiometric survey can be an effective tool to evaluate pavement surfaces that need maintenance.
4. Spectroradiometric analysis can be used to create a new efficient road classification procedure.

Moving on, a similar research has been done by Alexiou et al. (2010), they investigated asphalt road conditions with the use of hyperspectral remote sensing. According to Alexiou et al. (2010) 'Advances in hyperspectral remote sensing technology have shown capabilities to derive physical and chemical material properties on a very detailed level'. The researchers took high quality spectral measurements with the GER1500 radiometer in order to create a spectral library. The spectral library contained roads with difference in age and roads with the same age. After the analysis of the spectral signatures and the processing methods that were used to detect the road conditions, the researchers concluded to the following results:

1. The three parameters that affect the pavements condition and its reflectance are the quality, road circulation and age.
2. New paved roads have low reflectance which is controlled by the asphalt's chemistry.
3. The old and worn pavements are observed with a significant increase in reflectance but in contrast, an old pavement with good quality does not have significant increase in reflectance.
4. Circulation accelerates the deterioration of the pavement.
5. Pavements with high reflectance are observed to have cracks but, due to their structure and the local increase of hydrocarbon absorption the percentage of the assessed reflectance is being reduced.

These results provide confirmatory evidence that hyperspectral remote sensing is capable of mapping road conditions.

Additionally, Noronha et al. (2002) have undertaken a research similar to the ones explained above. To explain, the researchers prefer to use spectroscopy and hyperspectral remote sensing in order to assess condition of the pavement system and to obtain the road centreline. As Noronha et al. (2002) state in their research remote sensing could be characterized as quick and low cost methods to examine the road centreline condition and extraction. In order to develop a spectral library of the materials, the researchers used a 224 band AVIRIS hyperspectral imagery, a 4m imagery and about 6000 field gathered spectra. To analyze the spectral library and the remote sensing data, the researchers used the public domain program MultiSpec which can process and analyze high dimensional and hyperspectral remote sensing data sets (Landgrebe and Biehl 2001). The researchers use the Bhattacharyya distance as a separability measure, which according to the recent literature it is a useful measure of separability of band prioritization to decrease the dimensionality of hyperspectral data sets and to select the most appropriate spectral bands for data analysis (Chang et al 1999). Finally the researchers concluded to the following results:

1. The analysis of the AVIRIS data can be said that is successful but still it has some errors. It may be possible to improve the success of centerline extraction and recognition using contextual object oriented image classification which are based on geometric morphology, topology and elevation data from sensors like LiDAR.
2. It is proved that it is possible to map pavement type and condition. The age of the pavement can be determined.
3. The pavement's health is not detectable in 4 m imagery.

Lastly the researchers' recommends that a sensor needs to be designed with lower spectral resolution for the reason that much of the discriminating ability of hyperspectral remote sensing is located within a few wave bands.

Similarly, Herold et al. (2004) in his research uses remote sensing to map urban road infrastructure. The researcher developed a comprehensive regional spectral library with measurements that were taken with a field spectrometer and from high resolution remotely sensed data. The spectral library was used to analyze the spectral properties of the materials of the pavement (type, age and condition). The primary method that was used in this research is the Bhattacharyya distance. Bhattacharyya distance can calculate the statistical distance between two Gaussian distributions (Kailath, 1967) and incorporates first and second order statistics. Then the data were classified using a maximum likelihood classification algorithm. The analysis of the data has shown that:

1. It is possible to describe general pavement age and surface deformations.
2. The quality parameters of the pavement are undetectable at spatial sensor resolutions of 4 m.
3. The problems in spectral classification of road surfaces are related to generic spectral similarities with asphalt road materials.

In addition with the studies that were explained above the study below is about rigid pavement system. There are not many studies about the rigid pavement systems for the reason that, the most common type of pavement that is being used is the flexible pavement.

Martin Herold University of Santa Barbara has developed and analyzed a spectral library from 350 nm to 2500 nm in order to investigate the spectral complexity and spectral characteristics of urban environments. Field spectra were acquired with the use of a full range spectrometer. The spectral library that was created contained more than 4500 individual spectra. The Bhattacharyya distance was used to calculate the statistical distance and to choose the most appropriate spectral bands for data analysis. This research concluded to the following findings:

1. Rigid pavement systems have higher reflectance than the flexible pavement systems.
2. Rigid pavement systems materials are comprised of cement, gravel, water and various other ingredients. Significant absorptions appear in the shortwave infrared due to calcium carbonate with a feature at 2300 nm for calcite and at 2370 nm for dolomite.
3. The reflectance of rigid pavement systems decreases as the age of the system increases.

5 Methodology

5.1 Research Methodology

Research methodology can be defined as a systematic and ordinal approximation obtained regarding the collection and analysis of data in order to that information can be achieved from those data (Jankowicz, 2005). Generally, methodology is the procedure where the researcher uses some basic methods in order to collect data for the research. This chapter will focus at the research methodology that was used in the context of this research. Moreover, this chapter will justify the methods that were used to collect data and the process that was followed in order to complete the investigation

5.2 Study Area

The study focused in the Limassol urban area; three sets of data were taken from one parking lot (flexible pavement), four sets of data were taken from two concrete walkways and two sets of data from a road with an average low traffic (flexible pavement).

Each data set is consisted from measurements that were taken over areas with cracks/deformations (cracked) and areas with no cracks/deformations (un-cracked). The locations that were measured are shown in the table below. Pictures of the cracked areas of each pavement system are shown in the Appendix A.

Table 1: Pavement systems information

Name: construction date	Type	Latitude	Longitude
3 years (Set1)	Rigid	34°40'18.43	33° 2'40.54
3 years(Set 2)	Rigid	34°40'18.05	33° 2'39.92
5 years (Set 1)	Rigid	34°40'14.86	33° 2'28.91
5 years (Set 2)	Rigid	34°40'15.02	33° 2'29.08
10-15 years (Set 1)	Flexible	34°40'25.55	33° 2'19.87
10 -15years (Set 2)	Flexible	34°40'25.20	33° 2'19.98
10-15 years (Set 3)	Flexible	34°40'24.79	33° 2'20.18
20-30 years (Set1)	Flexible	34°40'30.02	33° 2'21.83
20 -30years (Set 2)	Flexible	34°40'29.82	33° 2'21.63

* the coordinates of the pavement systems were acquired from Google Earth

5.3 Data acquisition

The measurements that were obtained were with the use of the field spectroradiometer HR1024. This spectroradiometer can detect reflectance within the wavelength range of 350 – 2500 nm. The lense that was used on the spectroradiometer was 4°. The measurements that were taken from the area with no cracks were taken with the spectroradiometer approximately 1 meter from the ground and in addition the ones from areas with cracks were taken with the spectroradiometer to be at 0.3 meter from ground. Furthermore the field spectroradiometer is very sensitive so when it is used, any movement of the handler is going to be visible in the measurements as noise. Also any other noises from the vehicles passing or the surrounding environment might affect the measurements. To add, the spectroradiometer will have measurements that will be distorted or absorbed as a result of the atmospheric absorption. Atmospheric absorption occurs when gases that comprise the atmosphere such as water, carbon dioxide and ozone, absorb radiation in some wavelengths while at the same time allowing radiation of different wavelengths to pass through them. The wavelengths that are absorbed by these gases are called absorption bands. The absorption bands in the data sets this research are between 1850-1940 nm and between 2280-2500nm. The figure below shows the wavelengths at which electromagnetic radiation will penetrate the atmosphere.

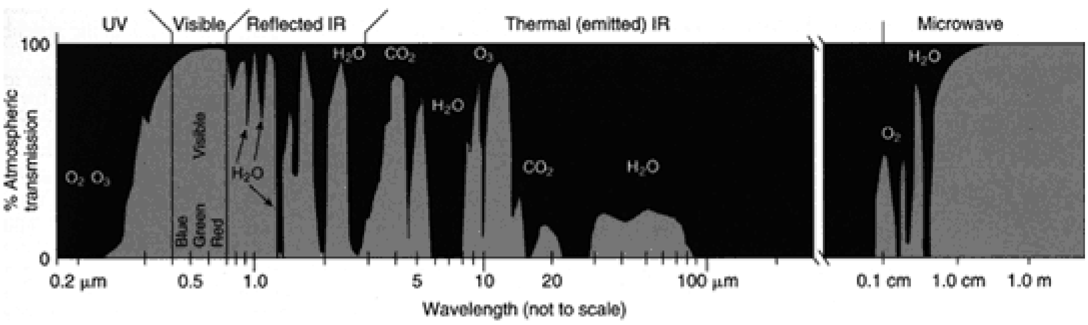

Figure 5: Atmospheric absorption bands. Source: NASA

5.4 Data processing & analysis

In order to process the data and to analyze them, several graphs were plotted so to be able to observe how the reflectance of the pavement systems reacts with the age. Moreover graphs with the range of the wavelength were plotted to study the range between the pavement systems. Statistical analysis was used and more specifically the T- test was established in order to examine whether there is significant difference between the healthy pavement systems and the ones that had cracks/deformations. The utility of T – test is that it can compare the actual difference between the two data sets. After the completion of the T-test a correlation analysis was performed to examine the data from the spectroradiometer. To be accurate the Pearson correlation coefficient was used. This correlation coefficient is a measure of the strength of linear relationship between two variables. It draws a line of best fit and the observer can with ease observe how far the data points are to this line.

Moving on, after the completion of the Pearson correlation coefficient, the Euclidean distance was used in order to identify spectral regions which are able to distinguish the spectral diversity of the pavement systems due to cracks. In simply words Euclidean distance is the distance between a pair of observations.

Lastly, after the Euclidean distance a spectral experiment took place. To undertake this spectral experiment the HR1024 spectroradiometer was used on a flexible pavement system (20-30 years) in an area of 2m x 0.7m. Measurements were taken for every 10 cm along the 2m line and it was repeated 7 times in order to cover the necessary area. This procedure was repeated two times in order to have two data sets. The figures below show the actual cracks and a diagram of the cracks showing at which points the measurements were taken. The first crack which is a vertical one appears on the 80^{th} cm along the 2 meter line, which is approximately the 8^{th} measurement. The second crack which is a horizontal one appears on the second repetition of measurements. The reason that this experiment needed to be carried out was to see whether the cracks are visible in curtain wavelengths. These curtain wavelengths were determined from the Euclidean distance results. Then with the use of Surfer, which is a program that can produce grid maps, diagrams and contours maps, diagrams of those wavelengths will be plotted in order to see whether the cracks are visible or not. To explain, when the analysis of the measurements and the statistical analysis of the sets taken from rigid and flexible pavement systems are completed, wavelengths are going to be generated. These wavelengths are the ones that were used to produce the diagrams and to check whether the cracks are visible or not. Also it is noted that there is not any background research on this experiment as this research is the first that will try to undertake it.

Figure 6: Actual cracks

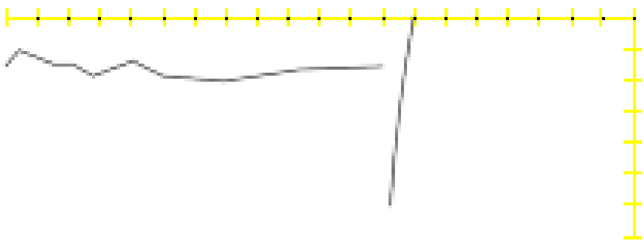

Figure 7: Diagram of cracks

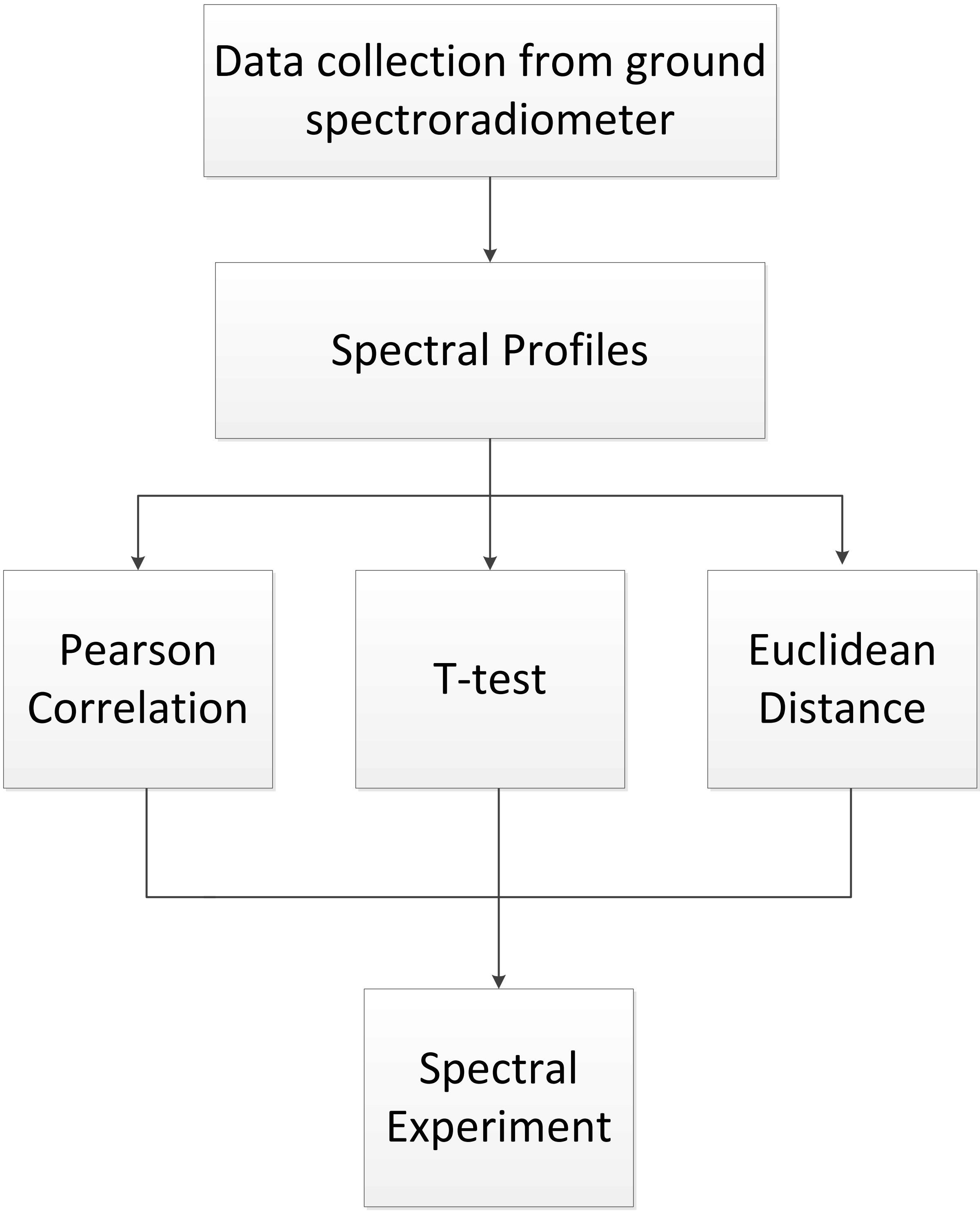

Figure 8: Flowchart of research methodology

6 Data analysis and discussion

6.1 Spectral profiles

This chapter will first present the data that were obtained from the HR 1024 spectroradiometer in a graphical manner. Later on, the statistical tests that were applied will be analyzed and discussed alongside with the findings.

The measurements from the spectroradiometer were categorized according to the data sets that were taken. The mean and standard deviation were calculated for the observations that each wavelength had from 350 nm to 2500nm in order to be able to show the range of each data set. When there is a small range it means that the standard deviation for the specific pavement system is small, which shows that the measurements that were taken are with no errors and the age of the pavement has not affected the measurements. In addition when there is high range it means that there is high standard deviation in the pavement system which shows that the age of the pavement system has affected the measurements.

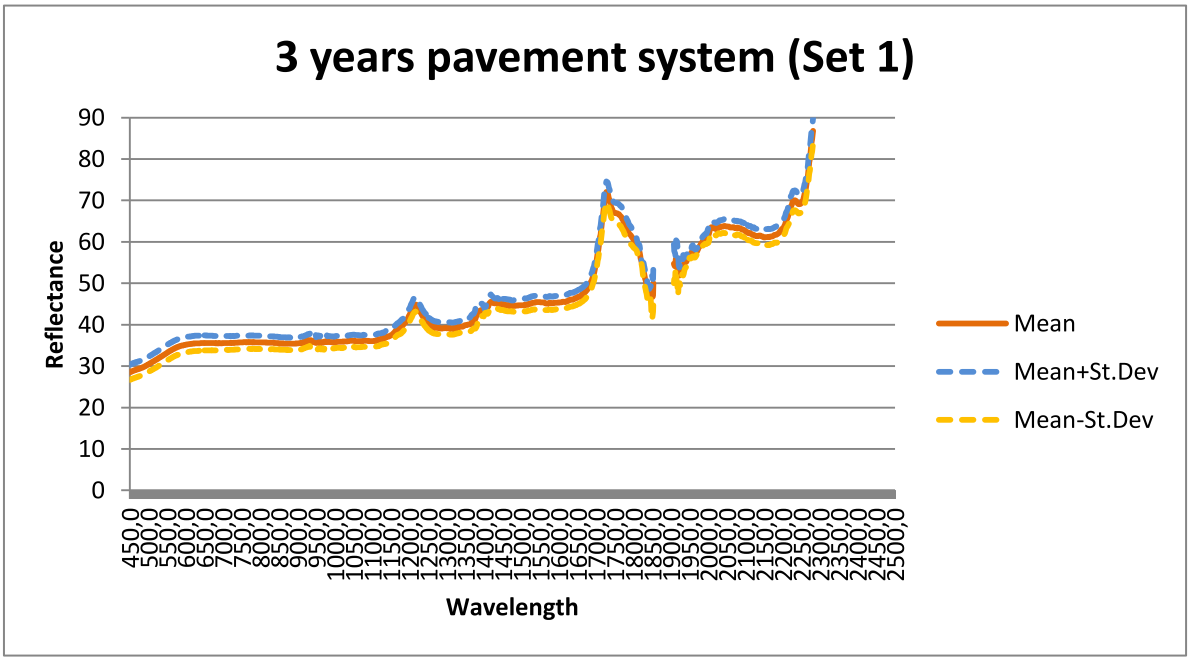

Figure 9: Range of the 3 years pavement system (Set 1) –Un-cracked (Rigid pavement system)

The data set 1 contains the measurements from a rigid pavement system with relatively low use. As it can be observed from the figure above, the range is relatively small between 450nm-1305nm which means that the measurements until that wavelength have no errors. The range increases between 1305nm – 2500 nm with the biggest increase located between 1590 nm to 1818 nm. This is probably because of the atmospheric absorption.

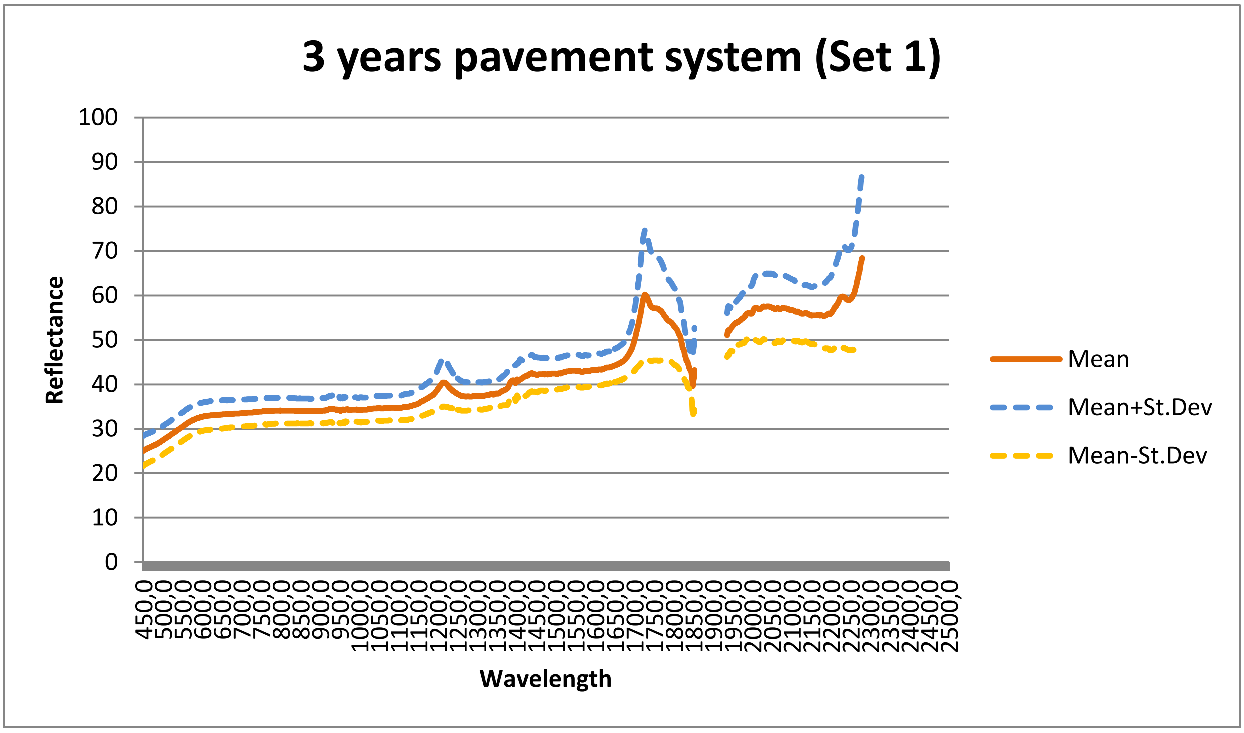

Figure 10: Range of the 3 years pavement system (Set 1) – Cracked (Rigid pavement system)

The figure above shows the measurements of set 1 which concerns the area with cracks. In this case, it is observed that the range of this data set is better than the previous, as it has a small range in almost every wavelength. Again between the wavelengths 1590 nm to 1818 nm it is observed an increase in the range which is probably a result of the atmospheric absorption.

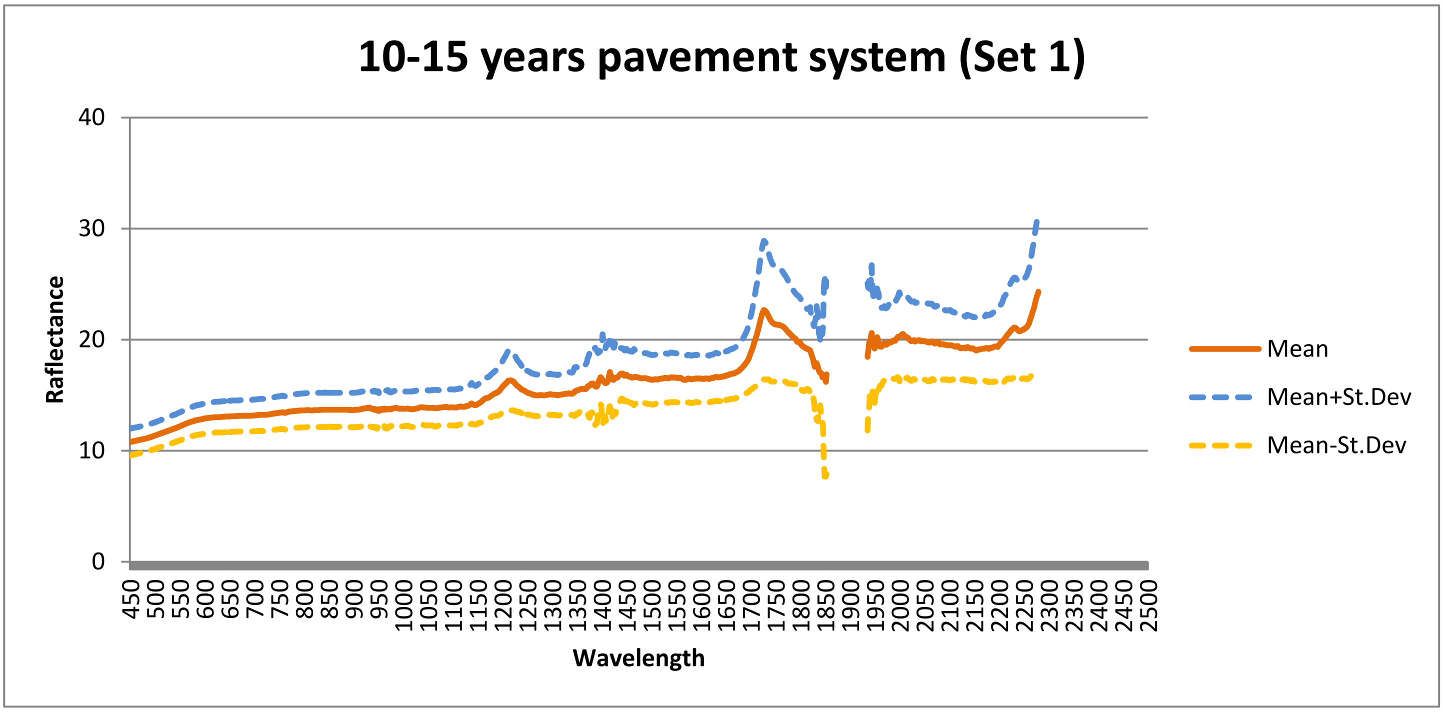

Figure 11: Range of the 10-15 years pavement system (Set 1) – Un-cracked (Flexible pavement system)

These measurements were taken on a flexible pavement system. That can be easily observed as the reflectance of the flexible pavement system is lower than the reflectance of rigid pavement system. It can be said that the range of flexible pavement system is better than the one of rigid pavement system, because the range is small throughout the wavelengths. Between the 1590 nm to 1818 nm an increase in the range is distinguished but in addition with the rigid pavement system it is not a big increase.

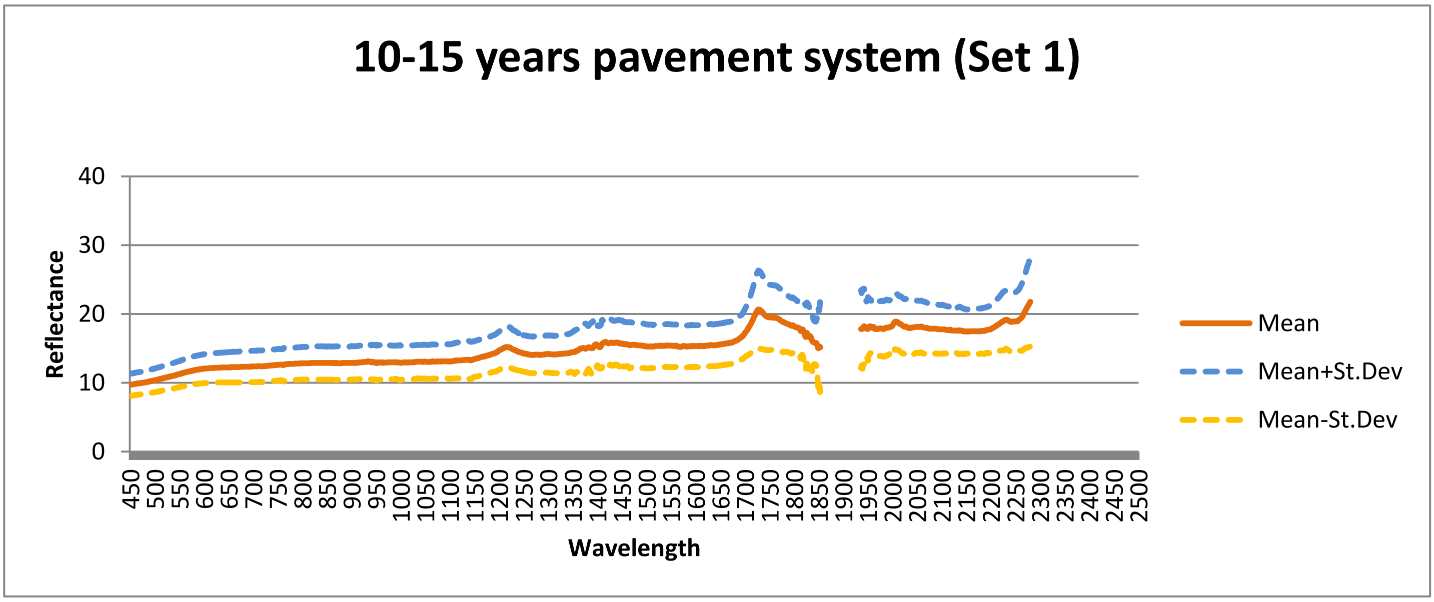

Figure 12: Range of the 10-15 years pavement system (Set 1) – Cracked (Flexible pavement system)

The range of this set which concerns the area with crack is small and it is close to the mean line which means that the measurements are good. Even between the wavelengths 1590 nm to 1818 nm, where atmospheric absorption happens, the range is relatively small compared with the other graphs.

The remaining spectral profiles of the flexible pavement system and the rigid pavement system are shown in the Appendix B as the range has the same attributes as the ones explained above.

After the completion of the spectral profiles with the range, it was found reasonable to compare the data sets between them and to discuss the outcome. Several graphs were plotted with data sets of the same material and the range. First this paper will present the graphs regarding the flexible pavement system and then the graphs of the rigid pavement system.

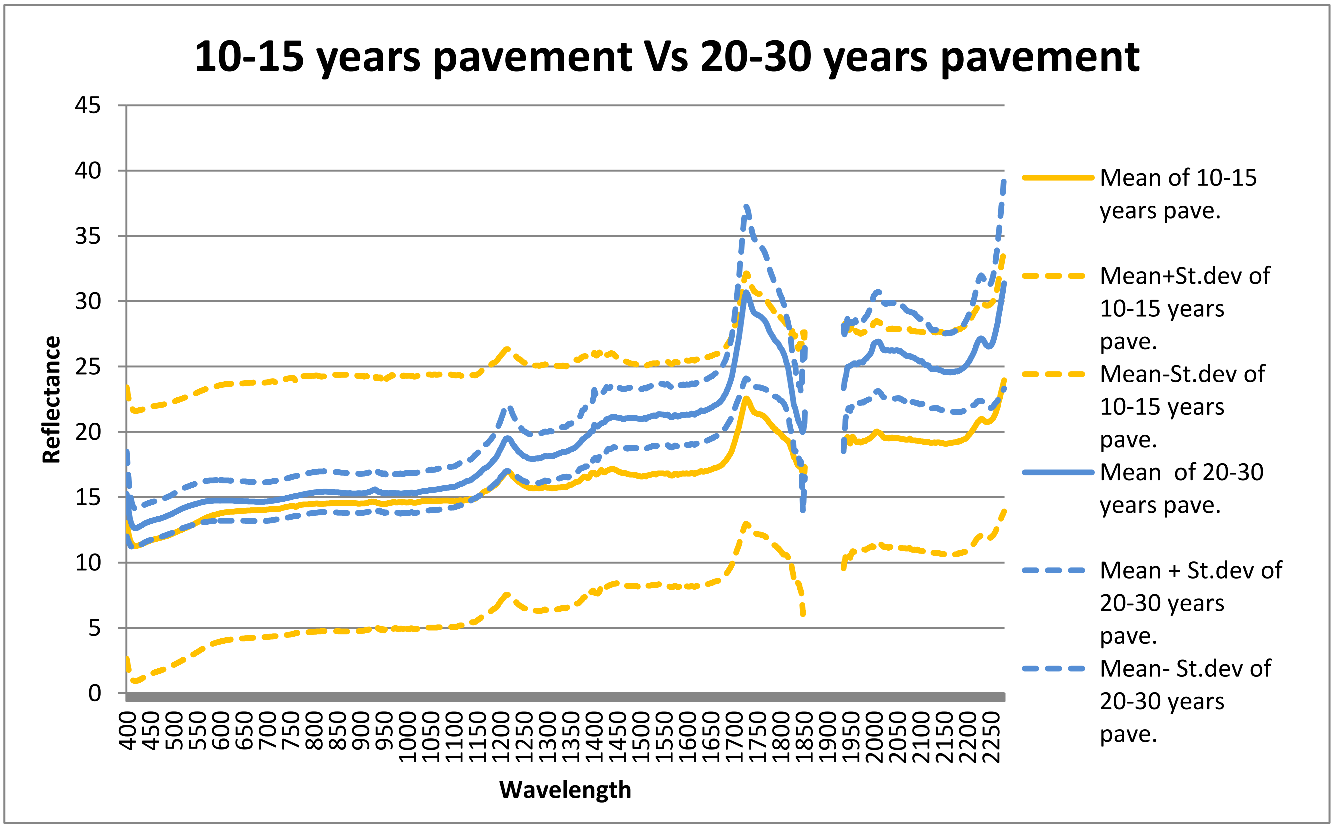

Figure 13: Range of 10-15 years flexible pavement Vs Range of 20-30 years flexible pavement – Un-cracked

To plot this graph, the average of the reflectance on each wavelength was calculated for both the flexible pavements in order to have a more specific view of the measurements. As it can be observed above, the range that the 10-15 years pavement system has is very big, in addition with the range of the 20-30 years pavement system which is relatively small and better. The outcome that can be expressed for this graph is that the measurements of the pavement 20-30 years are far better than the ones of the pavement 10-15 years, which was not expected.

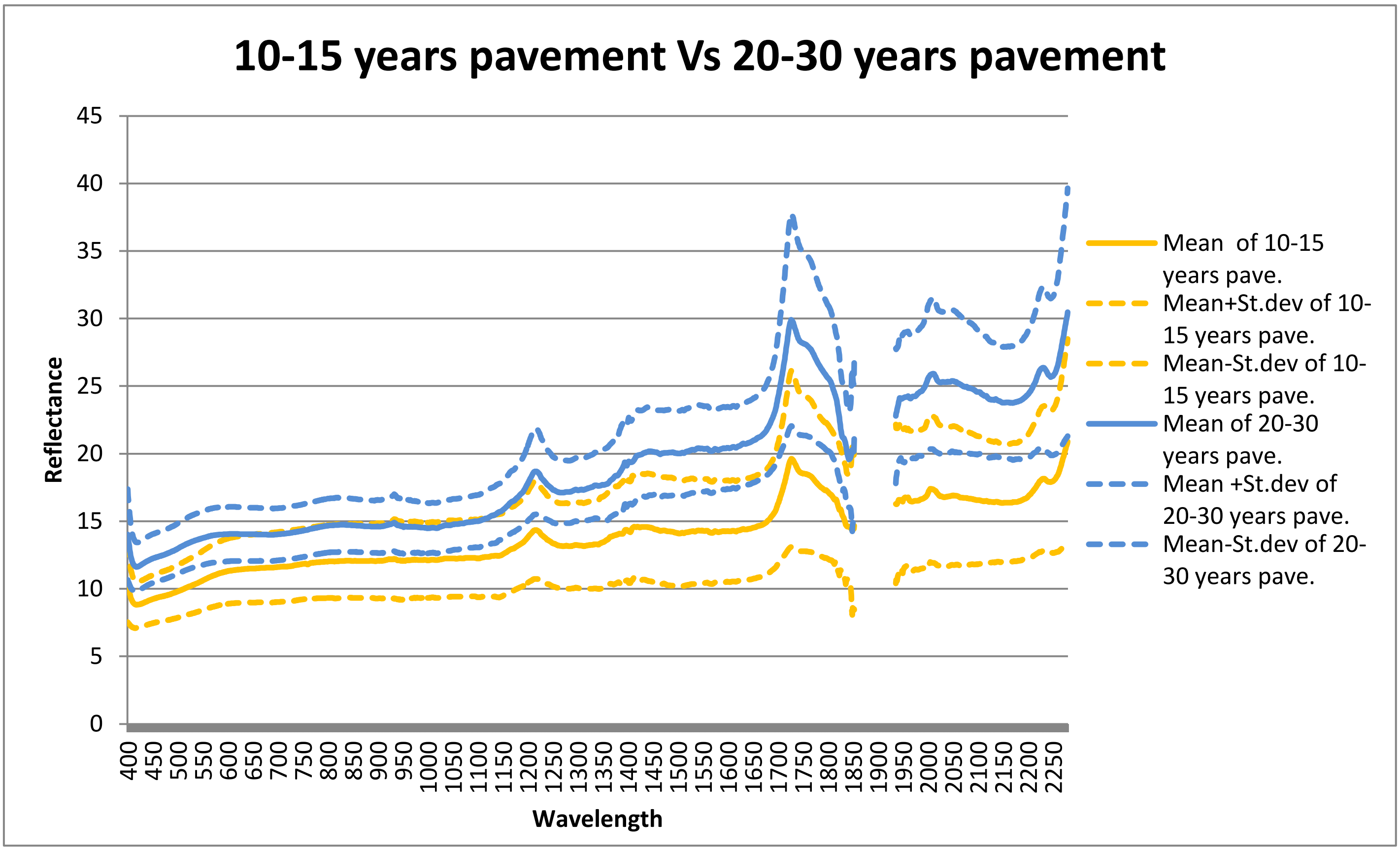

Figure 14: Range of 10-15 years flexible pavement Vs Range of 20-30 years flexible pavement – Cracked

In this graph the range of the 10-15 years pavement is small in addition with the one for the un-cracked so it can be said that the measurements that were taken for the crack are better than the ones taken for the un-cracked. To add the range of the 20-30 pavement system is small as previous which means that all measurements taken for this pavement un-cracked and crack have small standard deviation.

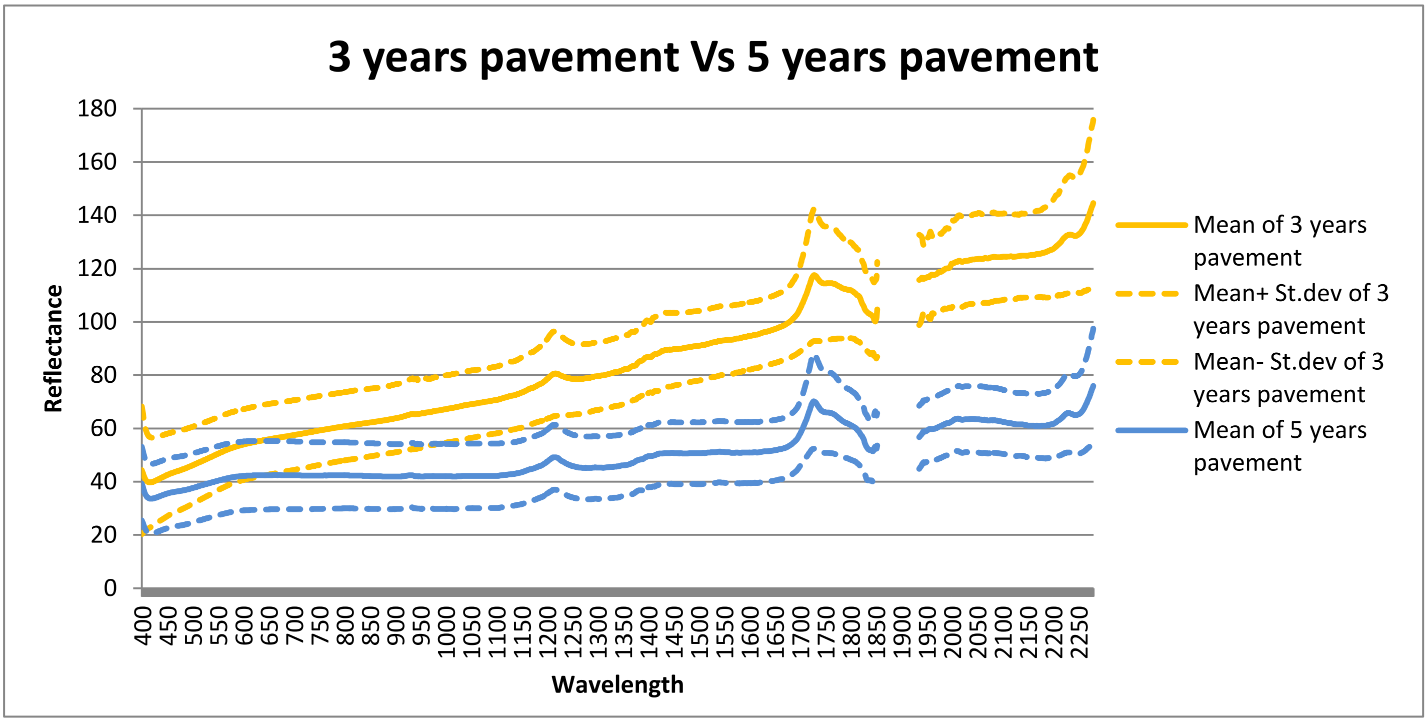

Figure 15: Range of 3 years rigid pavement Vs Range of 5 years rigid pavement – Un-cracked

The 3 years rigid pavement shows an increase in the reflectance as the wavelengths increases but its range is relatively small. In addition the 5 years rigid pavement does not have this increase in the reflectance. The reason that the 3 years rigid pavement presents this increase in its reflectance it is probably due to the fact that it is located near the sea. Factors like humidity and corrosion are playing a vital role in the increase of the reflectance.

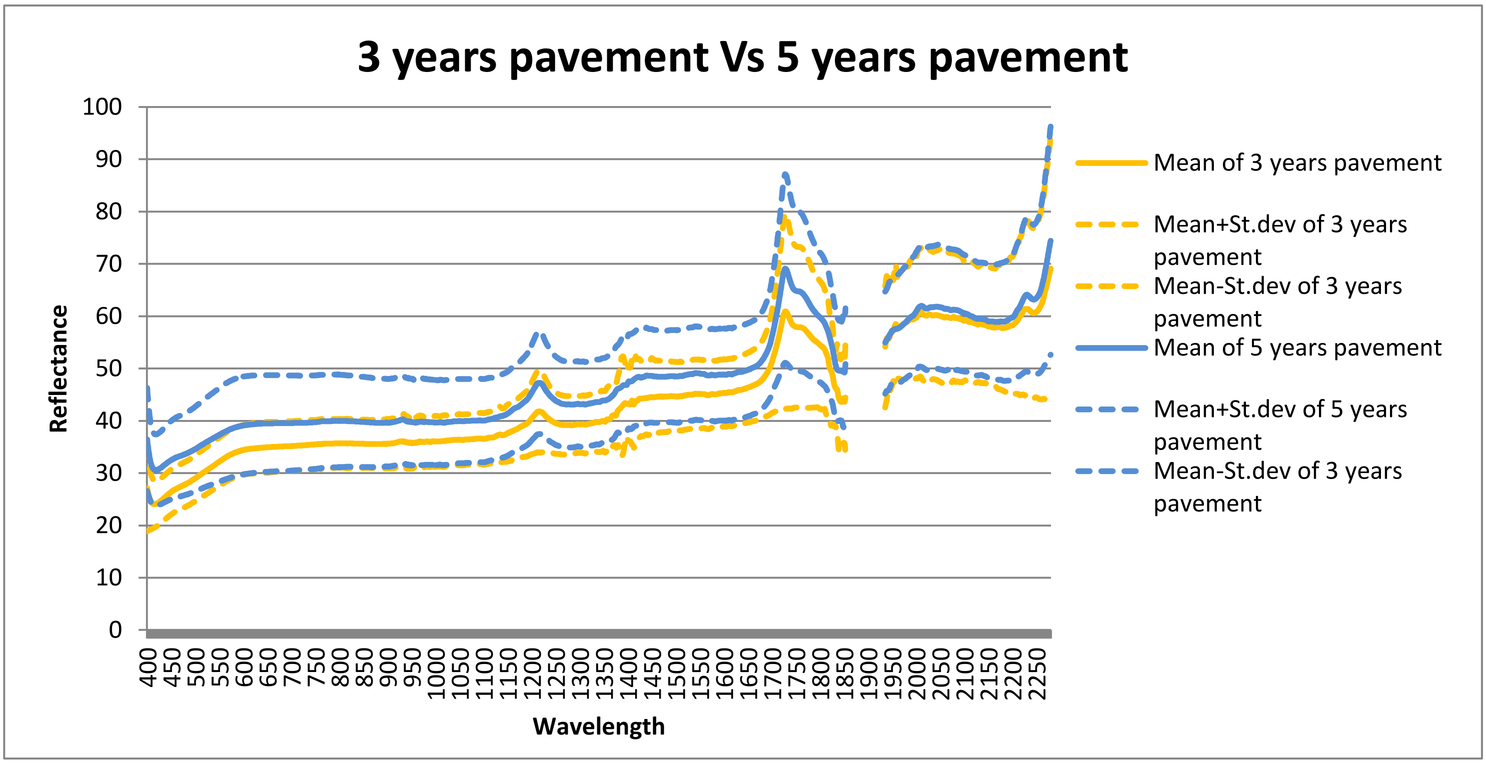

Figure 16: Range of 3 years rigid pavement Vs Range of 5 years rigid pavement – Cracked

In addition with the range of 3 years rigid pavement for the un-cracked area, the measurements that were taken for the crack area seems to be far better than the ones in the un-cracked area. The reflectance does not increase as previous and the range is small. The 5 years rigid pavement has a good range, and its reflectance values are higher than the 3 years rigid pavement.

Moving on, graphs were plotted to compare the un-cracked vs. cracked in the same pavement system. To plot these graphs, all the sets that were taken for each pavement system were added together in order to have a more general view of the pavement system.

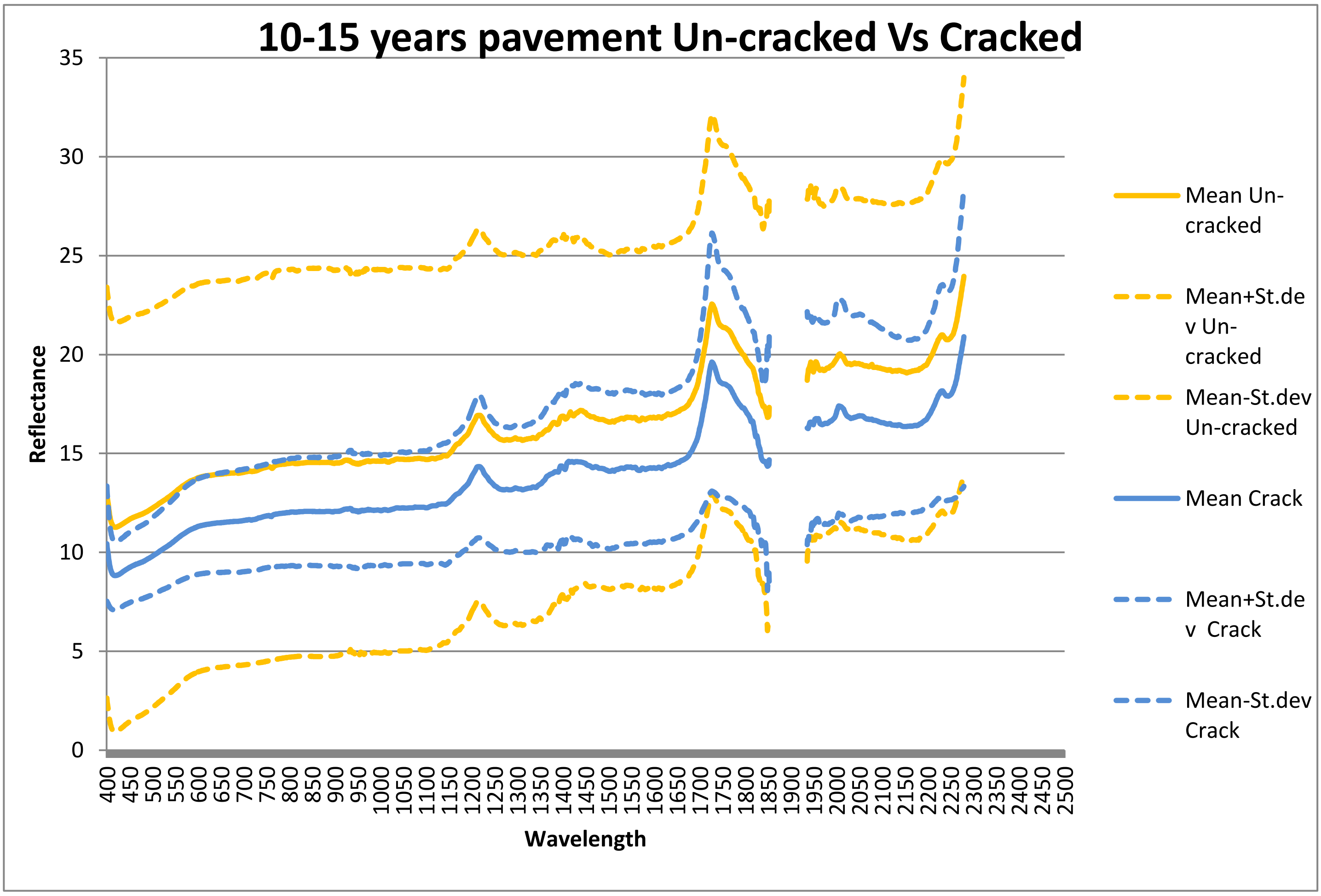

Figure 17: 10-15 years flexible pavement system Un-cracked Vs Cracked

In this figure, it is observed that the measurements for the un-cracked area are not good as the range is too big, this can be said with certainty as this flexible system in all the graphs that were plotted has a big range for the un-cracked area. In addition, the cracked area is small and has better measurements. It is distinguished that the areas with cracks have better range and lower values of reflectance.

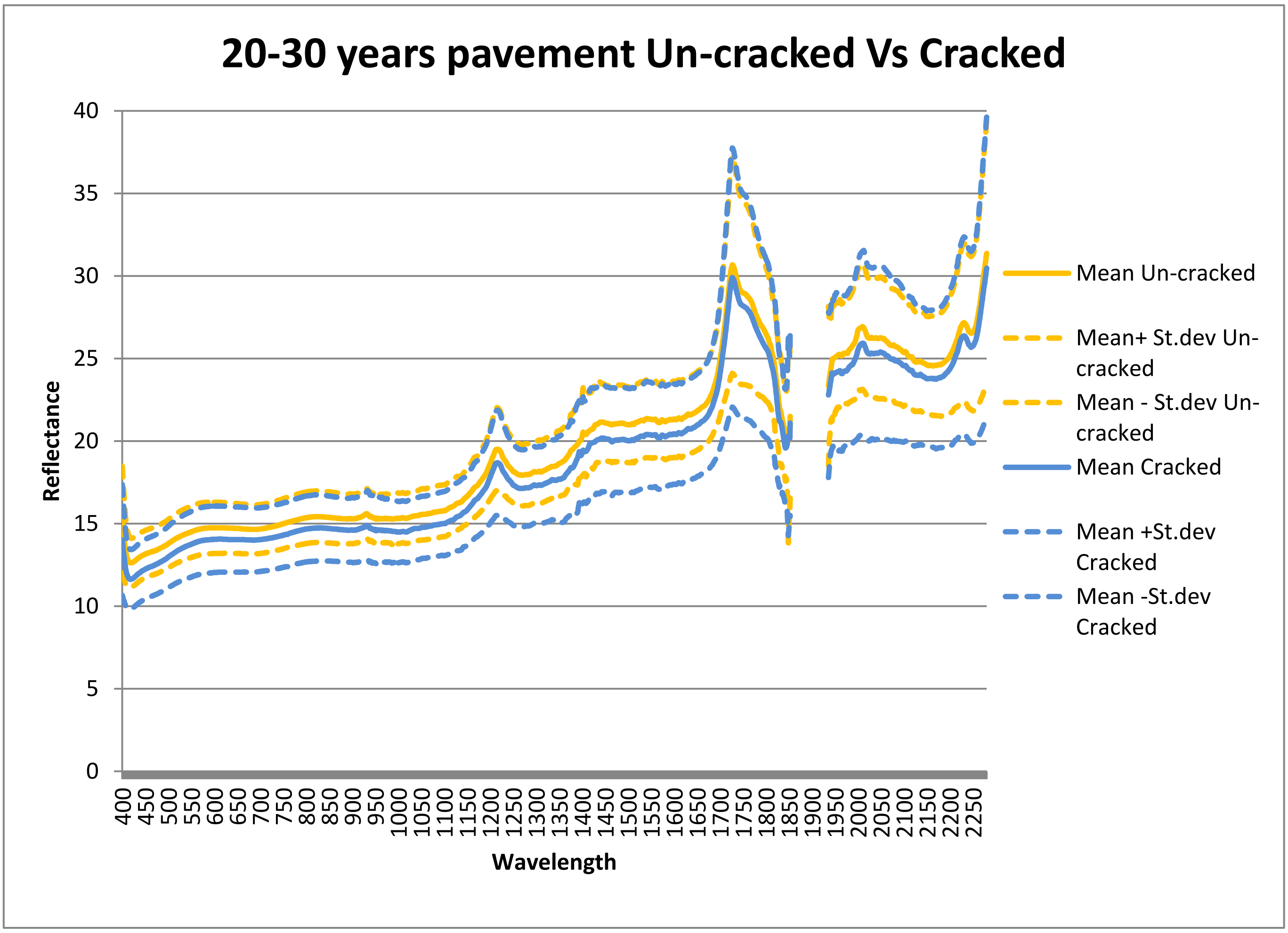

Figure 18: 20-30 years flexible pavement system Un-cracked Vs Cracked

When comparing figure 9 and figure 10 it can be observed that the 20-30 years flexible pavement has better range for the un-cracked areas and for the crack areas as well. Also it can be said that the oldest the road is then the higher reflectance it gets. This can be observed clearly through the graphs above. Lastly, the mean reflectance of the un-cracked area is nearly the same as the mean reflectance of the crack area, in addition with figure 9 where the mean reflectance of the crack area presents less reflectance than the mean reflectance of the un-cracked area.

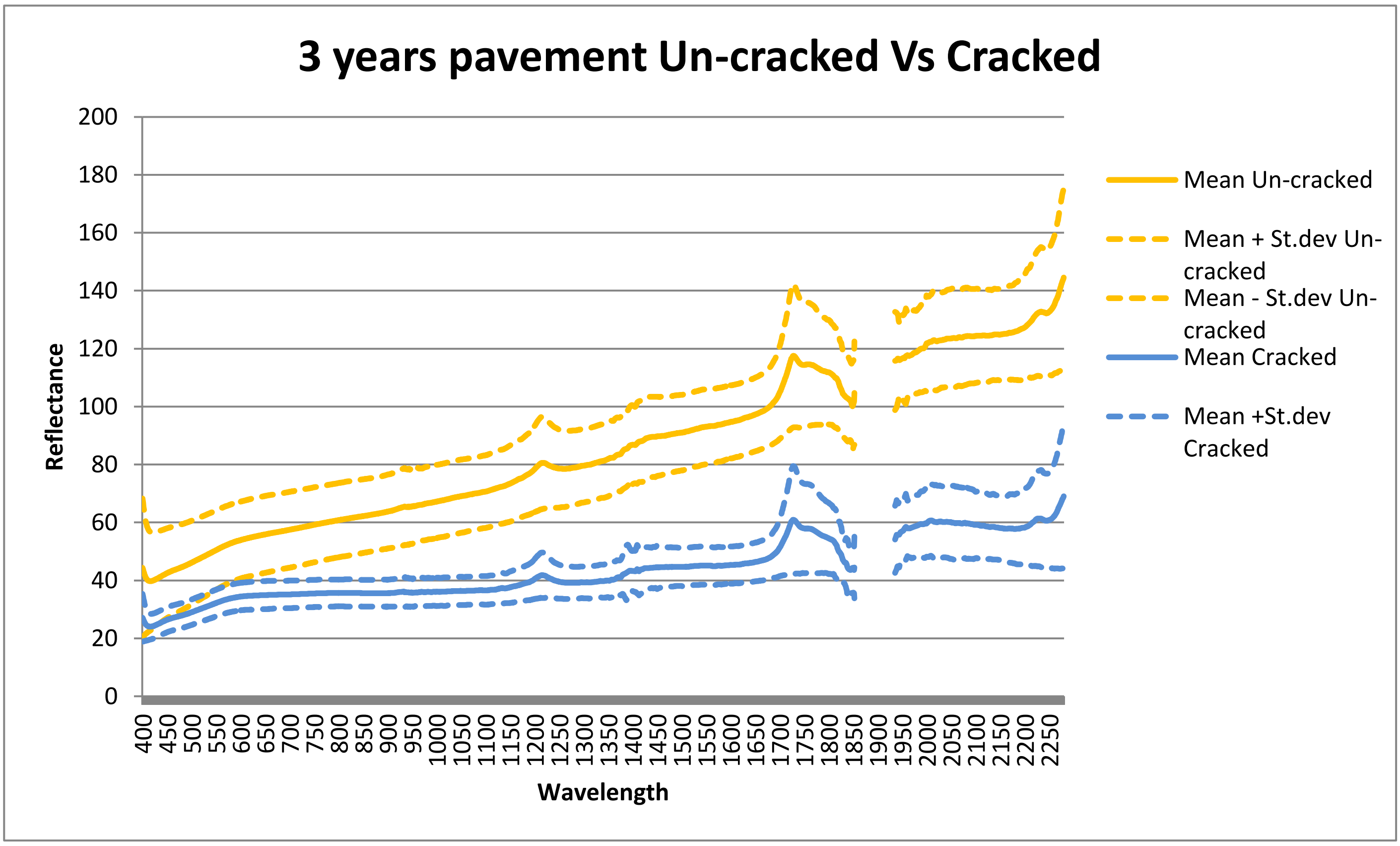

Figure 19: 3 years rigid pavement system Un-cracked Vs Crack

The above graph shows that the range for the un-cracked area is big and an increase in the reflectance as the wavelength increases. These two observations are not applicable for the cracked area as it has a good and small range and its reflectance does not increases.

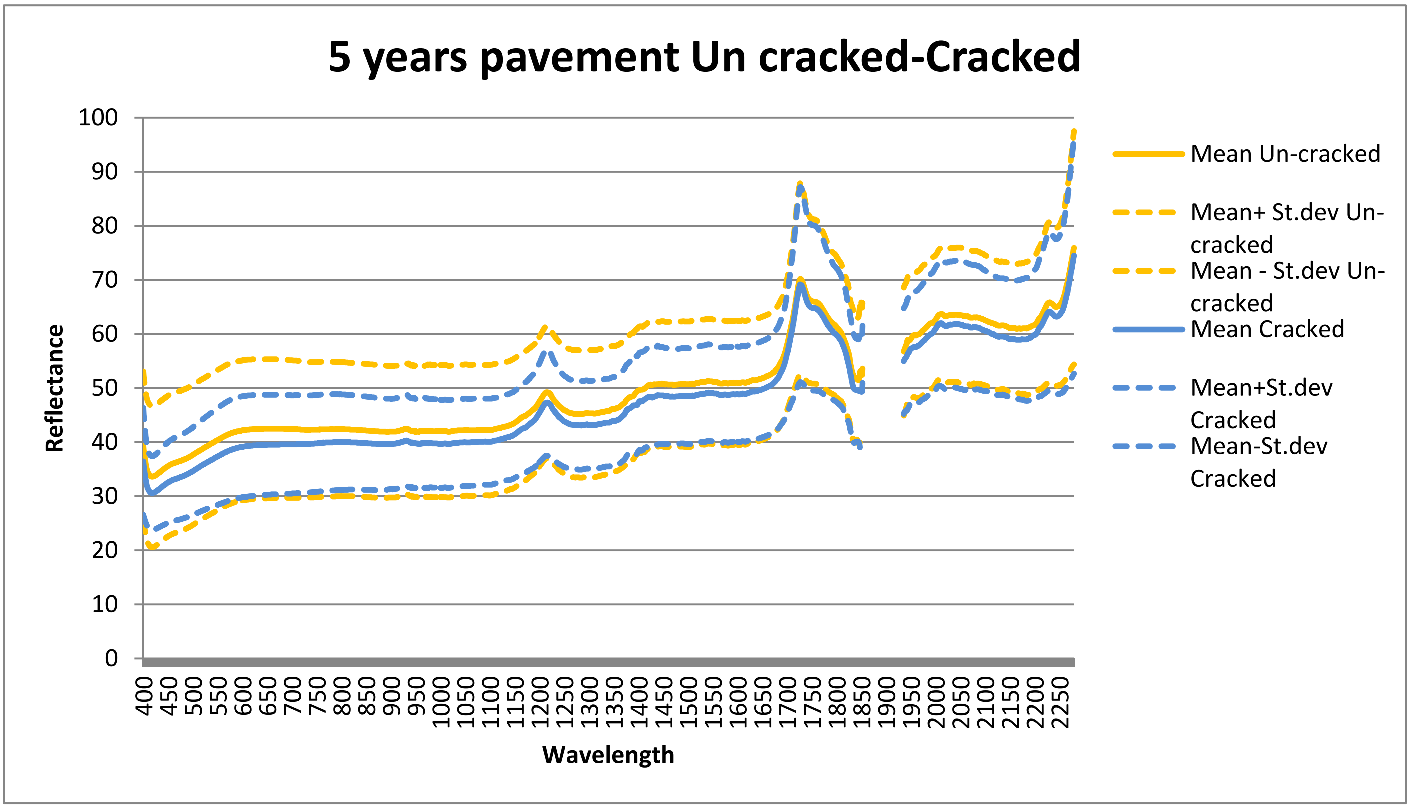

Figure 20: 5 years rigid pavement system Un-cracked Vs Crack

When comparing figure 11 with figure 12 it is observed that the 5 years rigid pavement system shows better values of reflectance than the 3 years rigid pavement system. Moreover it is noted that the reflectance of the oldest road is higher than the new one.

Lastly this paper will present two graphs for each pavement type with a comparison between un-cracked and cracked and one graph with the mean values of all the pavement systems.

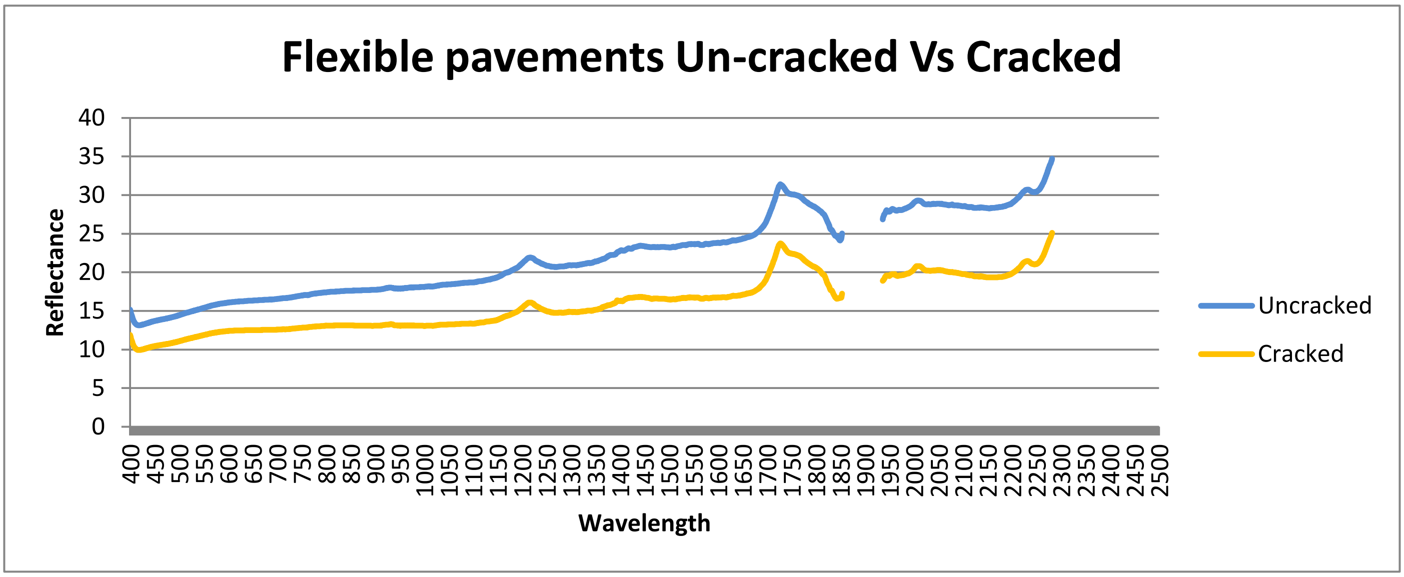

Figure 21: Flexible pavement system Un-cracked Vs Cracked

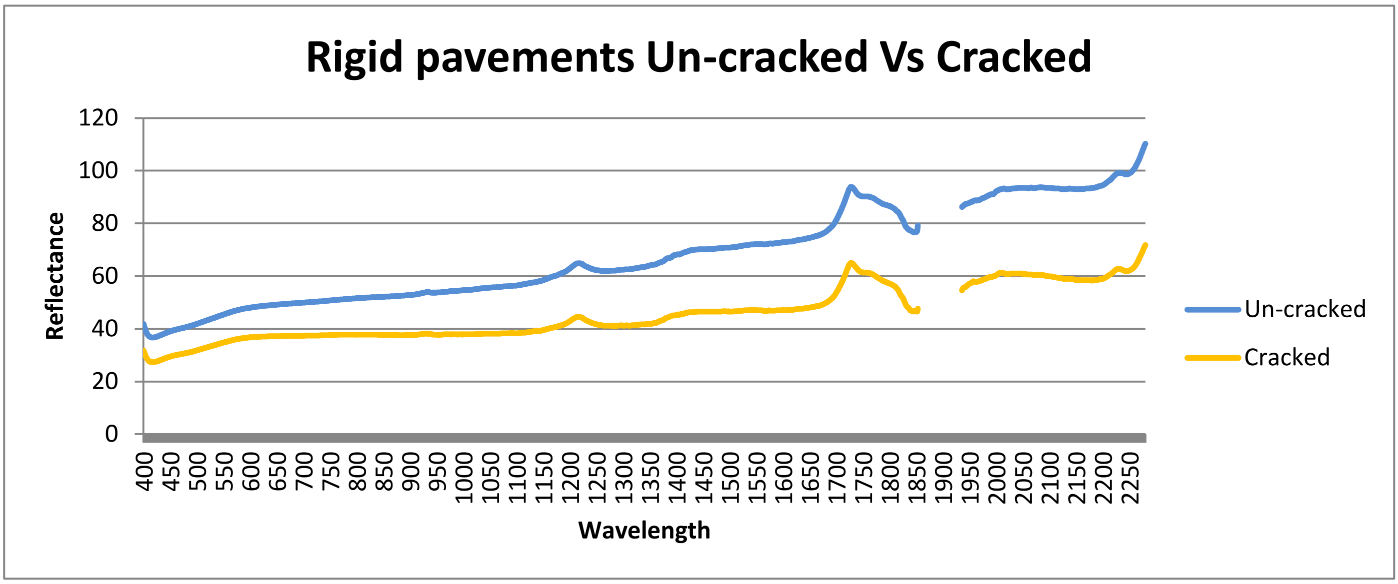

Figure 22: Rigid pavement system Un-cracked Vs Cracked

To plot these graphs all the mean values of reflectance for the good and the crack area, for each flexible system that was studied in this research were added for both flexible pavement system and rigid pavement system. The reason for this was to be able to compare the flexible pavement system with the rigid pavement system. When comparing figure 13 and figure 14 it can easily observed that the reflectance of rigid pavement system are much higher than the flexible pavement system. This can be said with 100% certainty as other researchers studying this topic have concluded to the same outcome. The highest value of the good area for the flexible pavement system is 35% in addition with the lowest value of the good area for the rigid pavement system which is 38%. The highest value of the crack area for the flexible pavement is 21% in addition with the lowest value of the rigid pavement which is 27%.

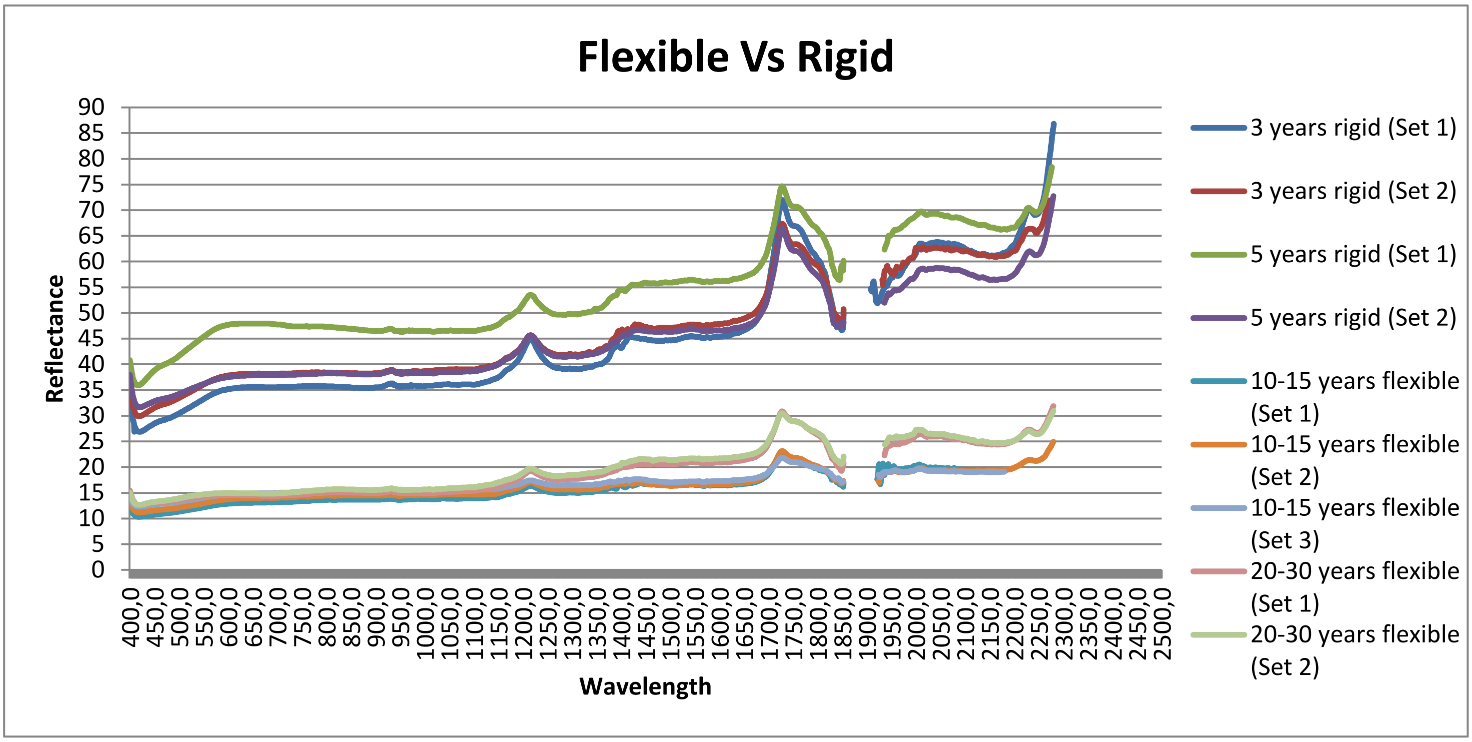

Figure 23: Flexible pavements systems against Rigid pavement systems

The above figure shows the difference between the two pavement systems (flexible and rigid) in terms of reflectance. It is easy to observe that the rigid pavement systems have much higher reflectance than the flexible pavement systems. According to Herold et al. (2004) 'the spectral signal from different types of road materials such as concrete and asphalt are different and hyperspectral sensing can easily distinguish between them. This can be observed with ease from the figure above.

6.2 T-test

First this research examined if there was a difference between the rigid pavement system and the flexible pavement system between all data sets. All the t-tests were calculated at 95% of significance. Before the t- test can take place it is needed to state two hypotheses, a null hypothesis and an alternate hypothesis. For all the t-test the two hypotheses are as follow:

- H1 (the alternate hypothesis): There is a statistical difference between the two data sets.
- H0 (the null hypothesis): There is not a statistical difference between the two data sets.

Table 2: t-test results between 3 years rigid pavement vs 10-15 flexible pavement

t-Test:3 years pavement(Rigid) Vs 10-15 years pavement(Flexible)		
	3 years	*10-15 years*
Mean	46,8	17,4
Df	3956	
t Stat	85,4	
P(T<=t) two-tail	0	
t Critical two-tail	1,9	

As it can be seen from the table above the t value calculated to be 85, 4 and the t critical value (two tail) calculated to be 1,9. As the t value is greater than the t critical the null hypothesis is rejected. As a result, it can be said that there is statistically important difference between the two data sets at the 95% level of certainty.

The rest t-tests which examined if there was a difference between rigid and flexible pavement system can be seen in the Appendix C.

The second t test was applied in order to examine if there was a difference between the un-cracked and the cracked area of the same pavement system.

Table 3: t-test results between the un-cracked and the cracked area of the same pavement type

t-Test: 3years set 1Un-cracked Vs Cracked		
	Un-cracked	*Cracked*
Mean	46,8	42,2
Df	3792	
t Stat	11,0	
P(T<=t) two-tail	5,4E-28	
t Critical two-tail	1,9	

In this t-test application the t value calculated to be 11.0 and the t critical calculated to be 1.9. t value is greater than the critical one therefore the null hypothesis is being rejected. There is a statistically important difference between the un-cracked and the cracked area of the same pavement type.

The remaining t-test which examined the un-cracked vs cracked of each data set can be seen in Appendix.

Moving on to the third t-test, which was applied in order to examine whether there is a difference between the un-cracked and the un-cracked area of different pavement systems but with the same material.

Table 4: t test results between the un-cracked area of set 1 and the un-cracked area of set 2

t-Test: 3 years un-cracked set 1 Vs set 2		
	Set 1	*Set 2*
Mean	45,8	47,0
df	3584	
t Stat	-2,9	
P(T<=t) two-tail	0,0	
t Critical two-tail	1,9	

It is distinguished that the t value calculated for this t-test is -2.9 which is lower than the t critical value which is 1.9. As a result of that, the alternate hypothesis is rejected and it can be said that there is not a statistical difference between the sample means.

The rest t-test that were applied on all data sets in the same way as above, can be found in the Appendix.

Lastly, the t-test was applied in a similar way with the previous t-test. To explain this t-test will investigate whether there is a difference or not between the cracked and the cracked area of different pavement systems with the same material.

Table 5: t-test results between 3 years (Set 1) cracked and 3 years pavement (Set 2) cracked

t-Test: 3 years cracked set 1 Vs set 2		
	Set 1	*Set 2*
Mean	41,6	45,7
df	3655	
t Stat	-11,8	
P(T<=t) two-tail	9,2E-32	
t Critical two-tail	1,9	

Again it is being observed that the t value calculated to be -11.8 which is much lower that the t critical value which was calculated to be 1,9. The alternate hypothesis is being rejected and it is clear that there is not a statistical difference between the two sample means.

6.3 Pearson Correlation Coefficient

As it was mentioned in the methodology chapter the Pearson correlation coefficient was used in order to investigate in each pavement system which wavelengths have low and high correlation. This research is interested in the wavelengths that have low correlation. To explain, when there is low correlation it means that the two sets are not correlated. These wavelengths with low correlation can be very helpful in the identification of the cracks from satellites; instead of taking readings on each wavelength the satellite will take readings at these wavelengths. The Pearson correlation coefficient was used in three different situations; first it was applied on reflectance values between the un-cracked and the cracked area of each pavement system, secondly it was applied on the reflectance values between the un-cracked and the un-cracked area of each pavement system and lastly it was applied on the cracked and the cracked area of each pavement system.

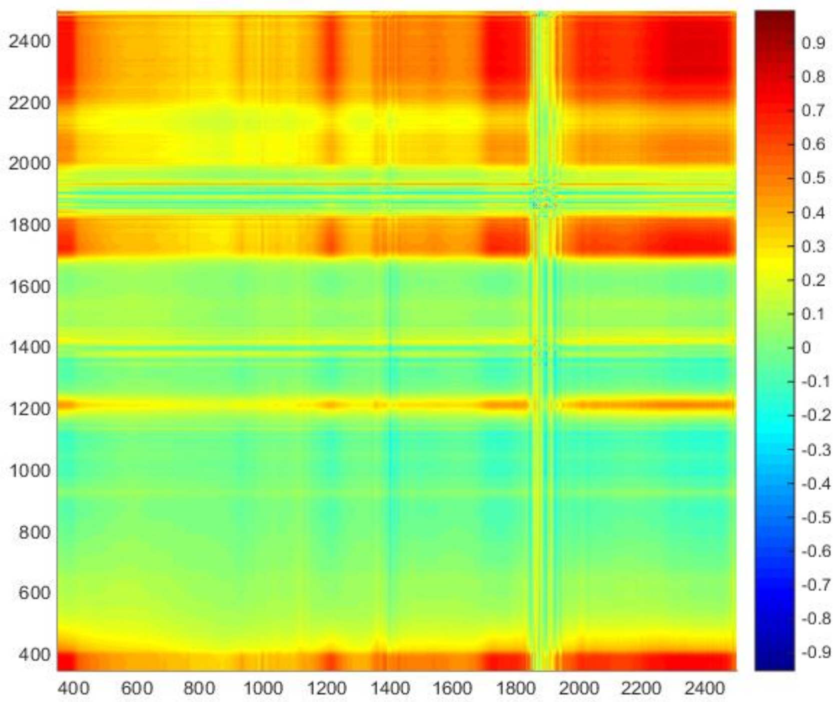

Figure 24: Correlation analysis of reflectance values from cracked against reflectance values of un-cracked from the 20-30 years flexible pavement system (Set 1)

As it is found (figure 1) a positive high correlation is observed between the wavelengths 2200-2400 nm. Moreover between the wavelengths 600-1200 nm and 1250-1600 nm (un-cracked area- y axis) a negative low correlation is observed. Lastly a low correlation is observed between the wavelengths 1800-2000 nm which probably is a result of the atmospheric absorption.

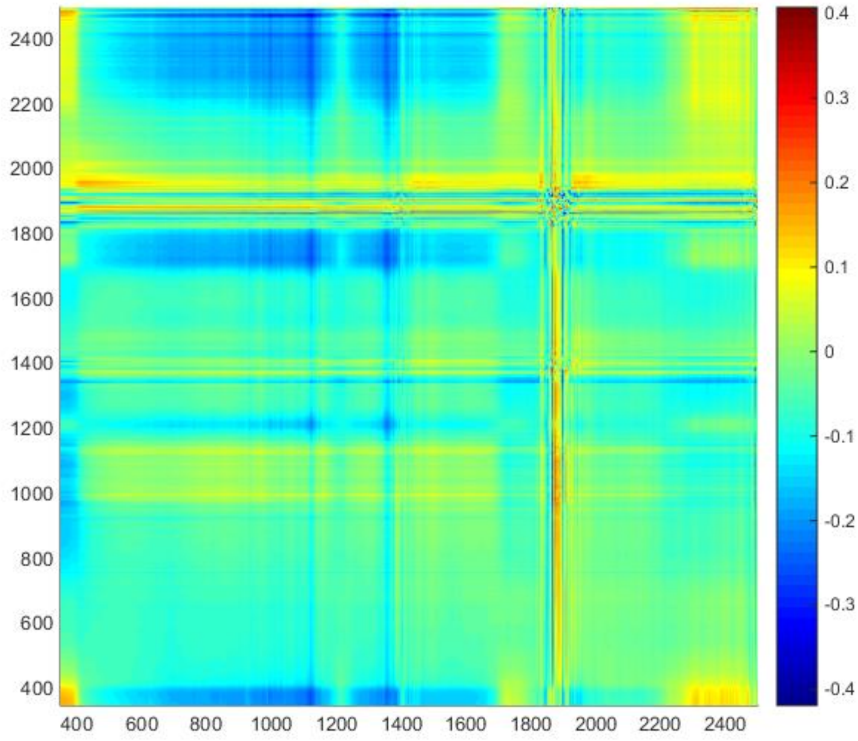

Figure 25: Correlation analysis of reflectance values from cracked against reflectance values of un-cracked from the 20-30 years flexible pavement system (Set 2)

The second set of data for the 20-30 years flexible pavement system has low correlation almost in each wavelength. The highest correlation value from the figure above is the 0.1 and it is located between the wavelengths 2200-2400 nm. Between the wavelengths 600-1400 nm (cracked area-x axis) it is observed a low negative correlation. These correlation results were not expected as the observed correlations are much lower than the previous set of data.

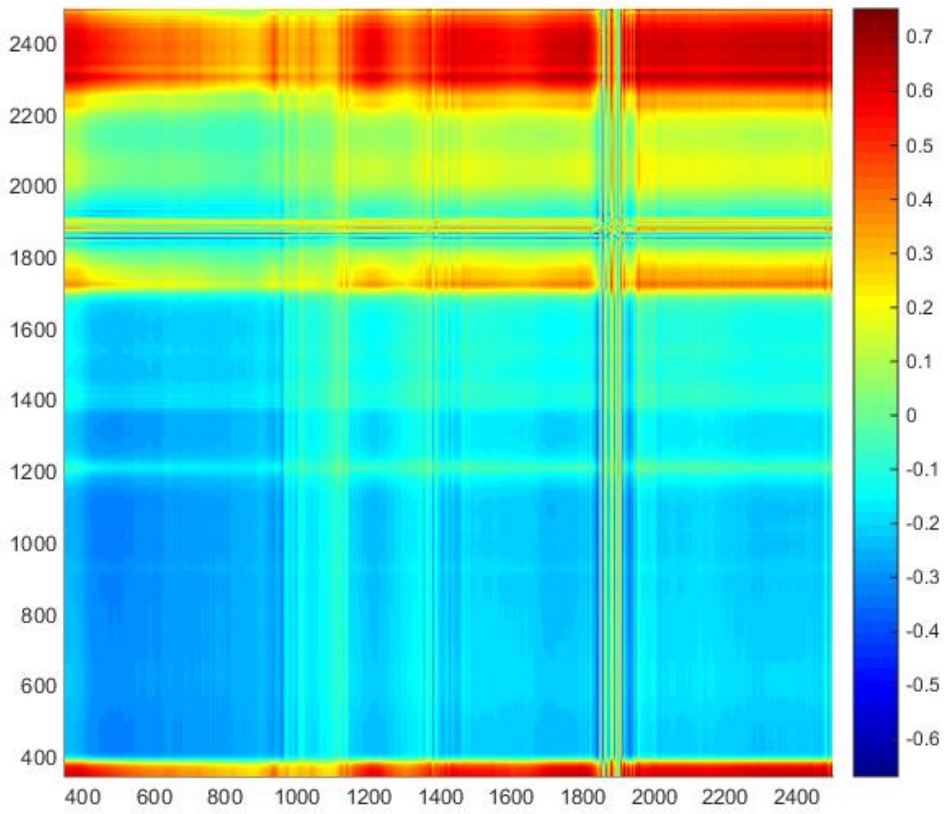

Figure 26: Correlation analysis of reflectance values from cracked against reflectance values of un-cracked from the 5 years rigid pavement system (Set 1)

As it is found between the wavelengths 400-2400 nm is observed a positive high correlation (cracked area- x-axis). In the good area (un-cracked area - y-axis) high correlation is observed between 2200-2400nm. Moreover between the wavelengths 400-1750 (un-cracked area - y-axis) a negative low correlation is observed at around -0.1 and -0.2. Again between the wavelengths 1800-2000 a high correlation is observed but as it was stated above is due to the atmospheric absorption.

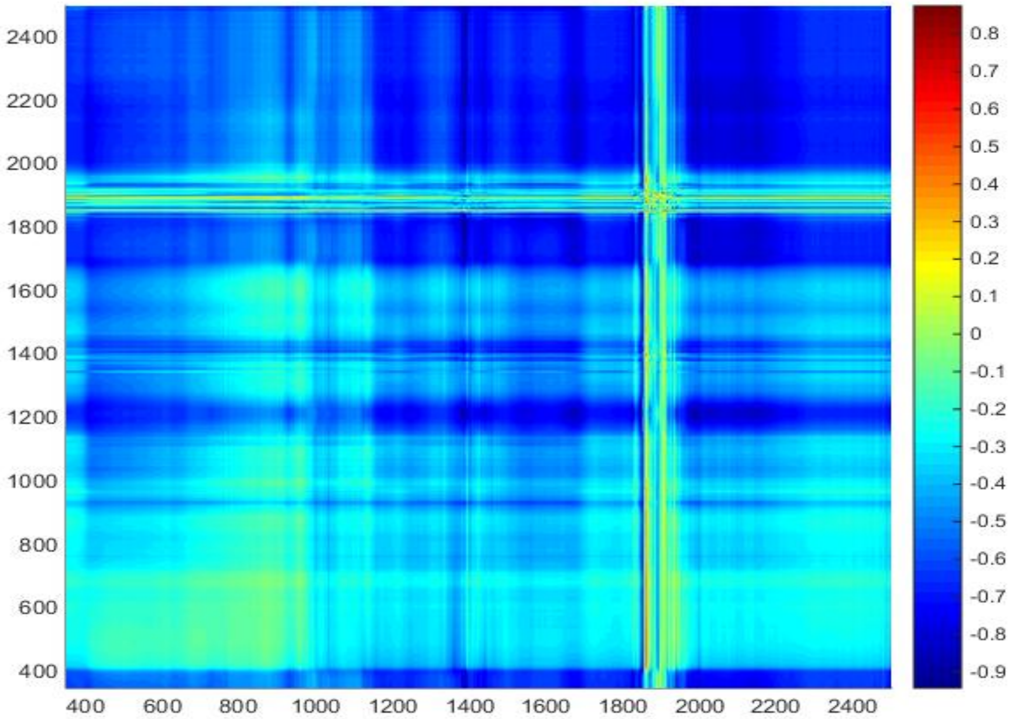

Figure 27: Correlation analysis of reflectance values from cracked against reflectance values of un-cracked from the 5 years rigid pavement system (Set 2)

The second data set from the same pavement system was measured in an area where it had no traffic and the cars were not passing over it. It differs from the previous figure (figure 3) as throughout the wavelengths a negative low correlation is observed; except the wavelengths 1800-2000 nm, where it is observed a positive low correlation. Between the wavelengths 1200-1800 and 2000-2400 (un-cracked area - y-axis) a negative low correlation is observed at-0.9. Lastly between the wavelengths 450-1200 (un-cracked area - y-axis) a negative low correlation is observed at -0.2.

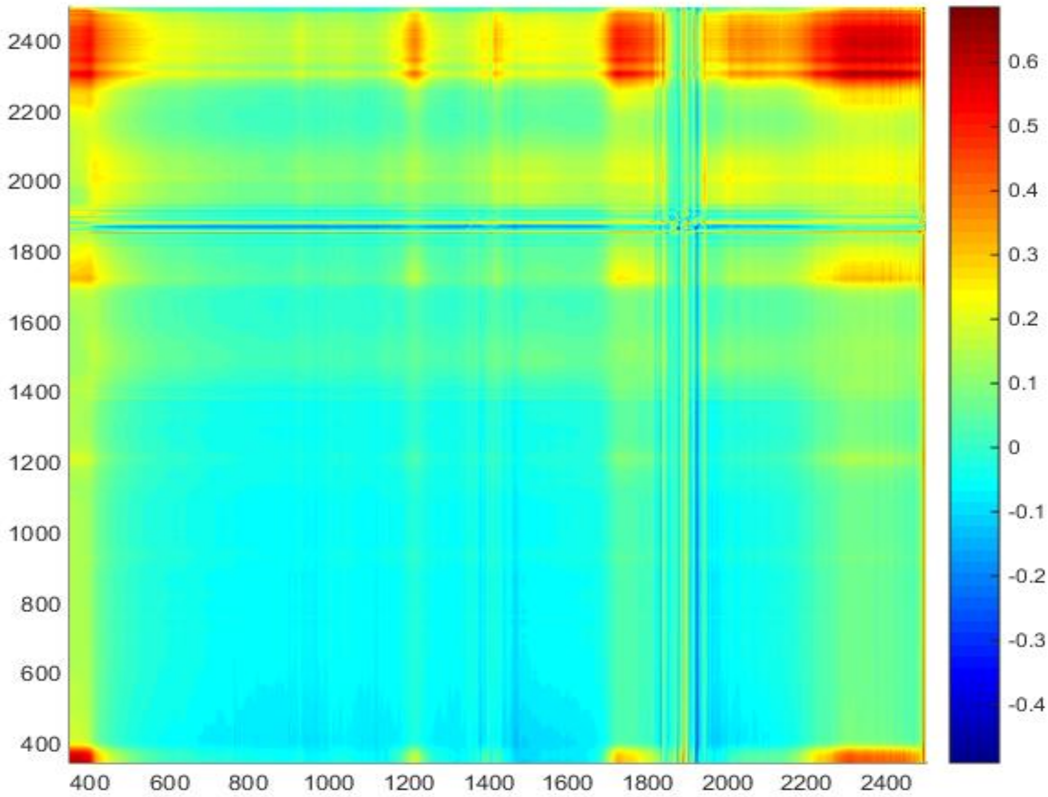

Figure 28: Correlation analysis of reflectance values from cracked against reflectance values of un-cracked from the 10-15 years flexible pavement system (Set 1)

As it is observed from the figure this pavement system has in general low correlation. To be exact, between the wavelengths 450 -1800 (un-cracked area- y-axis) it is observed a negative low correlation between the values 0 and -0.1. The highest positive correlation is observed at the wavelength 400(cracked area- x-axis) and 2400 (un-cracked area- y-axis).

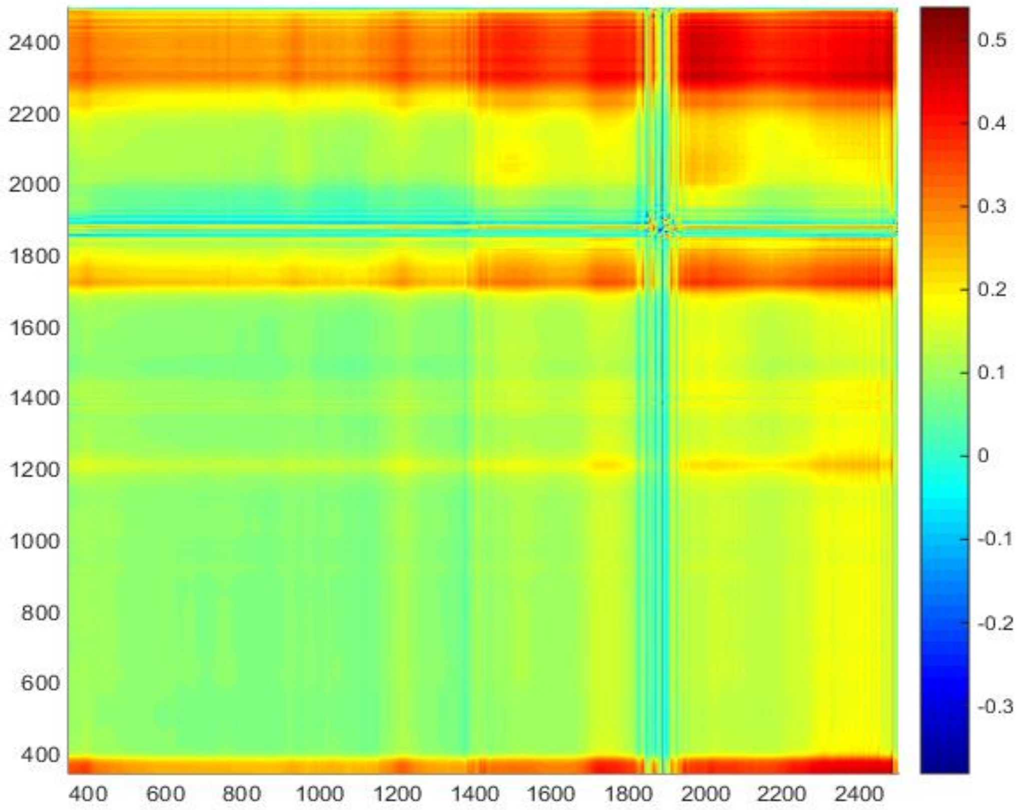

Figure 29: Correlation analysis of reflectance values from cracked against reflectance values of un-cracked from the 10-15 years flexible pavement system (Set 2)

The second data set from this flexible pavement system produced the above figure. It differs from the previous one as the correlation values are slightly higher than the previous figure. Between the wavelengths 400-1800 nm (un-cracked area-y-axis) a positive low correlation is observed at a range of 0.1-0.2. Between the wavelengths 2300-2400 nm (un-cracked area – y-axis) a relatively positive high correlation is observed.

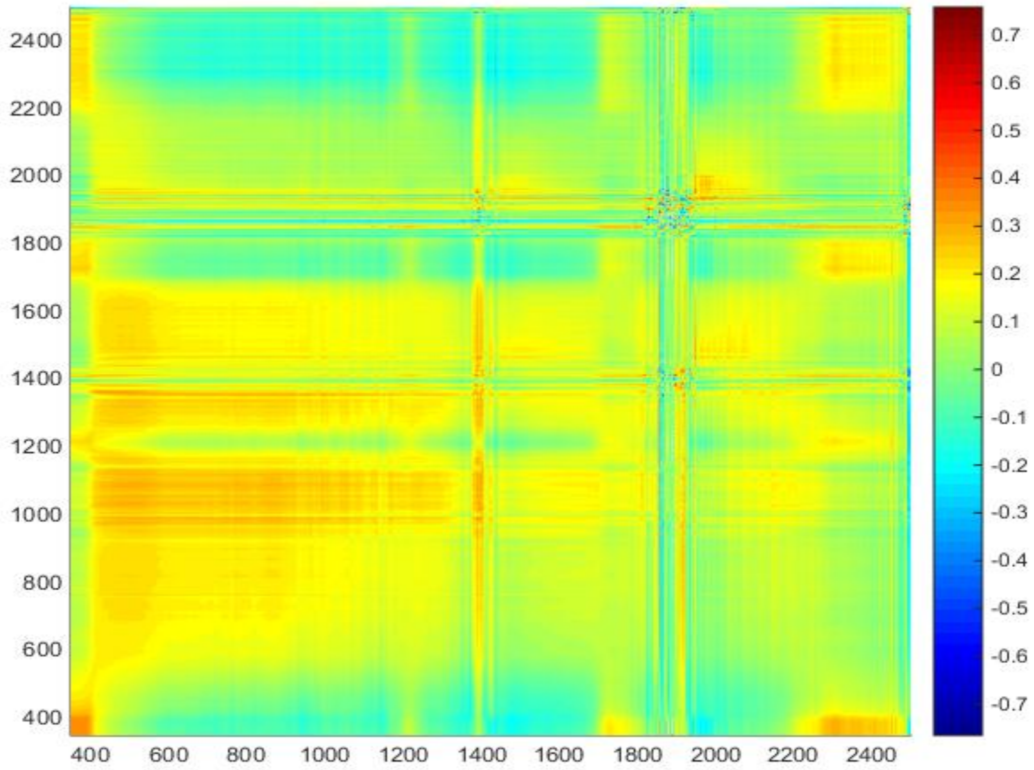

Figure 30: Correlation analysis of reflectance values from cracked against reflectance values of un-cracked from the 10-15 years flexible pavement system (Set 3)

The third data set from this flexible pavement system had an overall low positive correlation. Between 600-1600 nm (un-cracked area – y-axis) a positive low correlation at 0.2 is recorded. Moving on, in addition with the two previous figures, at the wavelengths 2300-2400 nm (un-cracked area – y -axis) is observed a negative low correlation at 0 and -0.1.

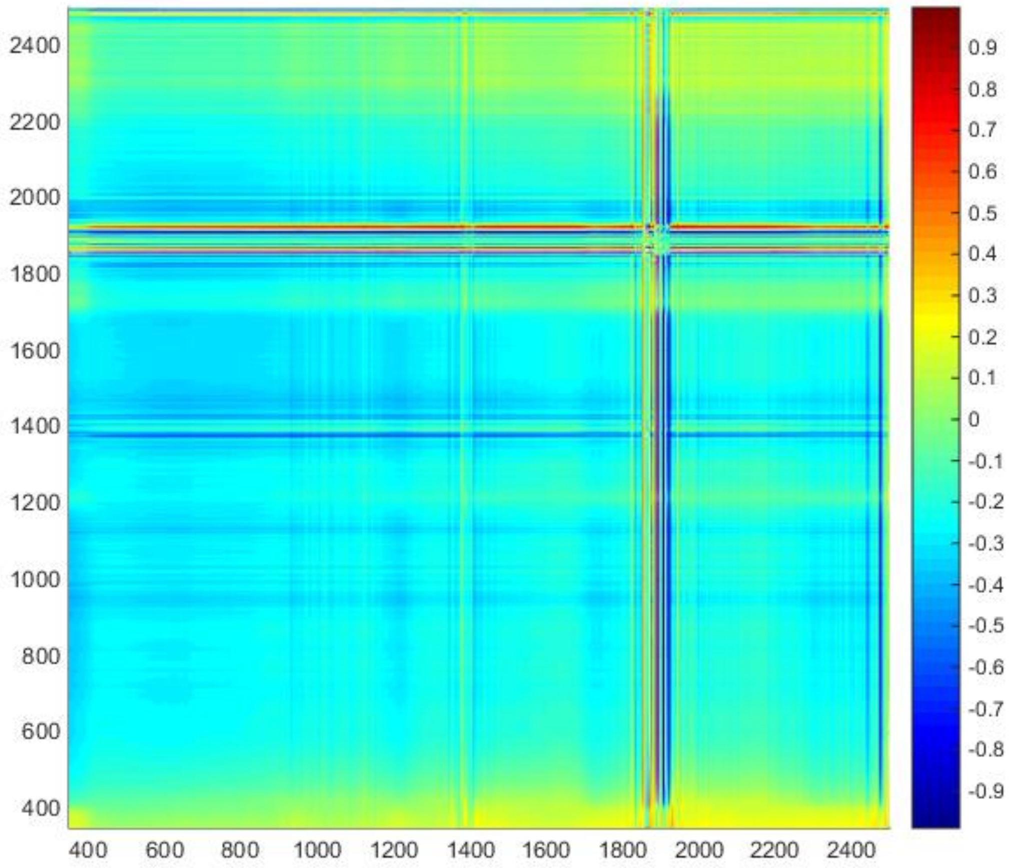

Figure 31: Correlation analysis of reflectance values from cracked against reflectance values of un-cracked from the 3 years rigid pavement system (Set 1)

This rigid pavement system has in most wavelengths negative low correlation. At the point 400 nm a positive low correlation is observed at 0.2 between the wavelengths 400-2400 (cracked area – x-axis). Moreover at the wavelengths 450-1800 nm (un-cracked area – y-axis) a negative low correlation is observed at -0.3. At the wavelengths 2300-2400 nm (un-cracked area – y-axis) a positive low correlation is observed. Lastly between the wavelengths 1800-2000 at both axes many correlations are observed in random values, as it can be seen from the figure it has a very low negative correlation at -0.9 but it also has a very high positive correlation at 0.9. These strange values of correlation are probably due to the atmospheric absorption.

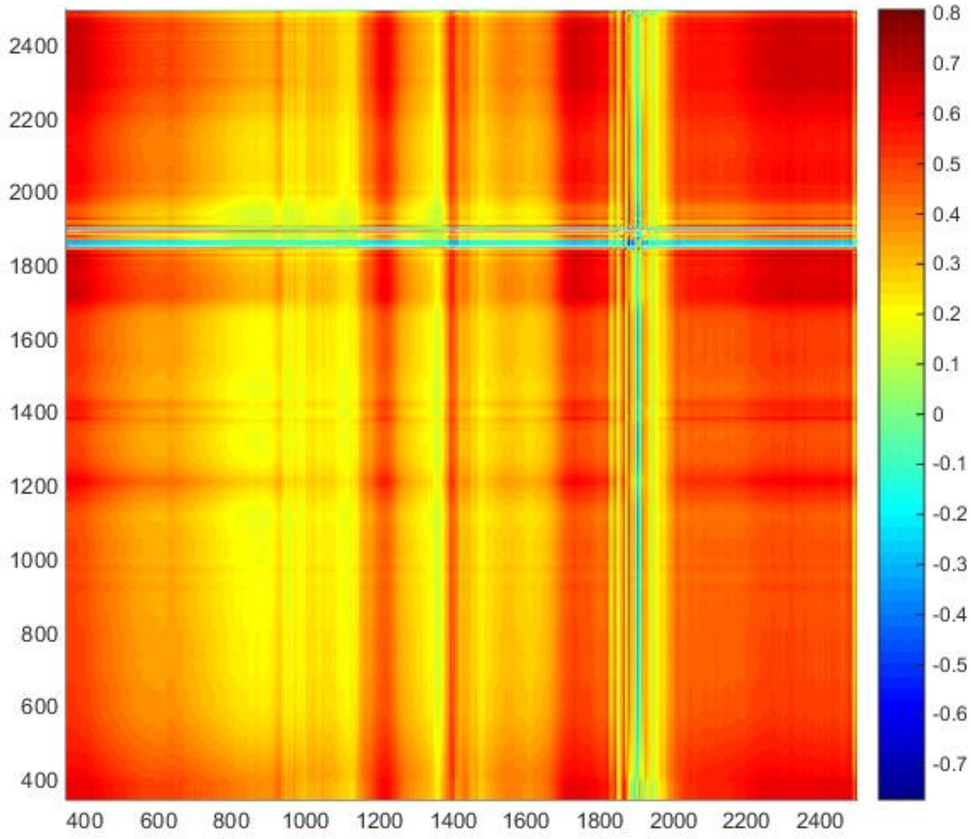

Figure 32: Correlation analysis of reflectance values from cracked against reflectance values of un-cracked from the 3 years rigid pavement system (Set 2)

As it is found, a high positive correlation is observed at 2000-2400 nm at both axes. Between the wavelengths 800-1150 nm (cracked area- x-axis) a positive low correlation is recorder at 0.2. These observed high values of correlation are probably a result of the humidity and the corrosion as this rigid pavement system is located exactly next to the sea.

Moving on, the results of the correlation between the un-cracked – un-cracked and the cracked –cracked will be shown. It was found good to show one diagram for each correlation for each pavement system. The remaining diagrams will be presented in Appendix D.

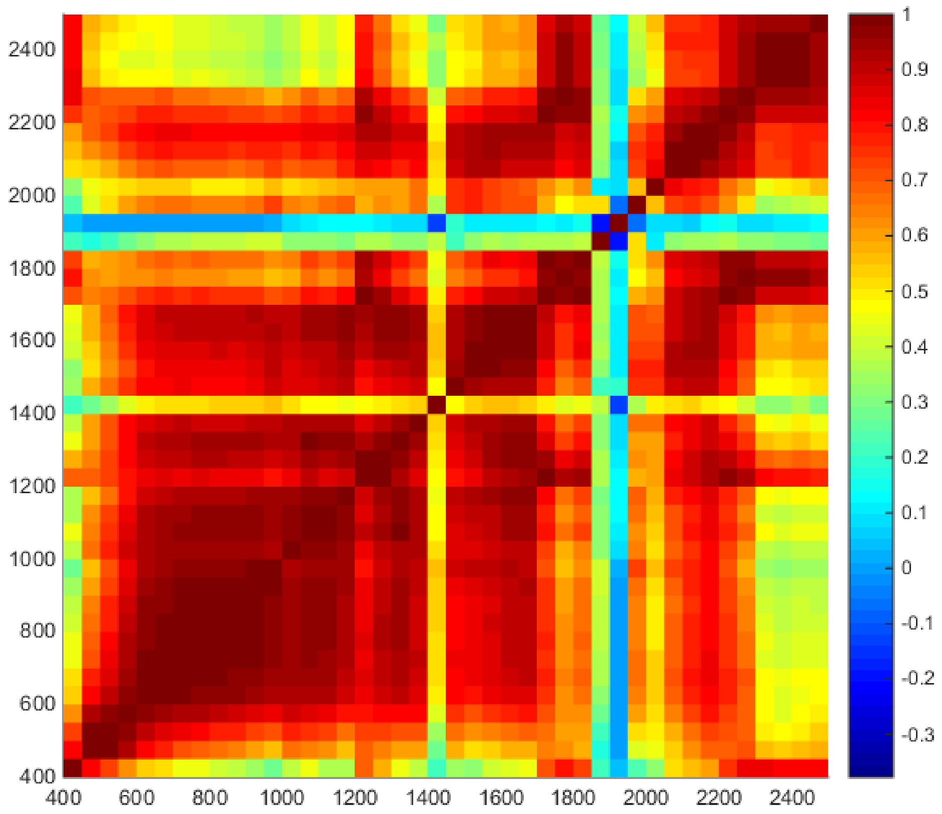

Figure 33: Correlation analysis of reflectance values from un-cracked against reflectance values of un-cracked from the 10-15 years flexible pavement system (Set 1)

The correlation values shown above were expected as it is logical to have a strong linear relationship between the two variables. It is found that there is negative correlation between the wavelengths 1800-2000 nm, but between these wavelengths atmospheric absorption occurs. Lastly a perfect positive correlation is observed diagonal on the diagram which was expected, and between the wavelengths 600-1200 nm.

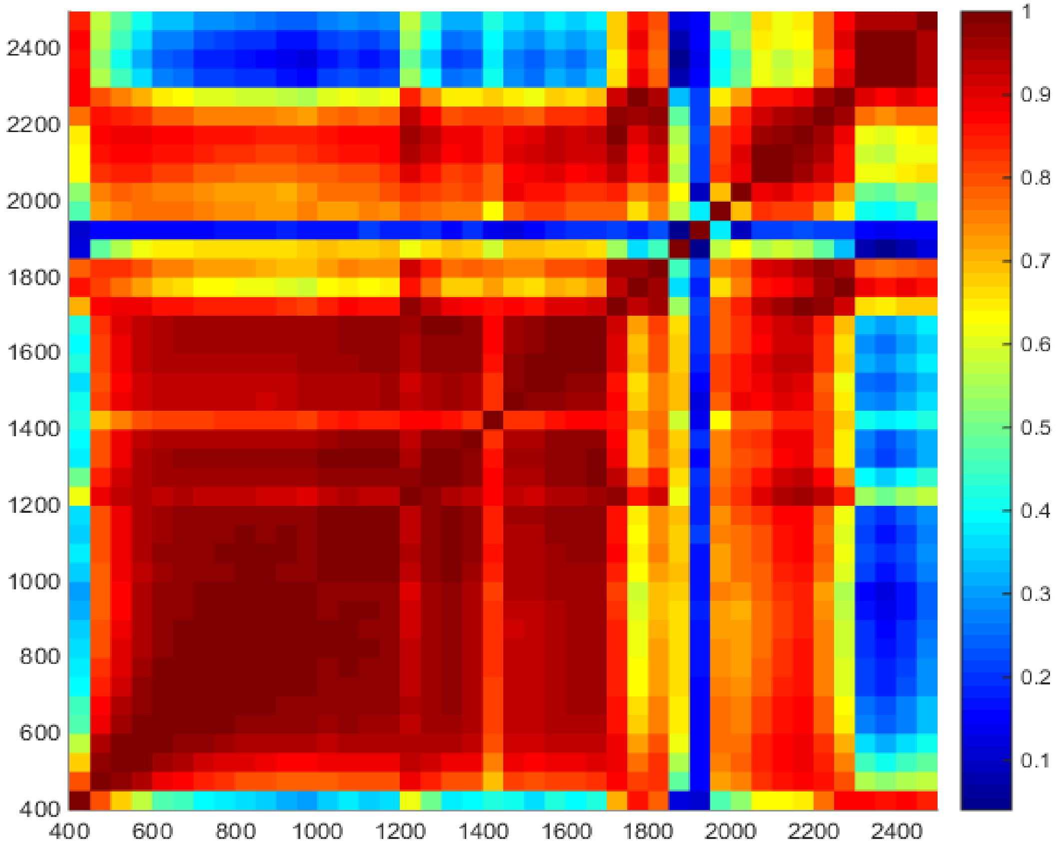

Figure 34: Correlation analysis of reflectance values from cracked against reflectance values of cracked from the 10-15 years flexible pavement system (Set 1)

As it is found there is not negative correlation as the lowest positive correlation is the 0.1. The absence of a negative correlation reveals that both of our variables move in the same direction. As it can be seen from the figure, most of the values are close to 1 which means that there is a strong linear relationship. Moreover it can be seen that a perfect positive correlation lies diagonal on the diagram which was expected. The lowest positive correlation can be seen in the wavelengths 1900-2000 nm and between the wavelengths 2250-2400 nm. This low positive correlation is probably due to the atmospheric absorption.

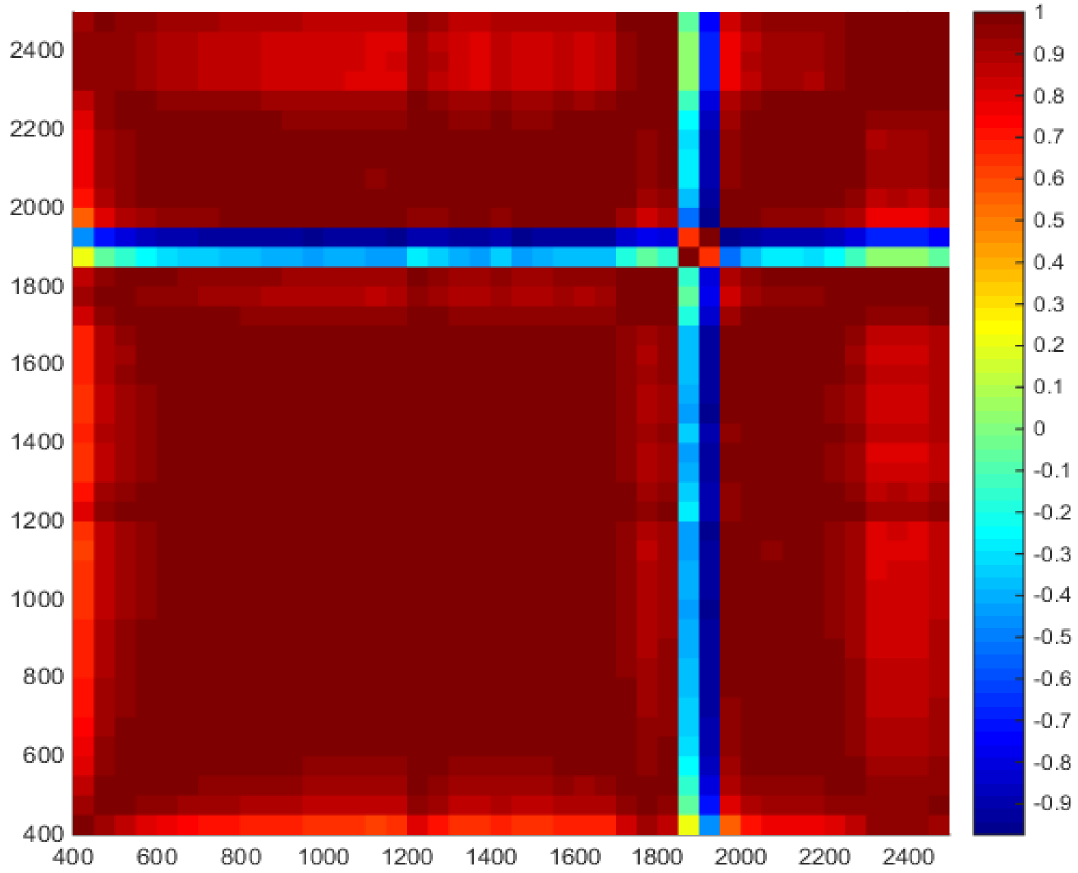

Figure 35: Correlation analysis of reflectance values from un-cracked against reflectance values of un-cracked from the 3 years rigid pavement system (Set 1)

The correlation between the data set of good for this rigid pavement system is very good as in almost every wavelength there is a perfect positive correlation. A negative low correlation is observed between the wavelengths 1800-200 nm but it will not taken in mind as it lies in the wavelengths that have atmospheric absorption.

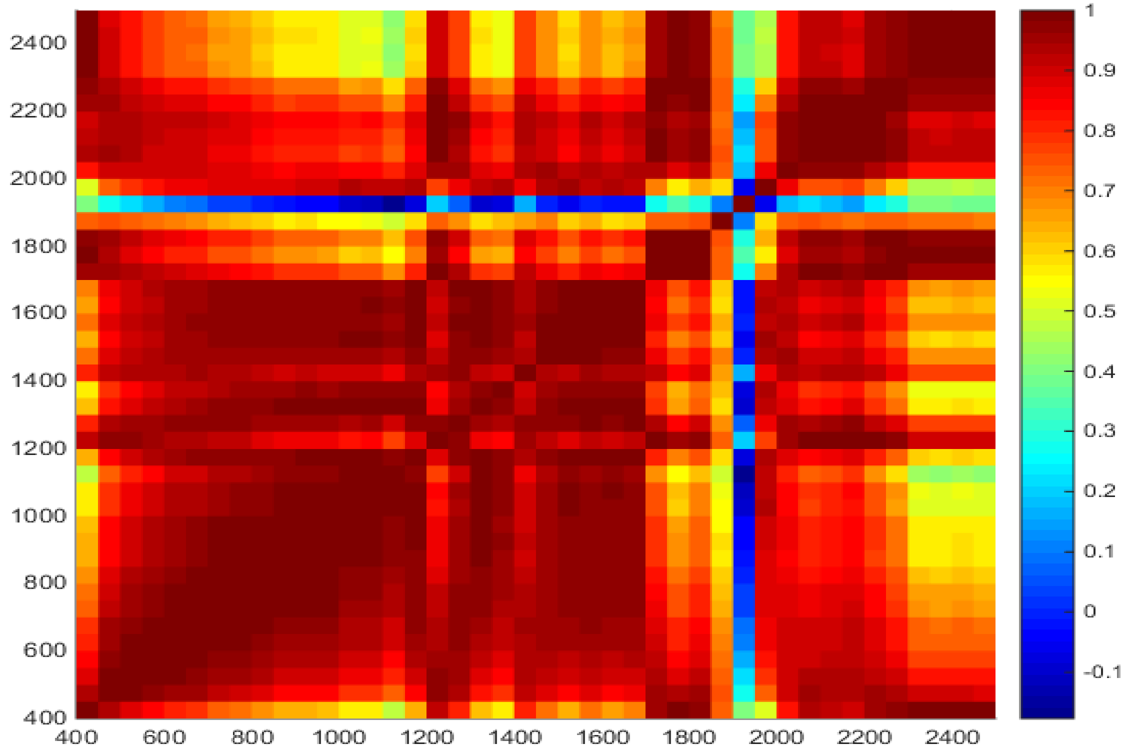

Figure 36: Correlation analysis of reflectance values from cracked against reflectance values of cracked from the 3 years rigid pavement system (Set 1)

The correlation diagram shows that there is a strong linear relationship between the two variables. It is distinguished that the most correlation values are from 0.9 to 1. The highest correlation value is 1 which is a perfect positive correlation and the lowest is -0.1 but it will be ignored as it appears in the wavelengths that have atmospheric absorption.

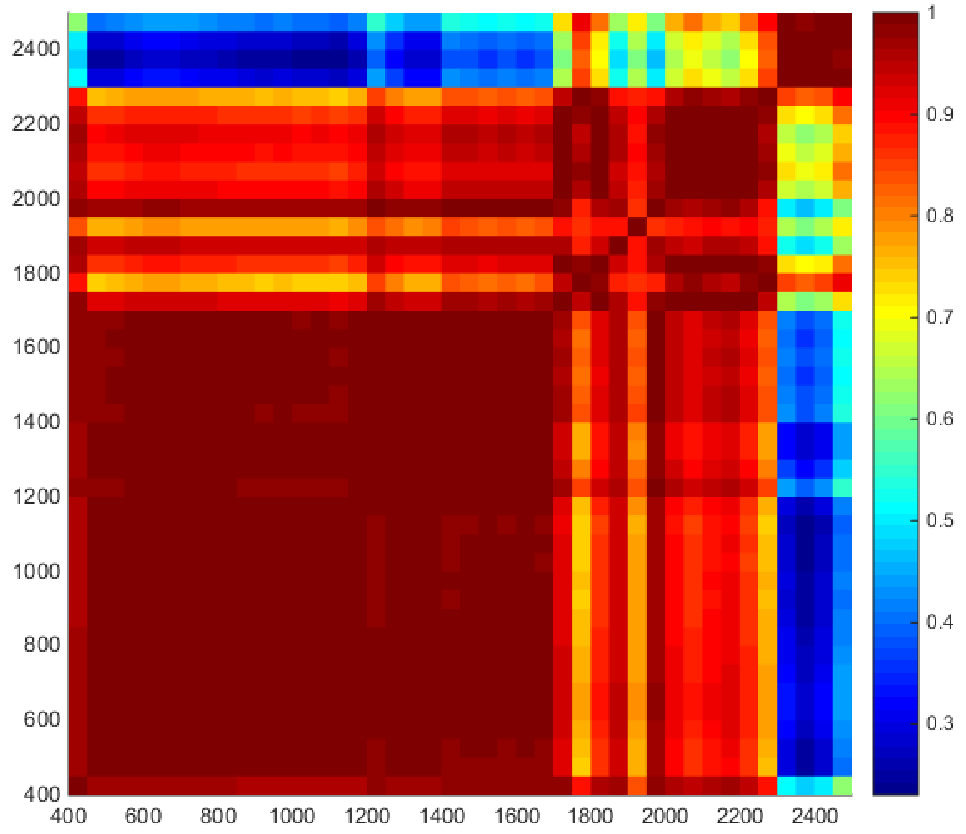

Figure 37: Correlation analysis of reflectance values from un-cracked against reflectance values of un-cracked from the 5 years rigid pavement system (Set 1)

As it is found between the wavelengths 400-1700 nm there is a perfect positive correlation, in addition with figure 12 which had perfect positive correlation in almost every wavelength. The lowest correlation is found to be 0.25 and it is observed between the wavelengths 2300-2400 nm. In this diagram the lowest correlation is recorded in different wavelengths than the previous which was between 1800-2000 but again it will be ignored as it comes under the wavelengths that have atmospheric absorption.

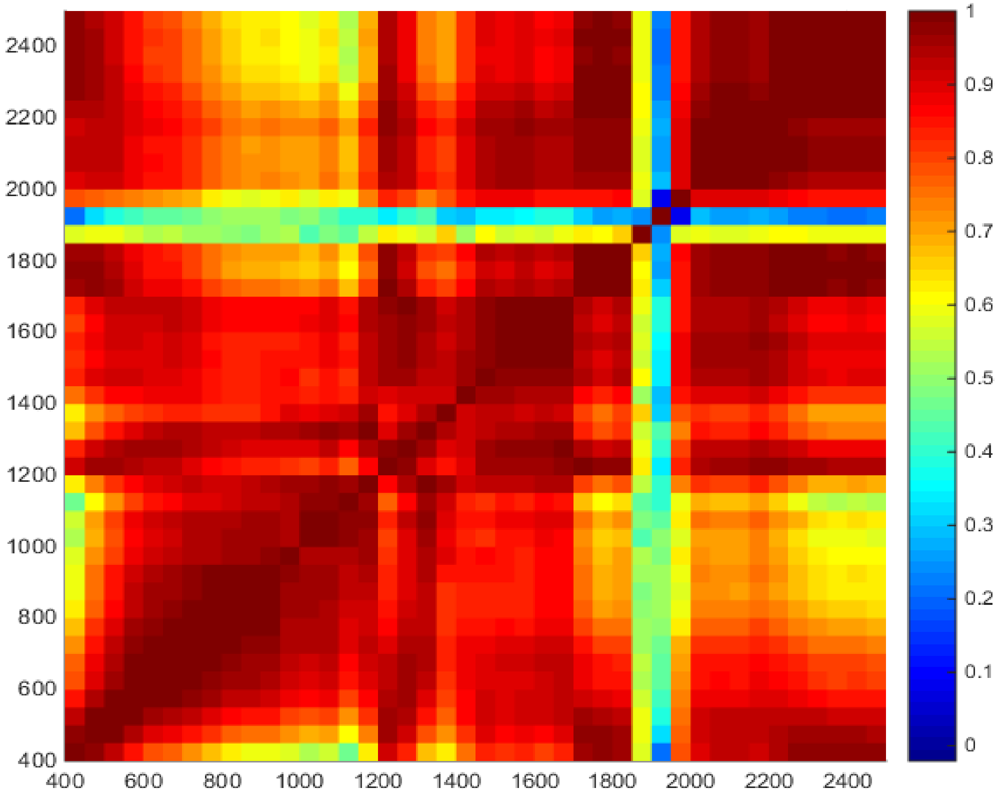

Figure 38: Correlation analysis of reflectance values from cracked against reflectance values of cracked from the 5 years rigid pavement system (Set1)

The above figure is similar to figure 13 which was expected as both are rigid pavement systems. There is not any negative correlation as the lowest correlation is observed to be 0 but again it is ignored as it comes under the wavelengths that have atmospheric absorption. The highest correlation is a perfect positive correlation and can be found diagonal on the diagram.

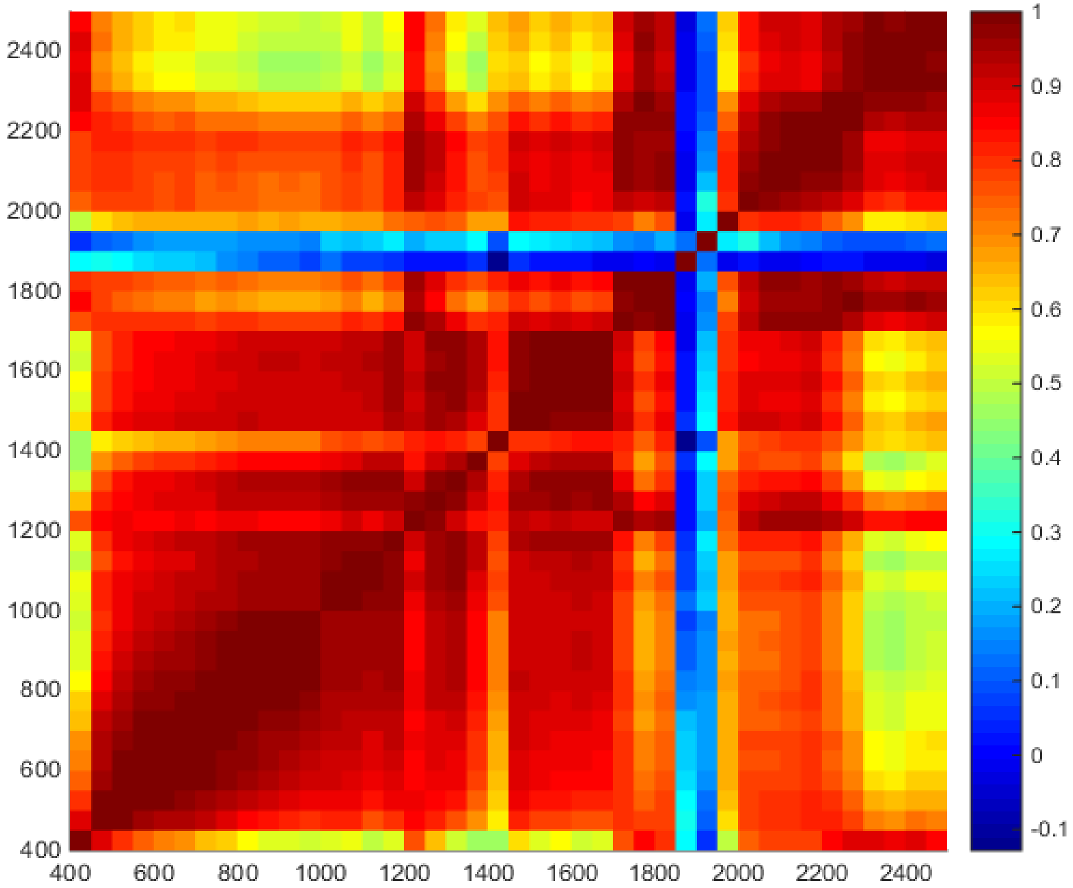

Figure 39: Correlation analysis of reflectance values from un-cracked against reflectance values of un-cracked from the 20-30 years flexible pavement system (Set 1)

As its found, the highest observed correlation is a perfect positive correlation and it can be seen diagonal on the diagram. The lowest correlation is recorder to be -0.1 and it lies between the wavelengths that have atmospheric absorption. The figure above is similar to figure 10 which was expected as both pavement systems are flexible, with only one difference which is that the 20-30 years flexible pavement system has higher values of correlation and a better linear relationship.

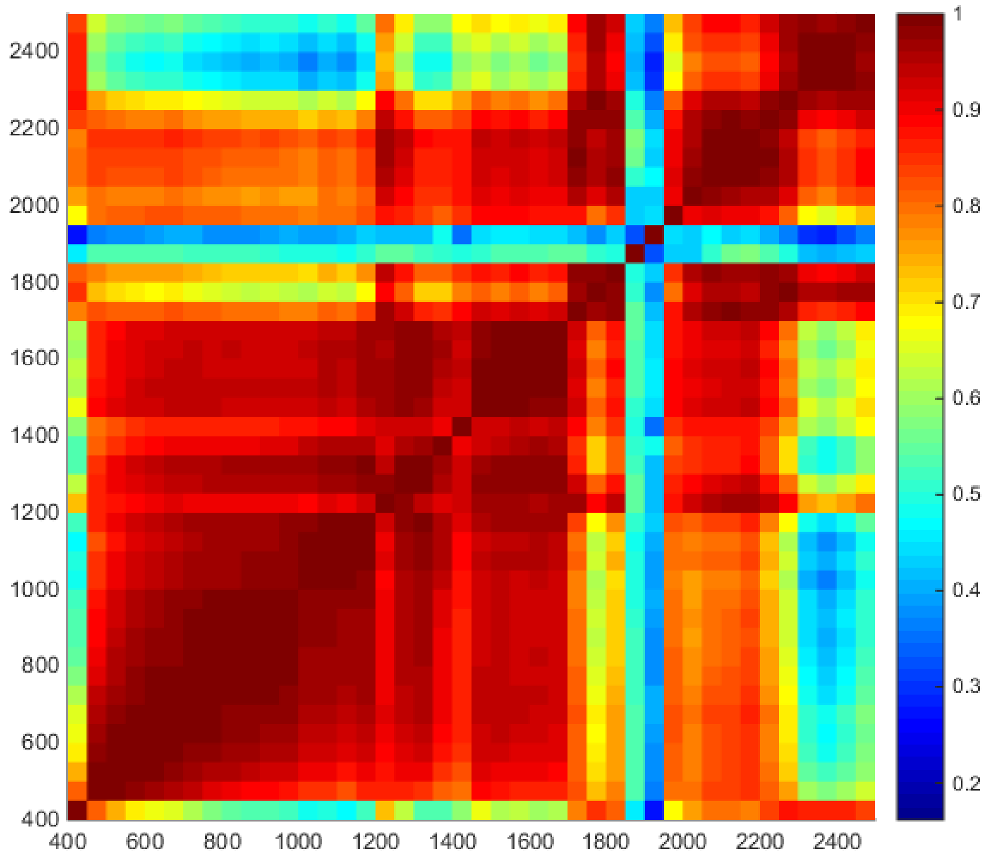

Figure 40: Correlation analysis of reflectance values from cracked against reflectance values of cracked from the 20-30 years flexible pavement system (Set 1)

The figure of this flexible pavement system shows that it has a variety of correlation values which was observed in figure 11 as well. The highest correlation is a perfect positive and it is found diagonal on the figure which was expected as the Pearson correlation is used on the same data e.g. the wavelength 400 is correlated with the same wavelength which have the same value. The lowest correlation is found to be 0.2 but it is in the range of wavelengths that have atmospheric absorption.

The findings from the Pearson correlation have shown that in each of the pavement systems, low correlation is observed in different range of wavelengths. These ranges of wavelengths will be compared with the results of the Euclidean distance and the wavelengths that will be used to monitor the pavements will be generated.

6.3 Euclidean distance

The Euclidean distance was used in order to identify spectral regions which are able to distinguish the spectral diversity of the pavement systems due to cracks. Moreover the Euclidean distance was used to examine the separability of the two variables and to identify the distance between those variables. The results were very promising as the highest value in each pavement system was at the same wavelengths except the rigid pavement system which is located next to the sea. The results are tabulated in the following tables:

Table 6: Separability results for the 20-30 years flexible pavement system (Set1)

Wavelength	450	550	650	750	850	950	1050
450	0.8						
550	2.1	1,4					
650	2,3	1,6	0,6				
750	2,5	1,8	0,9	0,6			
850	2,8	2,2	1,2	1,0	0,6		
950	2,8	2,1	1,2	0,9	0,5	0,6	
1050	3,0	2,3	1,3	1,1	0,7	0,7	0,7
1150	4,0	3,3	2,4	2,1	1,7	1,8	1,7
1250	5,6	4,9	4,0	3,7	3,3	3,4	3,3
1350	6,0	5,4	4,4	4,1	3,8	3,8	3,7
1450	8,4	7,7	6,8	6,5	6,1	6,2	6,1
1550	8,7	8,0	7,1	6,8	6,4	6,5	6,4
1650	9,2	8,5	7,6	7,3	6,9	7,0	6,9
1750	16,8	16,1	15,1	14,9	14,5	14,5	14,5

Table 7: Separability results for the 20-30 years flexible pavement system (Set 2)

Wavelength	450	550	650	750	850	950	1050
450	0,9						
550	2,4	0,8					
650	2,6	1,0	0,7				
750	3,0	1,3	1,0	0,7			
850	3,4	1,7	1,4	1,1	0,7		
950	3,3	1,7	1,4	1,1	0,7	0,7	
1050	3,6	2,0	1,6	1,3	0,9	1,0	0,9
1150	4,7	3,1	2,8	2,5	2,1	2,1	2,0
1250	6,2	4,6	4,2	3,9	3,5	3,6	3,4
1350	6,7	5,1	4,7	4,4	4,0	4,1	3,9
1450	9,2	7,6	7,3	7,0	6,6	6,6	6,5
1550	9,4	7,8	7,4	7,1	6,7	6,8	6,6
1650	9,9	8,3	8,0	7,6	7,2	7,3	7,2
1750	16,7	15,1	14,7	14,4	14,0	14,1	13,9

Table 8: Separability results for the 10-15 years flexible pavement system (Set1)

Wavelength	450	550	650	750	850	950	1050
450	1,0						
550	2,4	0,9					
650	3,3	1,7	0,8				
750	3,6	2,1	1,1	0,7			
850	3,9	2,3	1,4	1,0	0,7		
950	4,0	2,4	1,4	1,1	0,8	0,7	
1050	4,1	2,5	1,5	1,2	0,9	0,8	0,7
1150	4,4	2,8	1,8	1,5	1,2	1,1	1,0
1250	5,5	3,9	2,9	2,6	2,3	2,2	2,1
1350	5,7	4,1	3,1	2,8	2,5	2,4	2,3
1450	7,0	5,5	4,5	4,1	3,9	3,8	3,7
1550	6,1	5,2	4,2	3,9	3,6	3,5	3,4
1650	7,0	5,4	4,4	4,1	3,8	3,7	3,6
1750	11,7	10,1	9,1	8,8	8,5	8,4	8,3

Table 9: Separability results for the 10-15 years flexible pavement system (Set2)

Wavelength	450	550	650	750	850	950	1050
450	2,6						
550	4,0	2,7					
650	5,07	3,	2,9				
750	5,4	4,1	3,2	2,9			
850	5,6	4,3	3,4	3,1	2,9		
950	5,5	4,2	3,3	3,0	2,8	2,8	
1050	5,8	4,5	3,6	3,3	3,1	3,1	3,0
1150	6,0	4,7	3,8	3,5	3,3	3,4	3,2
1250	7,0	5,7	4,8	4,5	4,3	4,3	4,2
1350	6,9	5,6	4,7	4,4	4,2	4,2	4,1
1450	7,9	6,6	5,8	5,5	5,3	5,3	5,1
1550	7,7	6,4	5,6	5,3	5,1	5,1	4,9
1650	8,0	6,8	5,9	5,6	5,4	5,4	5,3
1750	12,9	11,6	10,8	10,5	10,3	10,3	10,1

Table 10: Separability results for the 10-15 years flexible pavement system (Set3)

Wavelength	450	550	650	750	850	950	1050
450	3,5						
550	4,8	3,6					
650	5,6	4,4	3,6				
750	6,0	4,8	4,0	3,7			
850	6,3	5,1	4,3	4,0	3,8		
950	6,1	4,9	4,1	3,8	3,6	3,6	
1050	6,	5,2	4,4	4,1	3,9	3,9	3,7
1150	6,6	5,4	4,6	4,3	4,1	4,1	3,9
1250	7,4	6,2	5,4	5,1	4,9	4,9	4,7
1350	7,4	6,2	5,5	5,2	5,0	5,0	4,7
1450	8,3	7,1	6,3	6,0	5,8	5,8	5,6
1550	8,0	6,8	6,0	5,7	5,5	5,5	5,3
1650	8,3	7,1	6,3	6,0	5,8	5,8	5,6
1750	11,7	10,5	9,8	9,4	9,3	9,3	9,0

Table 11: Separability results for the 5 years rigid pavement system (Set1)

Wavelength	450	550	650	750	850	950	1050
450	0,8						
550	5,7	0,8					
650	8,2	1,7	0,8				
750	7,7	1,1	1,3	1,3			
850	7,2	0,	1,8	1,8	1,5		
950	6,6	0,0	2,4	2,4	2,1	1,6	
1050	6,9	0,3	2,1	2,1	1,8	1,3	1,5
1150	8,0	1,5	1,0	0,98	0,7	0,2	0,3
1250	10,7	4,1	1,6	1,6	1,8	2,4	2,2
1350	11,1	4,6	2,0	2,1	2,3	2,8	2,7
1450	16,2	9,7	7,1	7,2	7,4	7,9	7,8
1550	16,7	10,1	7,6	7,6	7,8	8,4	8,2
1650	17,38	10,8	8,2	8,3	8,5	9,0	8,9
1750	31,0	24,5	21,9	21,9	22,2	22,7	22,5

Table 12: Separability results for the 5 years rigid pavement system (Set2)

Wavelength	450	550	650	750	850	950	1050
450	7,1						
550	10,5	7,2					
650	12,2	8,9	7,0				
750	12,4	9,1	7,2	6,7			
850	12,4	9,1	7,3	6,8	6,5		
950	12,5	9,2	7,3	6,8	6,5	6,2	
1050	12,8	9,6	7,7	7,2	6,9	6,5	6,2
1150	14,3	11,0	9,1	8,6	8,3	8,0	7,6
1250	16,55	13,2	11,3	10,9	10,5	10,2	9,8
1350	16,5	13,2	11,3	10,9	10,5	10,2	9,8
1450	20,8	17,5	15,6	15,1	14,8	14,4	14,1
1550	21,1	17,8	16,0	15,5	15,1	14,8	14,4
1650	21,7	18,4	16,5	16,	15,7	15,4	15,0
1750	36,5	33,2	31,3	30,8	30,5	30,1	29,8

Table 13: Separability results for the 3 years rigid pavement system (Set1)

Wavelength	400	450	550	650	750	850	950	1050
400	5,4							
450	3,4	3,0						
550	9,2	8,8	3,2					
650	12,2	11,9	6,2	3,4				
750	12,6	12,3	6,6	3,8	3,2			
850	12,7	12,3	6,6	3,8	3,2	3,0		
950	13,3	12,9	7,2	4,5	3,8	3,6	3,5	
1050	13,7	13,3	7,6	4,9	4,2	4,0	3,9	3,3
1150	15,4	15,1	9,4	6,6	6,0	5,7	5,6	5,0
1250	17,3	16,9	11,3	8,5	7,8	7,6	7,5	6,9
1350	18,07	17,7	12,0	9,2	8,6	8,4	8,2	7,6
1450	23,2	22,9	17,2	14,4	13,8	13,5	13,4	12,8
1550	23,4	23,0	17,3	14,5	13,9	13,7	13,5	12,9
1650	24,6	24,	18,5	15,7	15,1	14,9	14,7	14,1
1750	39,3	38,9	33,3	30,5	29,8	29,6	29,5	28,9
1850	Atmospheric absorption							
1950	37,8	37,5	31,8	29,0	28,4	28,1	28,0	27,4
2050	40,6	40,2	34,5	31,7	31,1	30,9	30,7	30,1
2150	38,5	38,1	32,4	29,6	29,0	28,8	28,6	28,0
2250	43,3	43	37,3	34,5	33,8	33,6	33,5	32,9

Table 14: Separability results for the 3 years rigid pavement system (Set2)

Wavelength	400	500	600	700	800	900	1000
400	7,5						
500	7,0	5,7					
600	2,2	0,9	5,8				
700	1,7	0,4	5,3	5,9			
800	1,4	0,1	5,0	5,5	5,9		
900	1,5	0,2	5,1	5,6	6,0	5,9	
1000	1,0	0,2	4,6	5,2	5,6	5,5	5,9
1100	0,6	0,6	4,2	4,8	5,2	5,1	5,5
1200	3,5	4,8	0,0	0,6	1,0	0,8	1,3
1300	2,2	3,5	1,3	1,9	2,3	2,1	2,6
1400	6,5	7,8	2,9	2,3	1,9	2,0	1,6
1500	7,5	8,8	3,9	3,3	2,9	3,0	2,6
1600	8,4	9,7	4,8	4,2	3,8	3,9	3,5
1700	14,8	16,1	11,2	10,6	10,3	10,4	9,9
1800	18,5	19,8	14,9	14,4	14,0	14,1	13,7
1900	Atmospheric absorption						
2000	23,4	24,7	19,8	19,3	18,9	19,0	18,6
2100	22,3	23,6	18,7	18,1	17,8	17,9	17,5
2200	21,8	23,1	18,2	17,7	17,3	17,4	17,0
2250	28,4	28,6	23,4	20,9	20,6	20,6	20,4

As it is found from the tables above the results from the application of the Euclidean distance are the same for all the pavement systems except the one that is located exactly next to the sea. It is found that the highest separability value is recorder at the wavelengths 450 and 1750 nm. These wavelengths will be used in the experiment later in a try to identify in those wavelengths the cracks.

6.4 Spectral grid experiment

As it was mentioned in the methodology chapter, two sets of data were taken from the 20-30 years flexible pavement system from 350 -2500 wavelength. The data were resample and then processed to the Surfer in order to produce the diagrams. According to Euclidean distance results the wavelengths that could show the cracks in the diagrams might be the 450 and 1750 nm. First the diagrams of 450 and 1750 and 1750/450 for the first data set will be presented followed by the diagrams of the same wavelengths for the second data set.

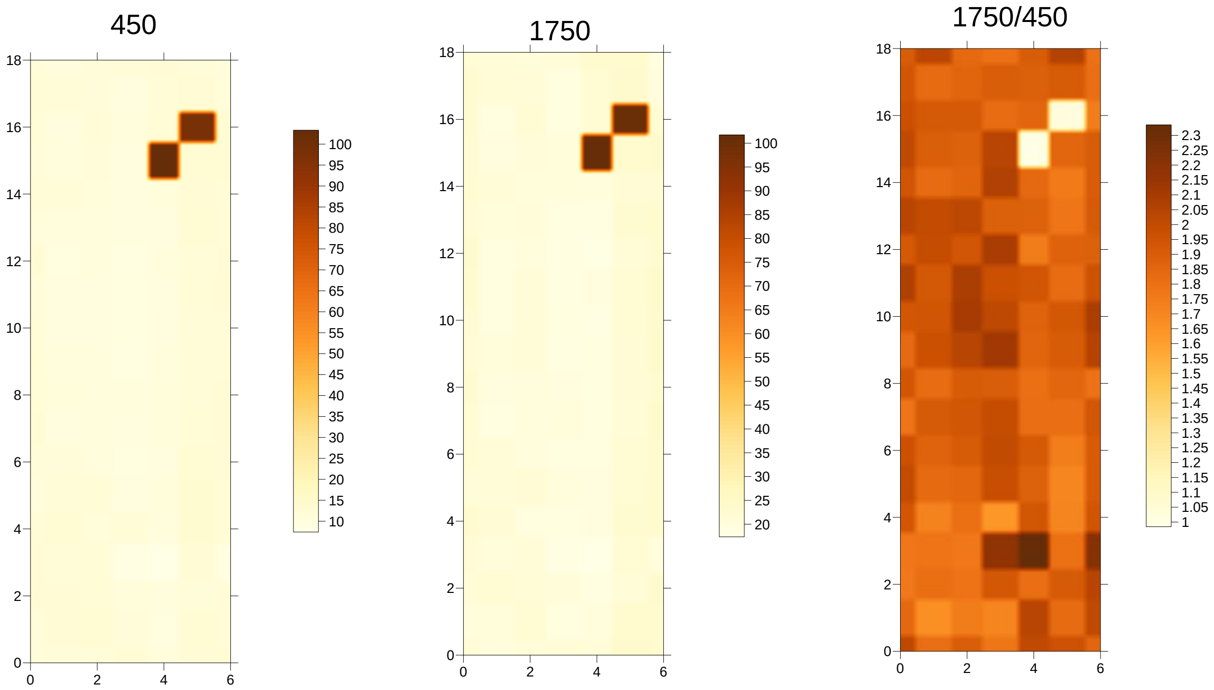

Figure 41: Diagrams of 450, 1750 nm and 1750/450nm for the first data set

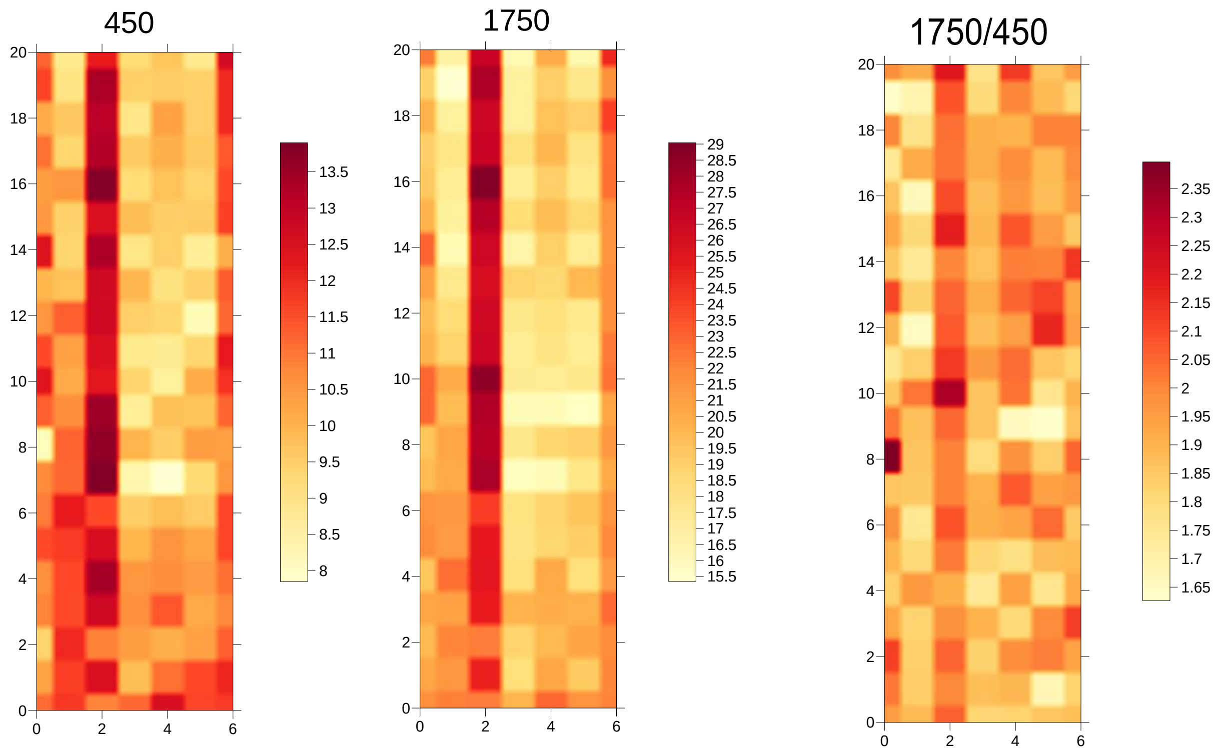

Figure 42: Diagrams of 450, 1750 nm and 1750/450nm for the second data set

As it is observed from the figures above, the experiment was not completed successfully for the reason that the cracks are not visible in any of the diagrams. Normally the first crack which is a vertical crack (See figure 6) should have appeared somewhere between the 8th and 9th (y-axis) measurement and the second crack which is a horizontal one should have appeared between 2nd and 3rd measurement (X-axis). It is clear that in order for this experiment to be successful further research is needed. Moreover one reason that might affect the results of the experiment is the number of data sets. This research took two data sets only, due to limited time so probably a lot more data sets are needed in order to succeed the experiment. Furthermore the pavement should be clean and the weather should be sunny with no clouds. These are probably the reasons that the experiment did not completed as expected.

6.5 Discussion

Through the analysis of the data, the statistical tests, the Pearson correlation, the Euclidean distance and the spectral experiment, it is curtain that road mapping can be achieved through ground spectrometry. After the completion of the graphs, this research found some important things; first of all the pavement type can be determined through the spectrometry. When comparing two asphalt pavement systems which differ in age, it is found that the pavement which is older shows an increase in the reflectance. In addition with the newer which has lower reflectance, but both pavements show an increase in reflectance towards 2200 nm. Also the oldest pavement system has small standard deviation – better range.

Moving on to the rigid pavements, it is observed that the rigid pavement which is located exactly next to the sea has strange values of reflectance. Its reflectance increases abruptly towards 1700 nm, which is probably a cause of the humidity of the sea salt and the corrosion.

To add it is observed that rigid pavements have higher values of reflectance than the flexible.

Lastly it is found that the cracked areas have lower reflectance than the un-cracked areas. This is because the un-cracked area ages faster than the cracked area, it loses its oily components, it is more exposed to the environment than the cracked and it has oxidation.

Through the application of t-test this research has shown that there is statistical difference between the cracked and the un-cracked, there is not any statistical difference between the un-cracked areas or the cracked areas.

The Pearson correlation showed the wavelengths that have low correlation. Within these wavelengths the cracks should be visible from satellites.

Last but not least, through the spectral grid experiment this research tried to identify the wavelengths that can reveal the deformations of the pavement. It is noted that during the experiment the flexible pavement system had dust and it was windy, facts that might have affected the measurements. Unfortunately the deformations are not visible in the wavelengths that were generated from the Euclidean distance results.

7 Conclusion

This research used a ground spectroradiometer in order to map the conditions of flexible and rigid pavement systems. Spectral signatures were taken from the pavement systems which were analysed through graphical manner. Then several t-test were applied in order to investigate differences in the means of the pavements. Following that, the Pearson correlation was used to investigate whether the pavements are correlated between them and to observe the wavelengths that have low correlation. Moving on, the Euclidean distance was used in order to observe regions of wavelengths that can show the deformations, and to identify the distance between the sets. Through the whole detailed research that took part, the following were resulted.

- It is easy to distinguish the pavement type through ground spectrometry as the reflectance of rigid pavement system are almost double than the reflectance of a flexible pavement system.
- The cracks in a pavement system rigid or flexible can be observed through ground spectrometry as they show a better range and lower values of reflectance than the areas with no cracks.
- Recently constructed pavement systems have low reflectance.
- As the age of the pavement increases the reflectance increases as well.
- The wavelengths with low correlation can be used to show the cracked areas through satellites
- Pavement systems that are near the sea show different attributes in terms of reflectance
- The cracked areas have lower reflectance than the un-cracked areas.
- There is not any statistical difference between the un-cracked areas or cracked areas of different pavement
- The wavelengths 1750nm and 450nm are the wavelengths that can show the deformations, with further research.

8 Recommendations

This research recommends other researches to undertake the spectral experiment as the results that this research got are promising, ignoring the fact that cracks are not visible in the diagrams. It is recommended to take more sets of data, as this research took only two sets and to take the measurements in good weather. With further research, the spectral experiment can be successful.

9 References

Agapiou, A., and Hadjimitsis, D. (2012). “Towards an archaeological index: identification of the spectral regions of stress vegetation due to buried archaeological remains.” *EuroMed*, 129–138.

Andreou, C., Karathanassi, V., and Kolokoussis, P. (2011). “Investigation of hyperspectral remote sensing for mapping asphalt road conditions.” *International Journal of Remote Sensing*, 32(21), 6315–6333.

Boucher, A. (2007). “Downscaling of Satellite remote sensing data: application to land cover mapping.” *Stanford University*, (August), 143.

Fuchs, I. F., and Jasienski, I. a. (2001). “Road pavements of cement concrete : Execution of Monolithic Pavements.” 20.

Green, O. (n.d.). “Spectral Bands.” 1–2.

Herold, M., Roberts, D. a, Gardner, M. E., and Dennison, P. E. (2004a). “Spectrometry for urban area remote sensing—Development and analysis of a spectral library from 350 to 2400 nm.” *Remote Sensing of Environment*, 91(3-4), 304–319.

Herold, M., Roberts, D., Noronha, V., and Smadi, O. (2008). “Imaging spectrometry and asphalt road surveys.” *Transportation Research Part C: Emerging Technologies*, 16(2), 153–166.

Herold, M., Roberts, D., Smadi, O., and Noronha, V. (2004b). “Road condition mapping with hyperspectral remote sensing.” *Aviris 2004*, 1–15.

Kuenzer, C., Dech, S., Arvidson, T., Barsi, J., Jhabvala, M., and Reuter, D. (2013). *Thermal Infrared Remote Sensing*.

Manzo, C., Mei, A., Salvatori, R., Bassani, C., and Allegrini, A. (2014). “Spectral modelling used to identify the aggregates index of asphalted surfaces and sensitivity analysis.” *Construction and Building Materials*, Elsevier Ltd, 61, 147–155.

Mei, A., Fiore, N., Salvatori, R., D’Andrea, A., and Fontana, M. (2012). “Spectroradiometric Laboratory Measures on Asphalt Concrete: Preliminary Results.” *Procedia - Social and Behavioral Sciences*, Elsevier B.V., 53, 514–523.

Mei, A., Salvatori, R., Fiore, N., Allegrini, A., and D’Andrea, A. (2014). “Integration of field and laboratory spectral data with multi-resolution remote sensed imagery for asphalt surface differentiation.” *Remote Sensing*, 6(4), 2765–2781.

Mohammadi, M. (2012). “Road classification and condition determination using hyperpsectral imagery.” *International Archives of the Photogrammetry, Remote Sensing* *and Spatial Information Sciences, Volume XXXIX-B7, 2012 XXII ISPRS Congress,* XXXIX(September), 141–146.

Noronha, V., Herold, M., Roberts, D., and Gardner, M. (2002). "Spectrometry and Hyperspectral Remote Sensing for Road Centerline Extraction and Evaluation of Pavement Condition." *National Consortium on Remote Sensing in transportation - Infrastructure Management (2002),* 12.

Pascucci, S., Bassani, C., Palombo, A., Poscolieri, M., and Cavalli, R. (2008). "Road Asphalt Pavements Analyzed by Airborne Thermal Remote Sensing: Preliminary Results of the Venice Highway." *Sensors 2008*, 8(2), 1278–1296.

Puttonen, E., Suomalainen, J., Hakala, T., and Peltoniemi, J. (2009). "Measurement of reflectance properties of asphalt surfaces and their usability as reference targets for aerial photos." *IEEE Transactions on Geoscience and Remote Sensing,* 47(7), 2330–2339.

Ramakrishnan, D., and Bharti, R. (2015). "Hyperspectral remote sensing and geological applications." *Current Science,* 108(5), 879–891.

Schnebele, E., Tanyu, B. F., Cervone, G., and Waters, N. (2015). "Review of remote sensing methodologies for pavement management and assessment." *European Transport Research Review,* 7(2).

Shahi, K., Shafri, H. Z. M., Taherzadeh, E., Mansor, S., and Muniandy, R. (2015). "A novel spectral index to automatically extract road networks from WorldView-2 satellite imagery." *The Egyptian Journal of Remote Sensing and Space Science*, Authority for Remote Sensing and Space Sciences, 18(1), 27–33.

Soediono, B. (1989). "No Title No Title." *Journal of Chemical Information and Modeling*, 53(Figure 1), 160.

Wells, G., Prest, H., and Russ, C. W. (2011). "Signal , Noise , and Detection Limits in Mass Spectrometry." 8.

Yun, H. C. (n.d.). "Extraction of road surface information using remote sensing." 1–8.

10. Appendices

10.1 Appendix A – pictures of the pavement systems

Figure 43: Rigid Pavement systems pictures

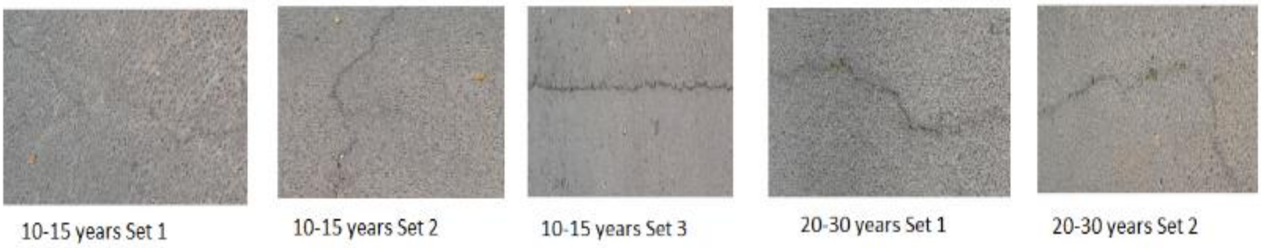

Figure 44: Flexible pavement systems pictures

10.2 Appendix B - Spectral profiles

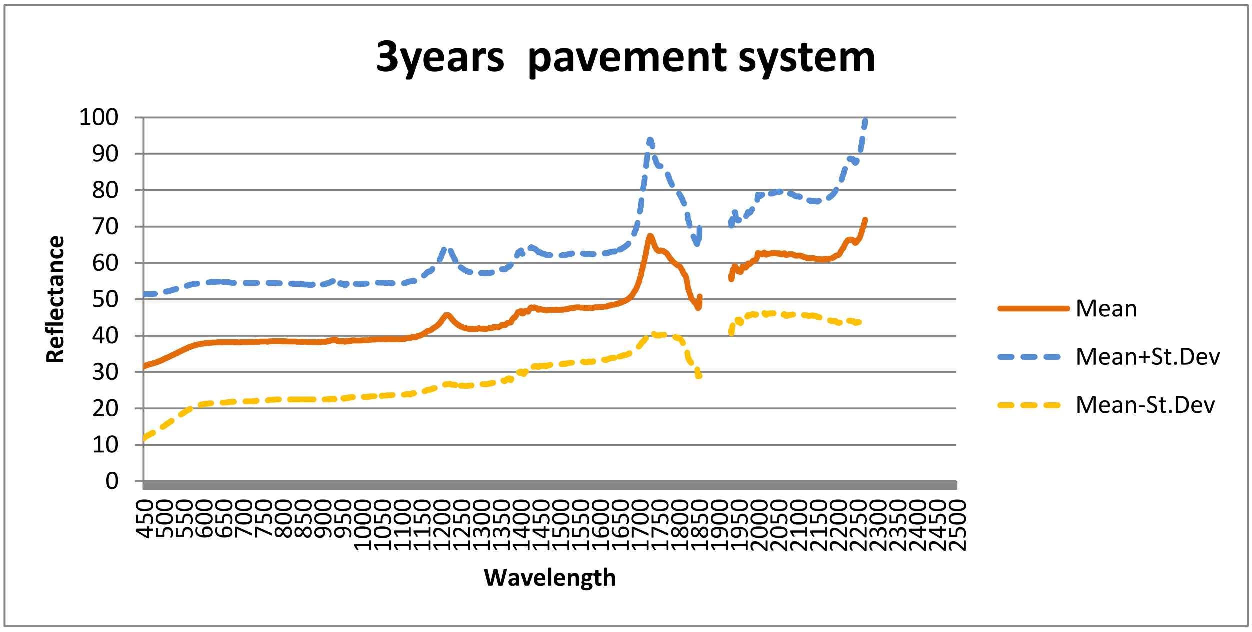

Figure 45: Range of the 3 years pavement system (Set 2) – Un-cracked (Rigid pavement system)

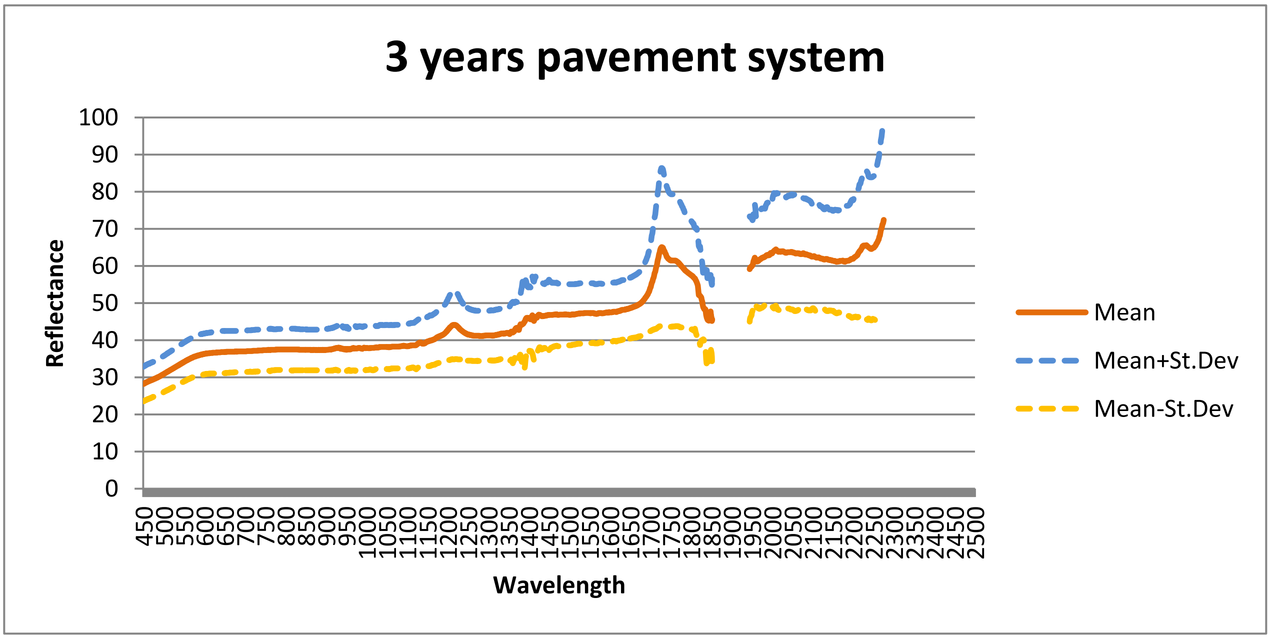

Figure 46: Range of the 3 years pavement system (Set 2) – Cracked (Rigid pavement system)

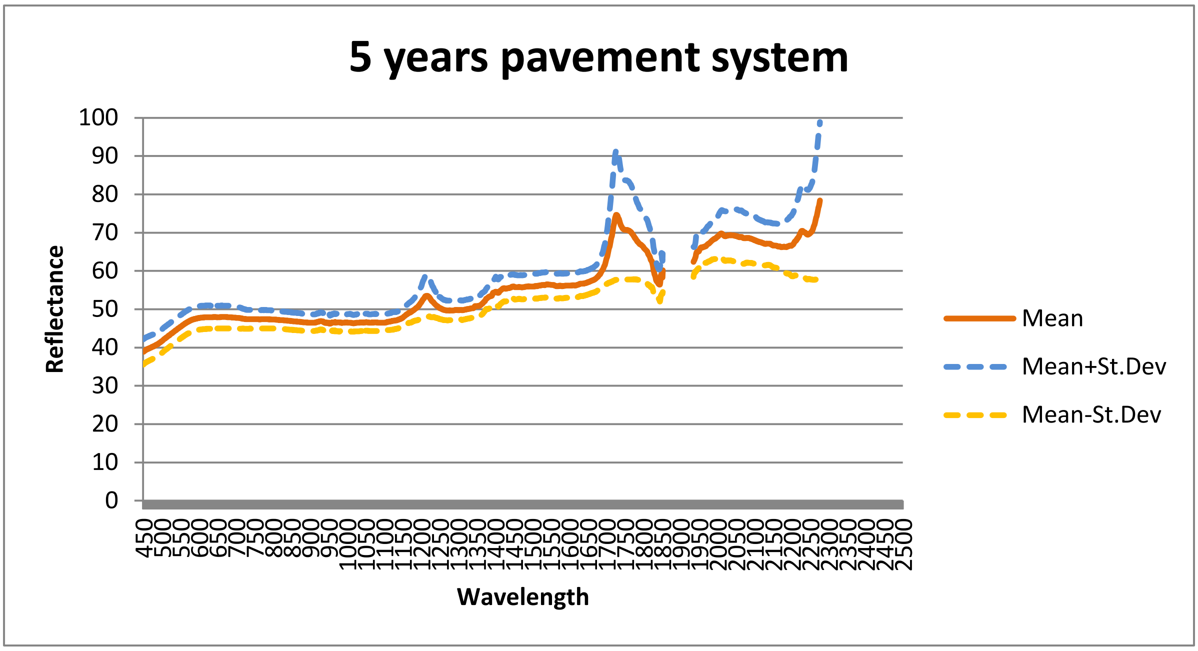

Figure 47: Range of the 5 years pavement system (Set 1) – Un-cracked (Rigid pavement system)

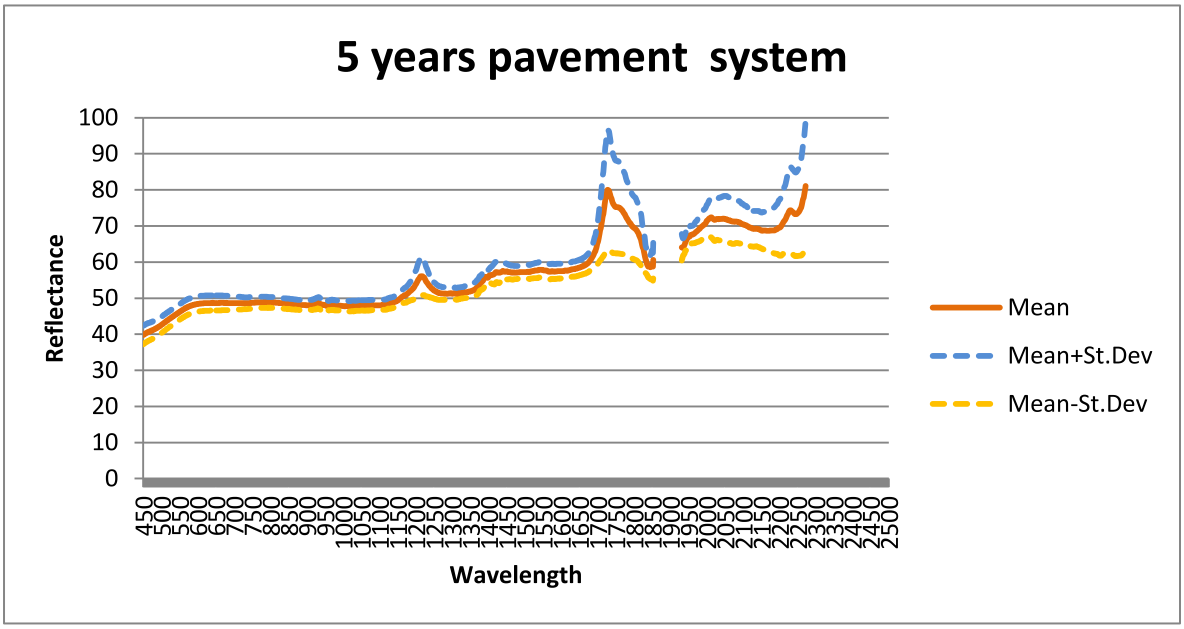

Figure 48: Range of the 5 years pavement system (Set 1) – Cracked (Rigid pavement system)

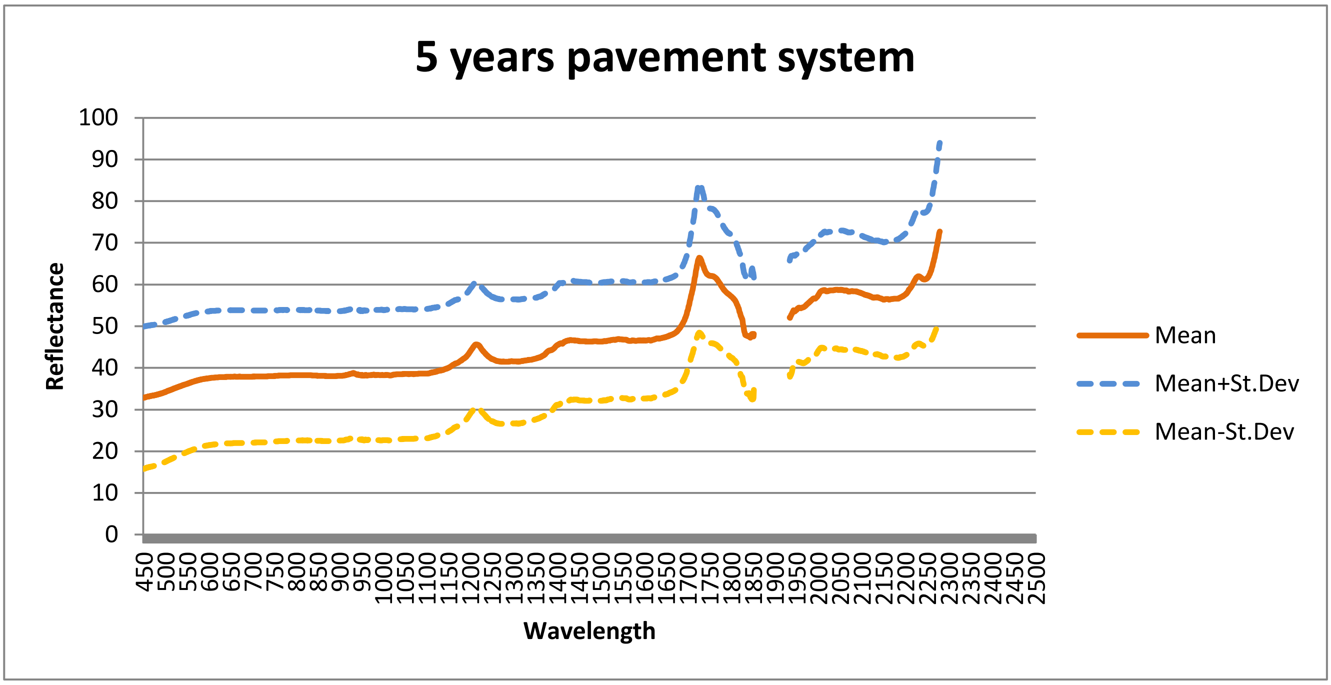

Figure 49: Range of the 5 years pavement system (Set 2) – Un-cracked (Rigid pavement system)

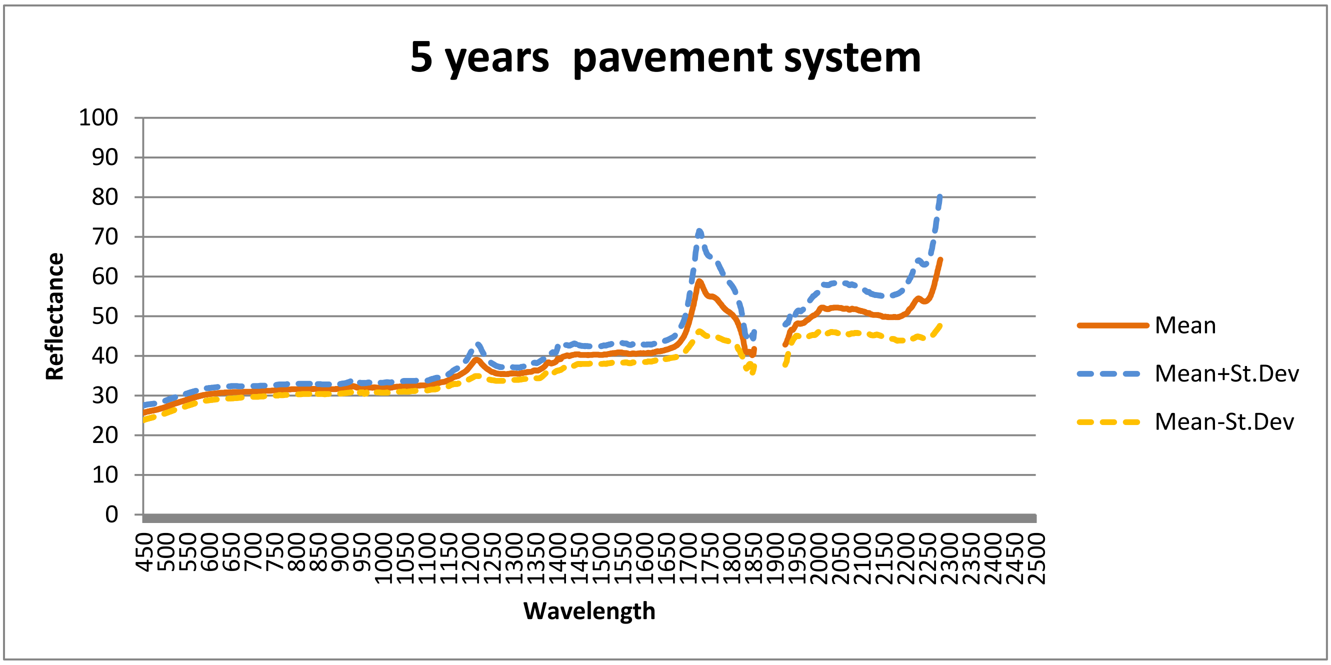

Figure 50: Range of the 5 years pavement system (Set 2) – Cracked (Rigid pavement system)

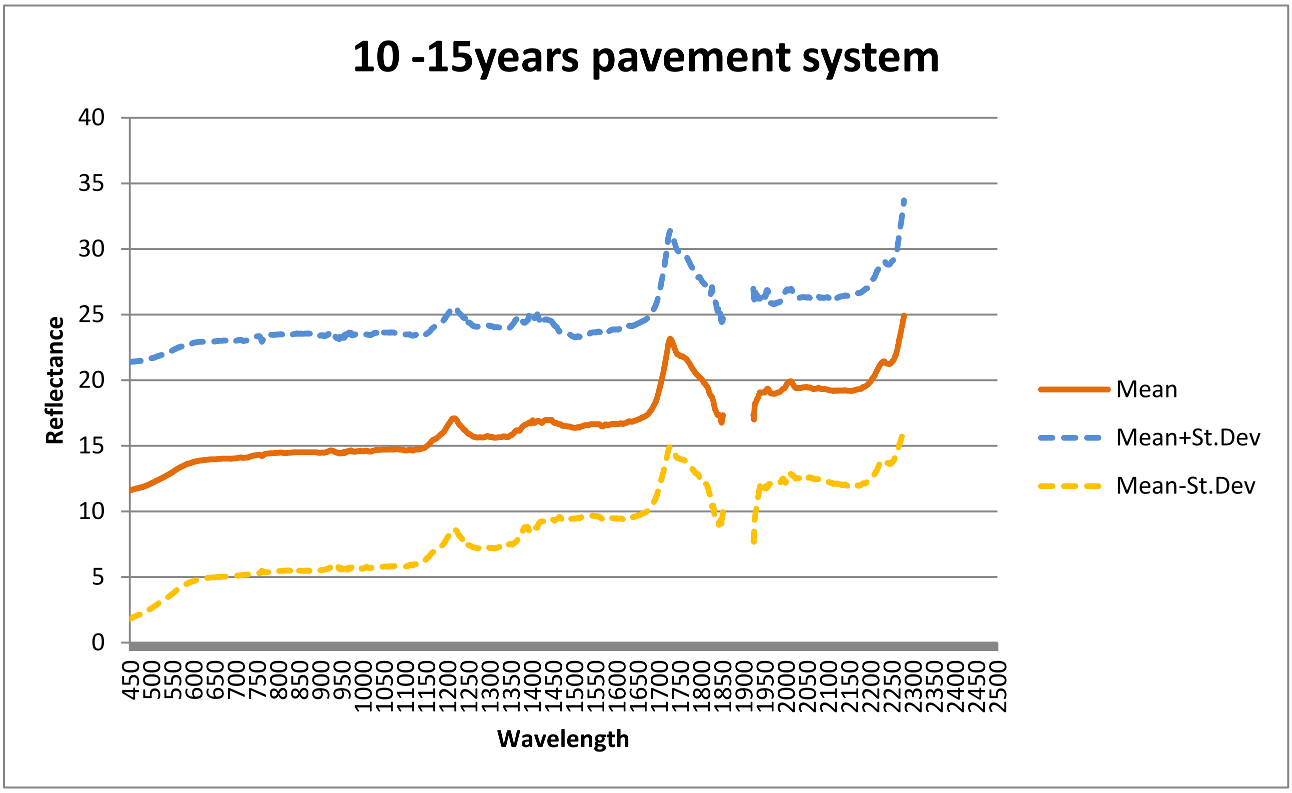

Figure 51: Range of the 10-15 years pavement system (Set 2) – Un-cracked (Flexible pavement system)

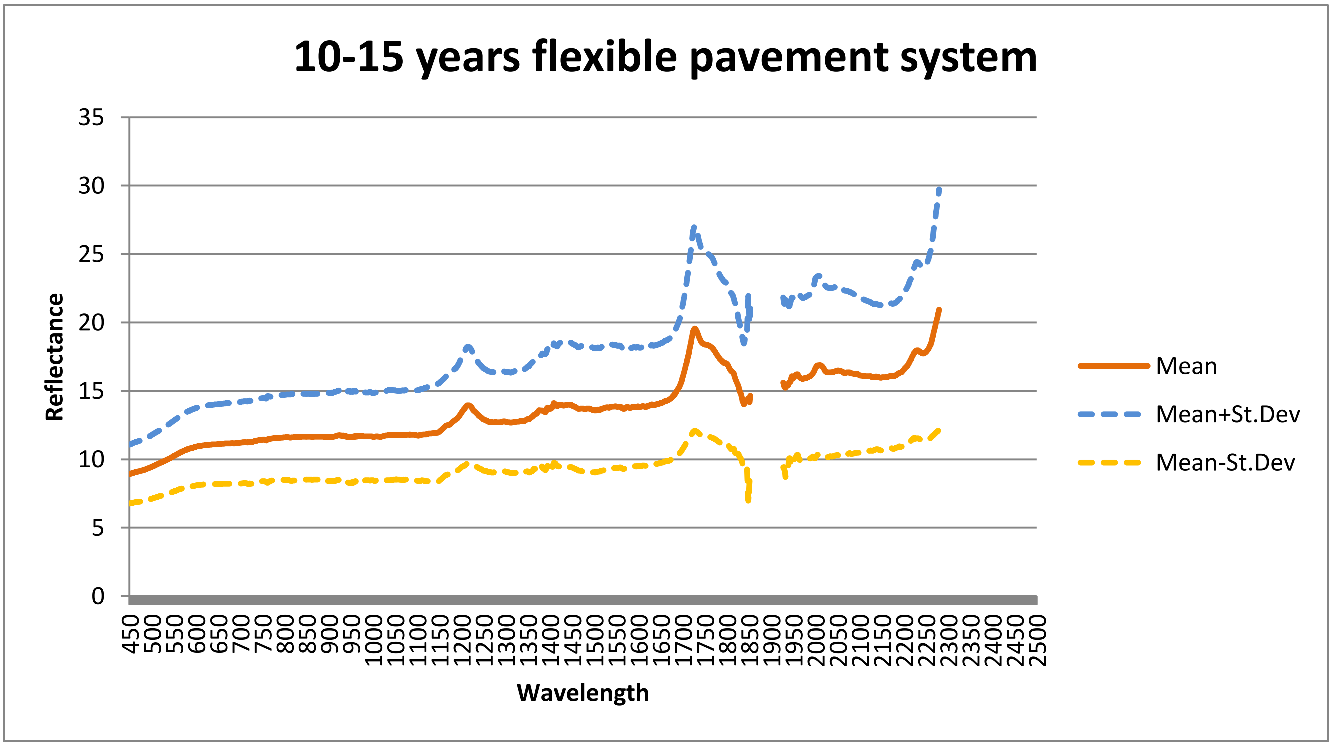

Figure 52: Range of the 10-15 years pavement system (Set 2) – Cracked (Flexible pavement system)

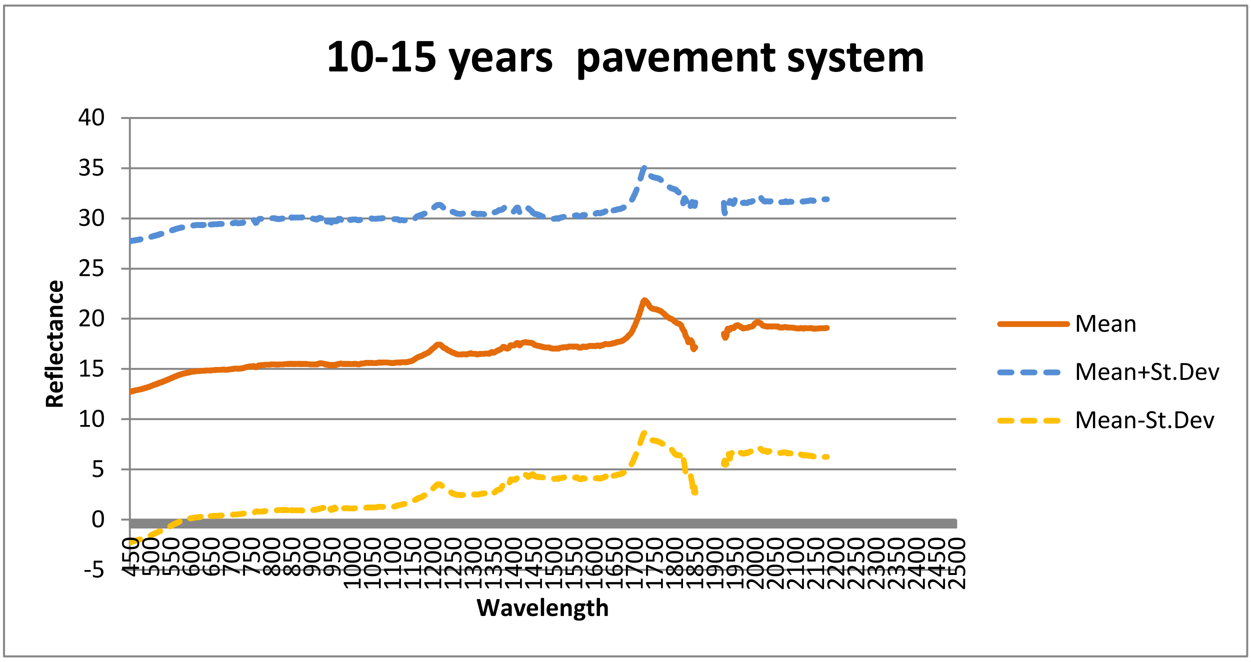

Figure 53: Range of the 10-15 years pavement system (Set 3) – Un-cracked (Flexible pavement system)

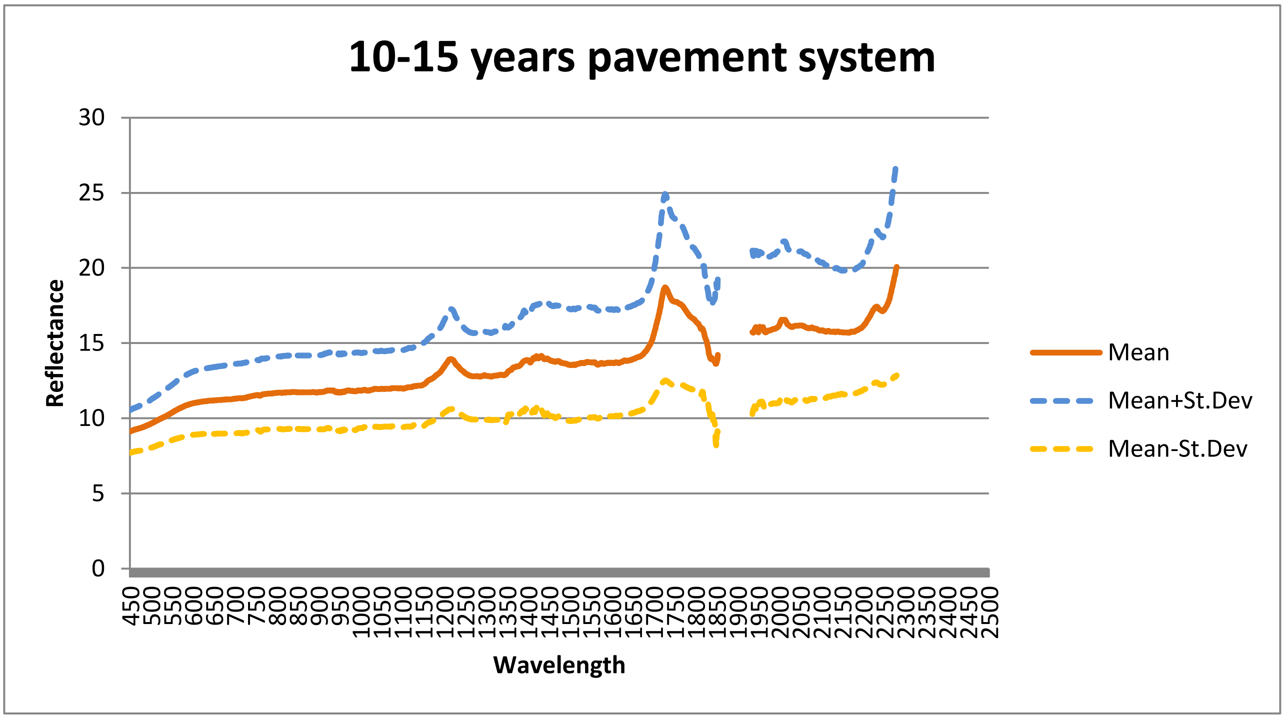

Figure 54: Range of the 10-15 years pavement system (Set 3) – Cracked (Flexible pavement system)

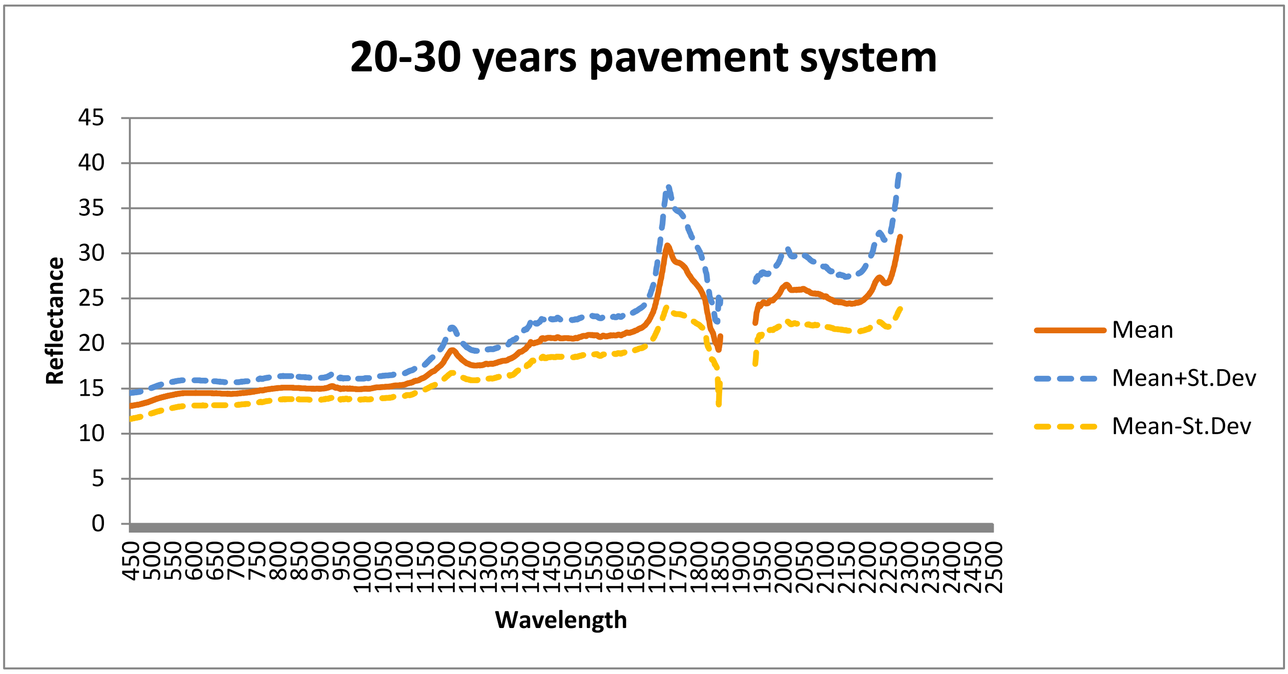

Figure 55: Range of the 20-30 years pavement system (Set 1) – Un-cracked (Flexible pavement system)

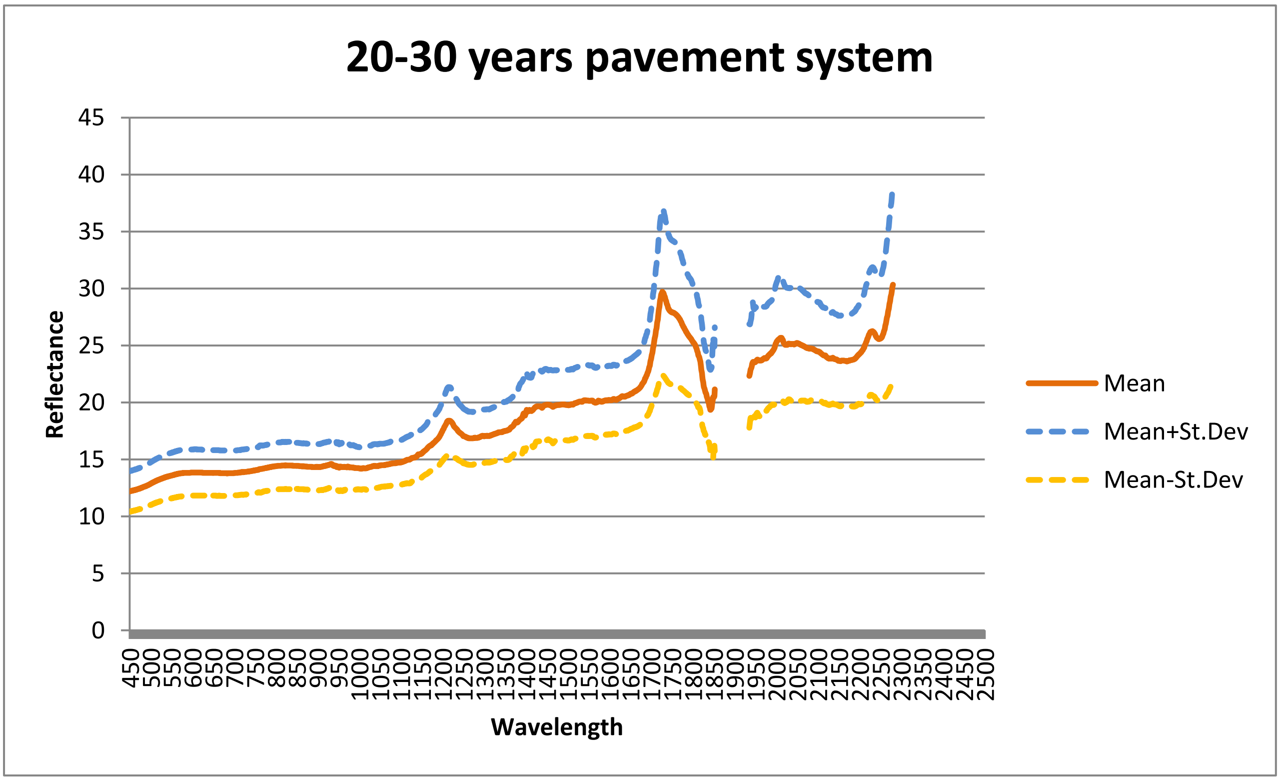

Figure 56: Range of the 20-30 years pavement system (Set 1) – Cracked (Flexible pavement system)

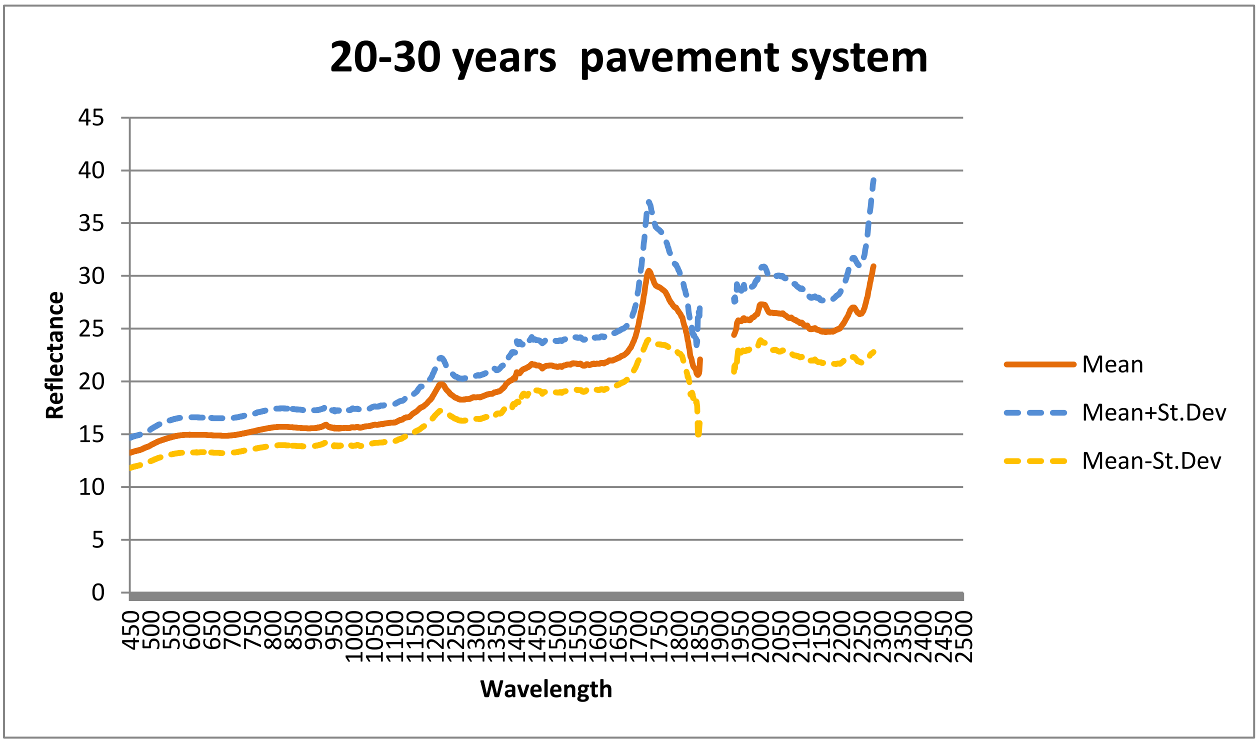

Figure 57: Range of the 20-30 years pavement system (Set 2) – Un-cracked (Flexible pavement system)

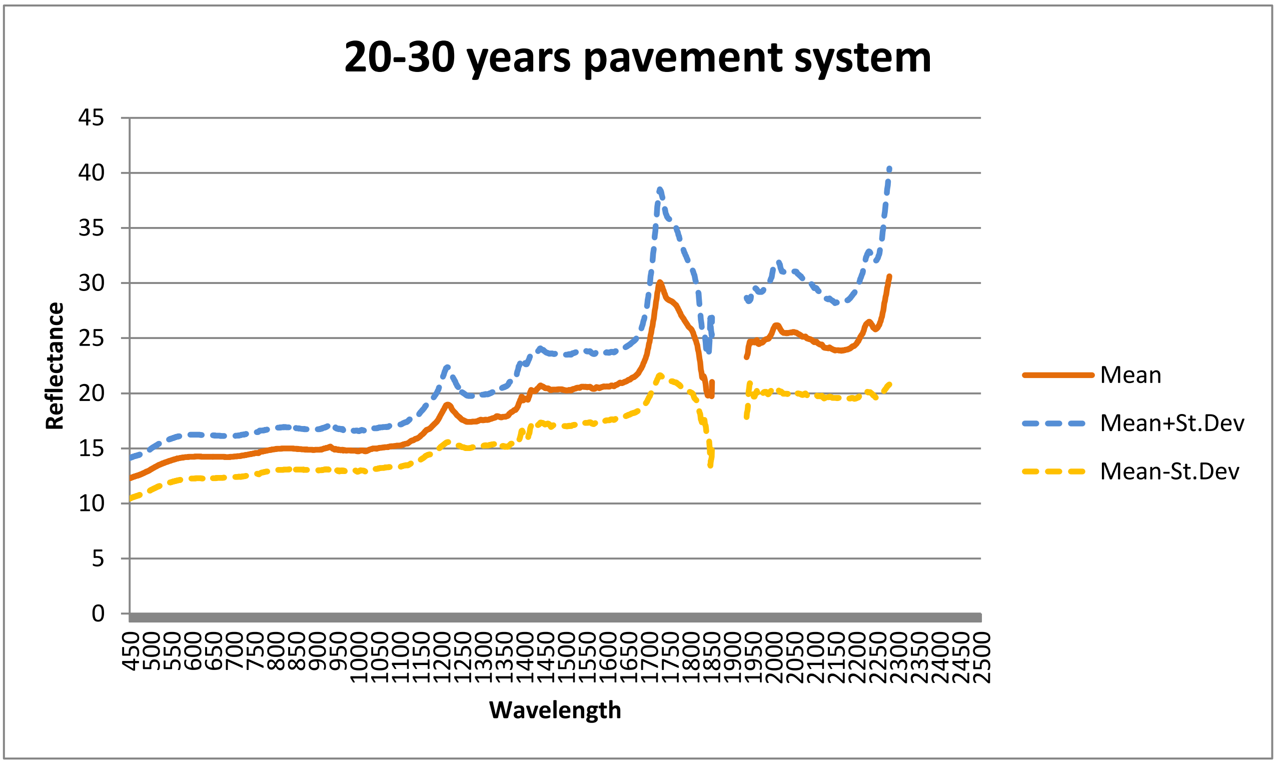

Figure 58: Range of the 20-30 years pavement system (Set 2) – Cracked (Flexible pavement system)

10.3 Appendix C - T-test

Table 15: t-test results between 3 years rigid pavement vs 10-15 flexible pavement

t-Test: 3 years pavement(Rigid) Vs 10-15 years pavement(Flexible)		
	3 years	*10-15 years*
Mean	47,06	17,98
df	3903	
t Stat	106,04	
P(T<=t) two-tail	0	
t Critical two-tail	2,57	

Table 16: t –test results between 5 years rigid pavement Vs 10-15 years flexible pavement

t-Test: 5 years pavement (Rigid) Vs 10-15 years pavement (Flexible)		
	5 years	*10-15 years*
Mean	54,94	17,94
df	3934	
t Stat	154,79	
P(T<=t) two-tail	0	
t Critical two-tail	2,57	

Table 17 : t –test results between 5 years rigid pavement Vs 20-30 years flexible pavement

t-Test: 5 years rigid Vs 20-30 flexible		
	5 years	*20-30 years*
Mean	46,71	21,15
df	3900	
t Stat	86,49	
P(T<=t) two-tail	0	
t Critical two-tail	2,57	

Second part of t-test

Table 18: t-test results between the un-cracked and the cracked area of the 3 years pavement

t-Test: 3 years pavement un-cracked vs cracked		
	Un-cracked	*Cracked*
Mean	47,06	45,75
df	3672	
t Stat	3,56	
P(T<=t) two-tail	0,00	
t Critical two-tail	1,96	

Table 19: t-test results between the un-cracked and the cracked area of the 5 years pavement (Set 1)

t-Test: 5 years pavement un-cracked vs cracked		
	Un-cracked	*Cracked*
Mean	54,94	56,65
df	3706	
t Stat	-4,88	
P(T<=t) two-tail	1,09E-06	
t Critical two-tail	1,96	

Table 20: t-test results between the un-cracked and the cracked area of the 5 years pavement (Set 2)

t-Test: 5 years pavement un-cracked vs cracked		
	Un-cracked	*Cracked*
Mean	46,71	40,71
df	3832	
t Stat	16,79	
P(T<=t) two-tail	4,03E-61	
t Critical two-tail	1,96	

Table 21: t-test results between the un-cracked and the cracked area of the 10-15 years pavement (Set 1)

t-Test: 10-15 years pavement un-cracked vs cracked		
	Un-cracked	*Cracked*
Mean	17,48	16,04
df	4120	
t Stat	9,44	
P(T<=t) two-tail	5,56E-21	
t Critical two-tail	1,96	

Table 22: t-test results between the un-cracked and the cracked area of the 10-15 years pavement (Set 2)

t-Test: 10-15 years pavement un-cracked vs cracked		
	Un-cracked	*Cracked*
Mean	17,98	14,82
df	4133	
t Stat	20,89	
P(T<=t) two-tail	2,91E-92	
t Critical two-tail	1,96	

Table 23: t-test results between the un-cracked and the cracked area of the 10-15 years pavement (Set 3)

t-Test:10-15 years pavement un-cracked vs cracked		
	Un-cracked	*Cracked*
Mean	17,94	14,56
df	4120	
t Stat	28,20	
P(T<=t) two-tail	3,4E-160	
t Critical two-tail	1,96	

Table 24 : t-test results between the un-cracked and the cracked area of the 10-15 years pavement (Set 1)

t-Test: 20-30 years pavement un-cracked vs cracked		
	Un-cracked	*Cracked*
Mean	21,15	20,27
Hypothesized Mean Difference	0	
df	4018	
t Stat	3,85	
P(T<=t) two-tail	0,00	
t Critical two-tail	1,96	

Table 25: t-test results between the un-cracked and the cracked area of the 10-15 years pavement (Set 2)

t-Test: 20-30 years pavement un-cracked vs cracked		
	Un-cracked	*Cracked*
Mean	21,57	21,04
df	4086	
t Stat	2,33	
P(T<=t) two-tail	0,019	
t Critical two-tail	1,96	

Third part of t-test

Table 26: t-test results between 5 years (Set 1) un-cracked and 5 years pavement (Set 2) un-cracked

t-Test: 3 years un-cracked set 1 Vs set 2		
	Set 1	*Set 2*
Mean	54,70	46,23
df	3692	
t Stat	25,14	
P(T<=t) two-tail	5,8E-129	
t Critical two-tail	1,96	

Table 27: t-test results between 10-15 years (Set 1) un- cracked and 10-15 years pavement (Set 2) un-cracked

t-Test: 10-15 years un-cracked set 1 Vs set 2		
	Set 1	*Set 2*
Mean	17,48	17,98
df	4122	
t Stat	-3,12	
P(T<=t) two-tail	0,00	
t Critical two-tail	1,96	

Table 28: t-test results between 20-30 years (Set 1) un- cracked and 20-30 years pavement (Set 2) un-cracked

t-Test: 20-30 years un-cracked set 1 Vs set 2		
	Set 1	*Set 2*
Mean	19,73	21,57
df	3778	
t Stat	-9,15	
P(T<=t) two-tail	8,63E-20	
t Critical two-tail	1,96	

Table 29: t-test results between 5 years (Set 1) cracked and 5 years pavement (Set 2) cracked

t-Test: 5 years cracked set 1 Vs set 2		
	Set 1	*Set 2*
Mean	56,65	39,64
df	3652	
t Stat	48,58	
P(T<=t) two-tail	0	
t Critical two-tail	1,96	

Table 30: t-test results between 10-15 years (Set 1) cracked and 10-15 years pavement (Set 2) cracked

t-Test: 10-15 years cracked set 1 Vs set 2		
	Set 1	*Set 2*
Mean	16,04	14,82
df	4124	
t Stat	8,65	
P(T<=t) two-tail	7,02E-18	
t Critical two-tail	1,96	

Table 31: t-test results between 20-30 years (Set 1) cracked and 20-30 years pavement (Set 2) cracked

t-Test: 20-30 years cracked set 1 Vs set 2		
	Set 1	*Set2*
Mean	20,27	21,04
df	4076	
t Stat	-3,43	
P(T<=t) two-tail	0,00	
t Critical two-tail	1,96	

10.4 Appendix D - Pearson Correlation

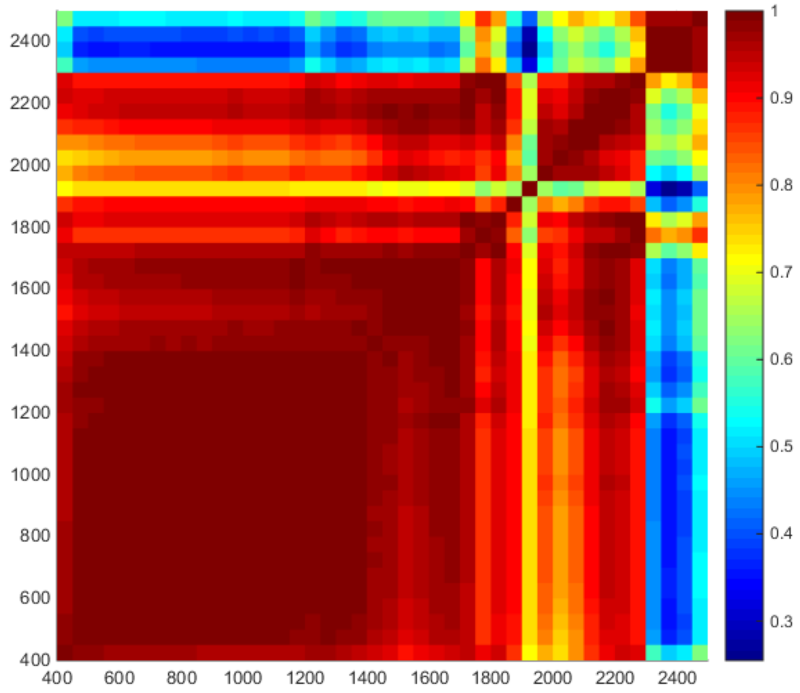

Figure 59: Correlation analysis of reflectance values from un-cracked against reflectance values of un-cracked from the 10-15 years flexible pavement system (Set 2)

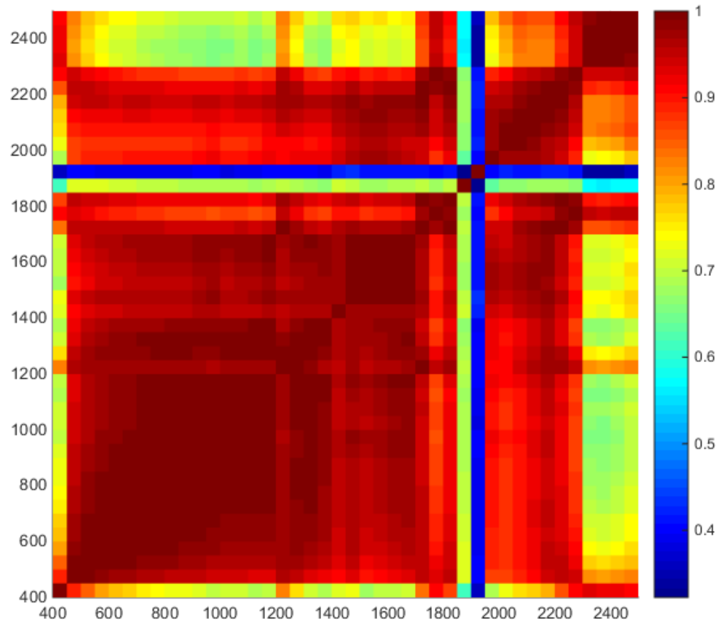

Figure 60: Correlation analysis of reflectance values from cracked against reflectance values of cracked from the 10-15 years flexible pavement system (Set 2)

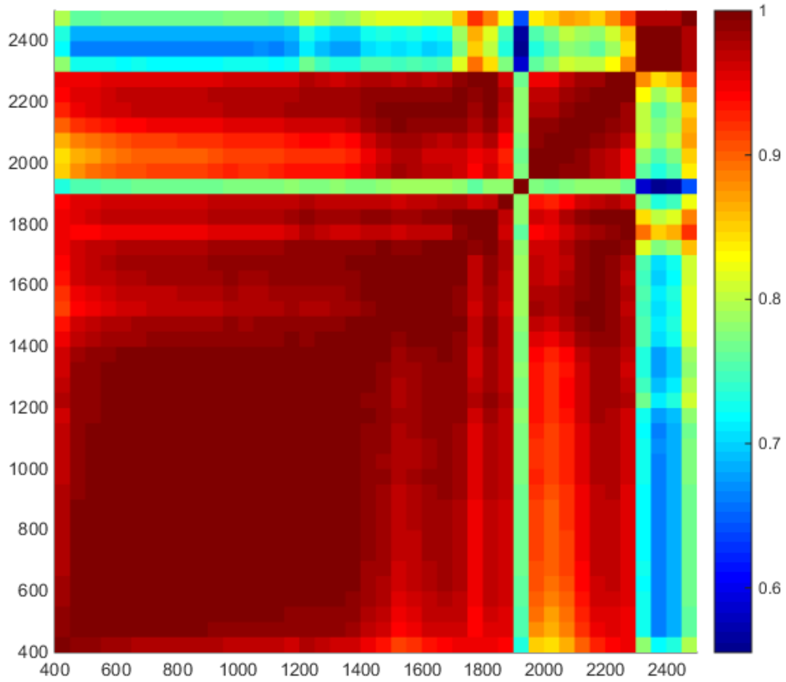

Figure 61: Correlation analysis of reflectance values from un-cracked against reflectance values of un-cracked from the 10-15 years flexible pavement system (Set 3)

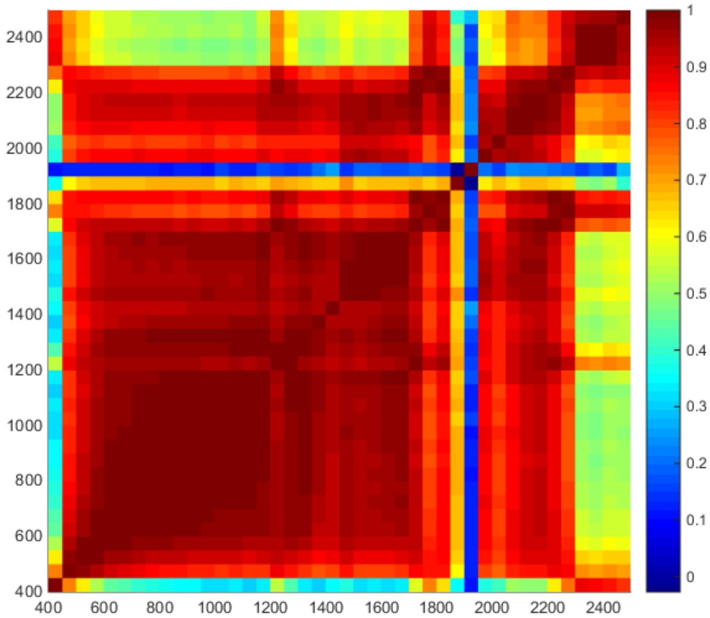

Figure 62: Correlation analysis of reflectance values from cracked against reflectance values of cracked from the 10-15 years flexible pavement system (Set 3)

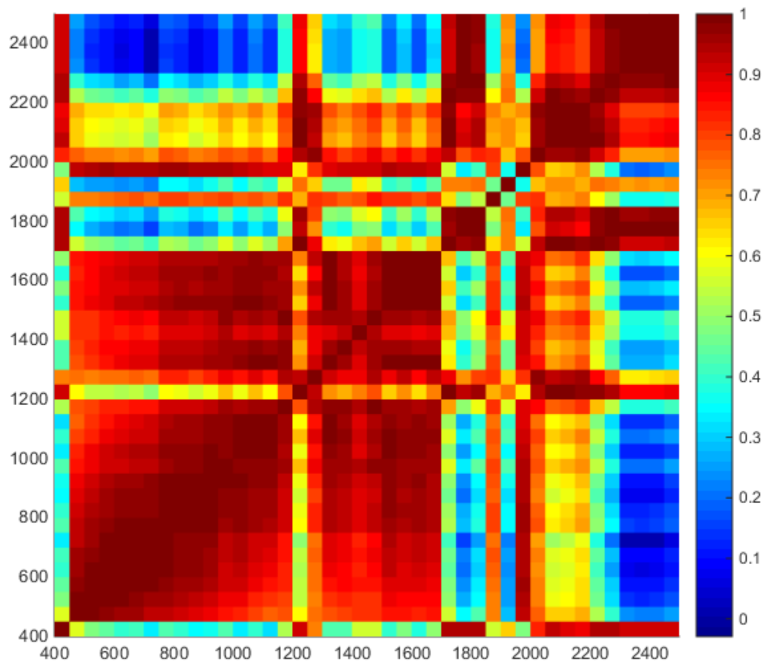

Figure 63: Correlation analysis of reflectance values from un-cracked against reflectance values of un-cracked from the 5 years rigid pavement system (Set 1)

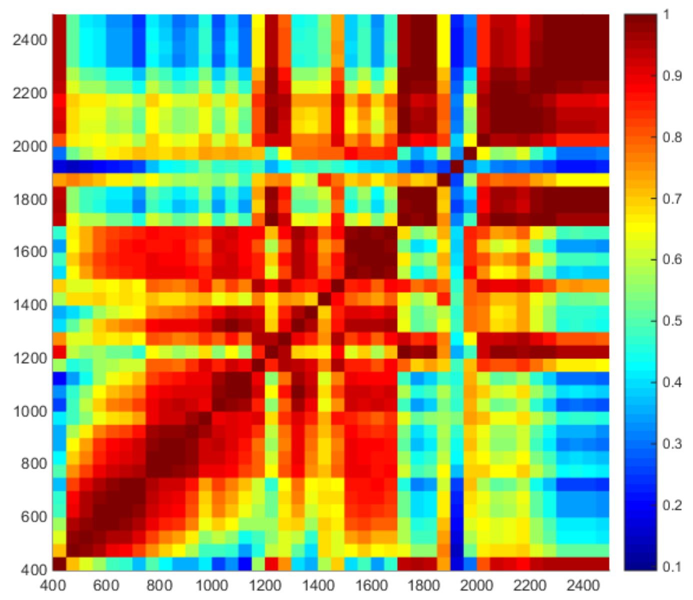

Figure 64: Correlation analysis of reflectance values from cracked against reflectance values of cracked from the 5 years rigid pavement system (Set 1)

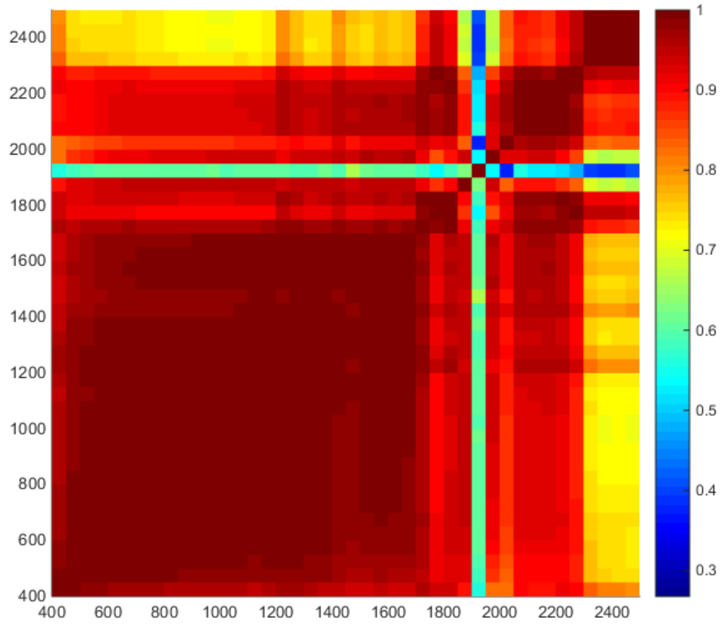

Figure 65: Correlation analysis of reflectance values from un-cracked against reflectance values of un-cracked from the 3 years rigid pavement system (Set 2)

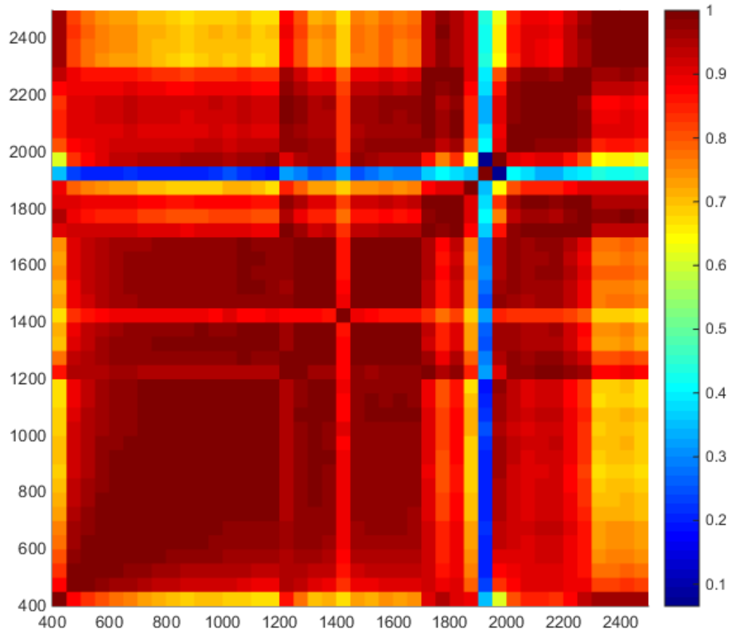

Figure 66: Correlation analysis of reflectance values from cracked against reflectance values of cracked from the 3 years rigid pavement system (Set 2)

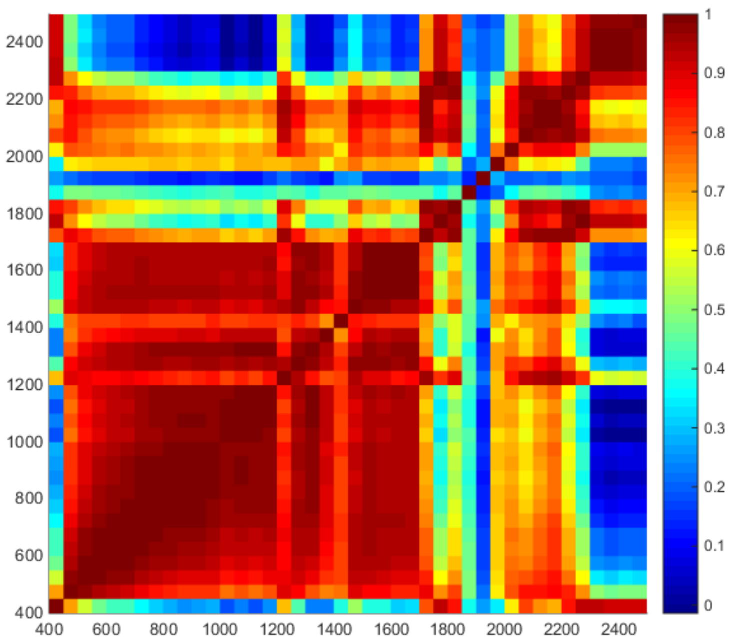

Figure 67: Correlation analysis of reflectance values from un-cracked against reflectance values of un-cracked from the 20-30 years flexible pavement system (Set 2)

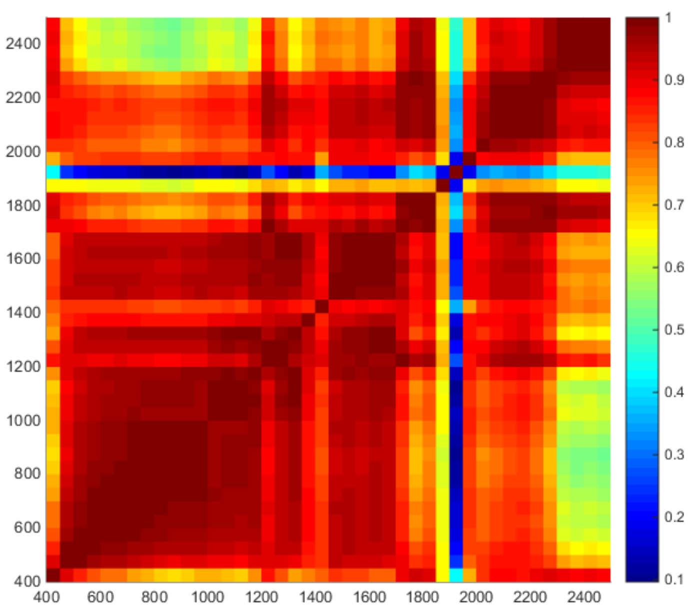

Figure 68: Correlation analysis of reflectance values from cracked against reflectance values of cracked from the 20-30 years flexible pavement system (Set 2)